

1980

# Stereoselective coordination of optically active amino acids and their derivatives to cobalt (III)

Larry Alan Meiske  
*Iowa State University*

Follow this and additional works at: <https://lib.dr.iastate.edu/rtd>

 Part of the [Inorganic Chemistry Commons](#)

## Recommended Citation

Meiske, Larry Alan, "Stereoselective coordination of optically active amino acids and their derivatives to cobalt (III) " (1980).  
*Retrospective Theses and Dissertations*. 7392.  
<https://lib.dr.iastate.edu/rtd/7392>

This Dissertation is brought to you for free and open access by the Iowa State University Capstones, Theses and Dissertations at Iowa State University Digital Repository. It has been accepted for inclusion in Retrospective Theses and Dissertations by an authorized administrator of Iowa State University Digital Repository. For more information, please contact [digirep@iastate.edu](mailto:digirep@iastate.edu).

## INFORMATION TO USERS

This was produced from a copy of a document sent to us for microfilming. While the most advanced technological means to photograph and reproduce this document have been used, the quality is heavily dependent upon the quality of the material submitted.

The following explanation of techniques is provided to help you understand markings or notations which may appear on this reproduction.

1. The sign or "target" for pages apparently lacking from the document photographed is "Missing Page(s)". If it was possible to obtain the missing page(s) or section, they are spliced into the film along with adjacent pages. This may have necessitated cutting through an image and duplicating adjacent pages to assure you of complete continuity.
2. When an image on the film is obliterated with a round black mark it is an indication that the film inspector noticed either blurred copy because of movement during exposure, or duplicate copy. Unless we meant to delete copyrighted materials that should not have been filmed, you will find a good image of the page in the adjacent frame.
3. When a map, drawing or chart, etc., is part of the material being photographed the photographer has followed a definite method in "sectioning" the material. It is customary to begin filming at the upper left hand corner of a large sheet and to continue from left to right in equal sections with small overlaps. If necessary, sectioning is continued again—beginning below the first row and continuing on until complete.
4. For any illustrations that cannot be reproduced satisfactorily by xerography, photographic prints can be purchased at additional cost and tipped into your xerographic copy. Requests can be made to our Dissertations Customer Services Department.
5. Some pages in any document may have indistinct print. In all cases we have filmed the best available copy.

University  
Microfilms  
International

300 N. ZEEB ROAD, ANN ARBOR, MI 48106  
18 BEDFORD ROW, LONDON WC1R 4EJ, ENGLAND

8019650

MEISKE, LARRY ALAN

STERESELECTIVE COORDINATION OF OPTICALLY-ACTIVE AMINO  
ACIDS AND THEIR DERIVATIVES TO COBALT(III)

*Iowa State University*

PH.D.

1980

University  
Microfilms  
International

300 N. Zeeb Road, Ann Arbor, MI 48106

18 Bedford Row, London WC1R 4EJ, England

Stereoselective coordination of optically active  
amino acids and their derivatives to cobalt(III)

by

Larry Alan Meiske

A Dissertation Submitted to the  
Graduate Faculty in Partial Fulfillment of the  
Requirements for the Degree of  
DOCTOR OF PHILOSOPHY

Department: Chemistry  
Major: Inorganic Chemistry

Approved:

Signature was redacted for privacy.

In Charge of Major Work

Signature was redacted for privacy.

For the Major Department

Signature was redacted for privacy.

For the Graduate College

Iowa State University  
Ames, Iowa

1980

## TABLE OF CONTENTS

	Page
GENERAL INTRODUCTION	1
Explanation of Dissertation Format	6
SECTION I. SYNTHESIS, SPECTRAL CHARACTERIZATION AND MOLECULAR STRUCTURE OF [N-(2- Pyridylmethyl)-L-aspartato][L- phenylalaninato]cobalt(III) trihydrate, [Co(PLASP) (L-Phe)] · 3H <sub>2</sub> O	7
INTRODUCTION	8
EXPERIMENTAL SECTION	11
RESULTS AND DISCUSSION	22
CONCLUSION	36
REFERENCES	38
SECTION II. SYNTHESIS AND SPECTRAL CHARAC- TERIZATION OF THE MIXED LIGAND COMPLEXES, [N-(2-Pyridylmethyl)- L-aspartato][amino acidato]- cobalt(III), Co(PLASP)(AA)	41
INTRODUCTION	42
EXPERIMENTAL SECTION	45
RESULTS AND DISCUSSION	52
CONCLUSION	79
REFERENCES	81

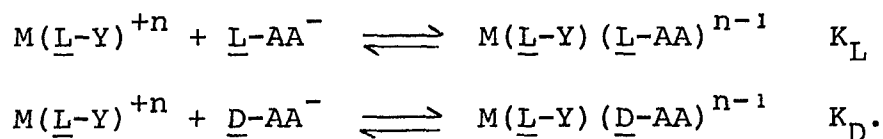
	Page
SECTION III. SYNTHESIS AND SPECTRAL CHARACTERIZATION OF fac- AND mer-[N-Carboxymethyl-L-β-(2-pyridyl)-α-alaninato][D-threoninato]cobalt(III), Co(N-Cm-L-Pyala)-(D-Thr) AND THE MOLECULAR STRUCTURE OF THE mer- ISOMER	82
INTRODUCTION	83
EXPERIMENTAL SECTION	86
RESULTS AND DISCUSSION	102
CONCLUSION	119
REFERENCES	121
SECTION IV. SYNTHESIS AND SPECTRAL CHARACTERIZATION OF THE MIXED LIGAND COMPLEXES, [N-Carboxymethyl-L-β-(2-pyridyl)-α-alaninato]-[amino acidato]cobalt(III), Co(N-Cm-L-Pyala)(AA)	124
INTRODUCTION	125
EXPERIMENTAL SECTION	130
RESULTS AND DISCUSSION	139
CONCLUSION	163
REFERENCES	168

	Page
SECTION V. SYNTHESIS AND SPECTRAL CHARACTERIZATION OF THE MIXED LIGAND COMPLEXES, [N-Carboxymethyl-L-histidinato][amino acidato]-cobalt(III), Co(N-Cm-L-Hist)(AA)	169
INTRODUCTION	170
EXPERIMENTAL SECTION	173
RESULTS AND DISCUSSION	179
CONCLUSION	203
REFERENCES	210
SUMMARY	211
LITERATURE CITED	220
ACKNOWLEDGEMENTS	221

## GENERAL INTRODUCTION

Ever since chemists resolved their first pair of enantiomers they have been searching for faster, simpler and more selective methods of achieving resolution. Synthetic chemists have used optically active compounds such as tartaric acid and brucine to selectively precipitate only one enantiomer out of solution. Enzymes have been used by biochemists to selectively degrade or metabolize only one enantiomer leaving the other unaffected. Analytical chemists have used optically active supports to separate enantiomers by chromatography. Optically active metal complexes have been used by inorganic chemists to selectively coordinate one enantiomer over the other. It is this latter use of enantioselectivity that is the major concern in the work presented here.

Enantioselectivity is used to define the difference in the interaction (or coordination) of a chiral center (or complex) with two optical isomers. Experimentally, enantioselectivity is detected by a difference in the two equilibrium constants,  $K_L$  and  $K_D$  for the reactions,





If  $K_L > K_D$  the  $M(\underline{L}-Y)^{+n}$  complex selectively coordinates  $\underline{L}-AA^-$  while the  $M(\underline{D}-Y)^{+n}$  complex selectively coordinates the  $\underline{D}-AA^-$  if  $K_D > K_L$ .

Enantioselectivity has been observed in several mixed ligand complexes where Y is a tetradentate ligand, M is a labile transition metal ion and  $AA^-$  is a bidentate amino acidate. For example, the Ni(II) and Cu(II) complexes of the N-(6-methyl-2-pyridylmethyl)- $\underline{L}$ -aspartate, 6MPLASP $^{2-}$  and N-(2-pyridylmethyl)- $\underline{L}$ -aspartate, PLASP $^{2-}$ , ligands (Figure 1) exhibit a stronger preference for coordinating an  $\underline{L}$ -amino acidate than a  $\underline{D}$ -amino acidate.<sup>1</sup> This was rationalized by assuming that the complex had the geometry shown in Figure 2a. In this structure the bulky R-group of an  $\underline{L}$ -amino acidate would not interact sterically with the carboxylate group trans to the pyridine and thus coordinate normally. On the other hand, the bulky R-group of a  $\underline{D}$ -amino acidate would interact sterically with the bulky pyridyl group and thus reduce the interaction between itself and the metal ion. The Ni(II) complexes of the N-carboxymethyl- $\underline{L}$ - $\beta$ -(2-pyridyl)- $\alpha$ -alaninate, N-Cm- $\underline{L}$ -Pyala $^{2-}$  (Figure 1), were observed to preferentially coordinate  $\underline{D}$ -amino acidates over their  $\underline{L}$ -enantiomers by a factor of  $\sim 4$ .<sup>2</sup> As for the 6MPLASP $^{2-}$  and PLASP $^{2-}$  ligands above,

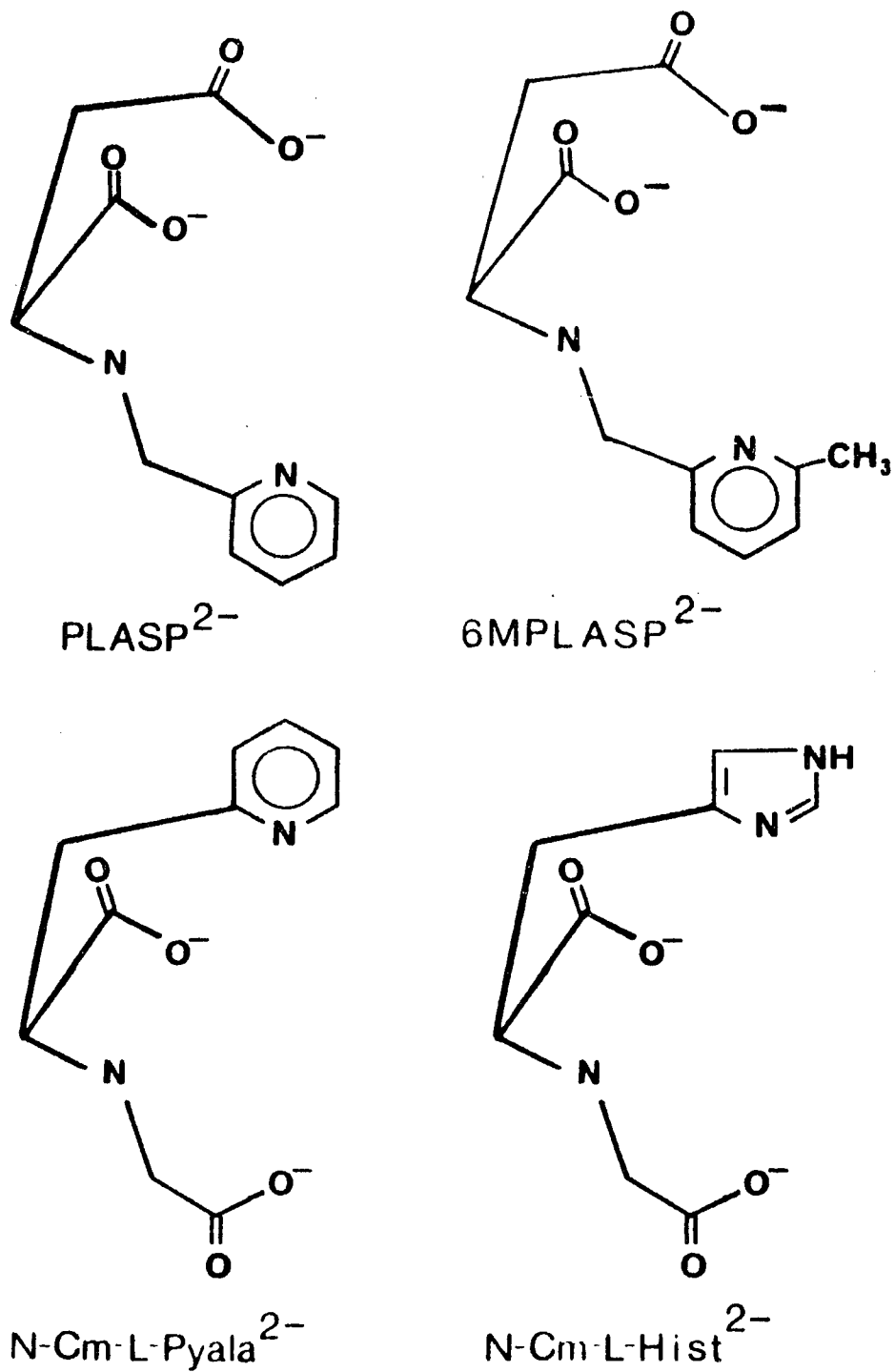


Figure 1. Various optically active tetradentate ligands.

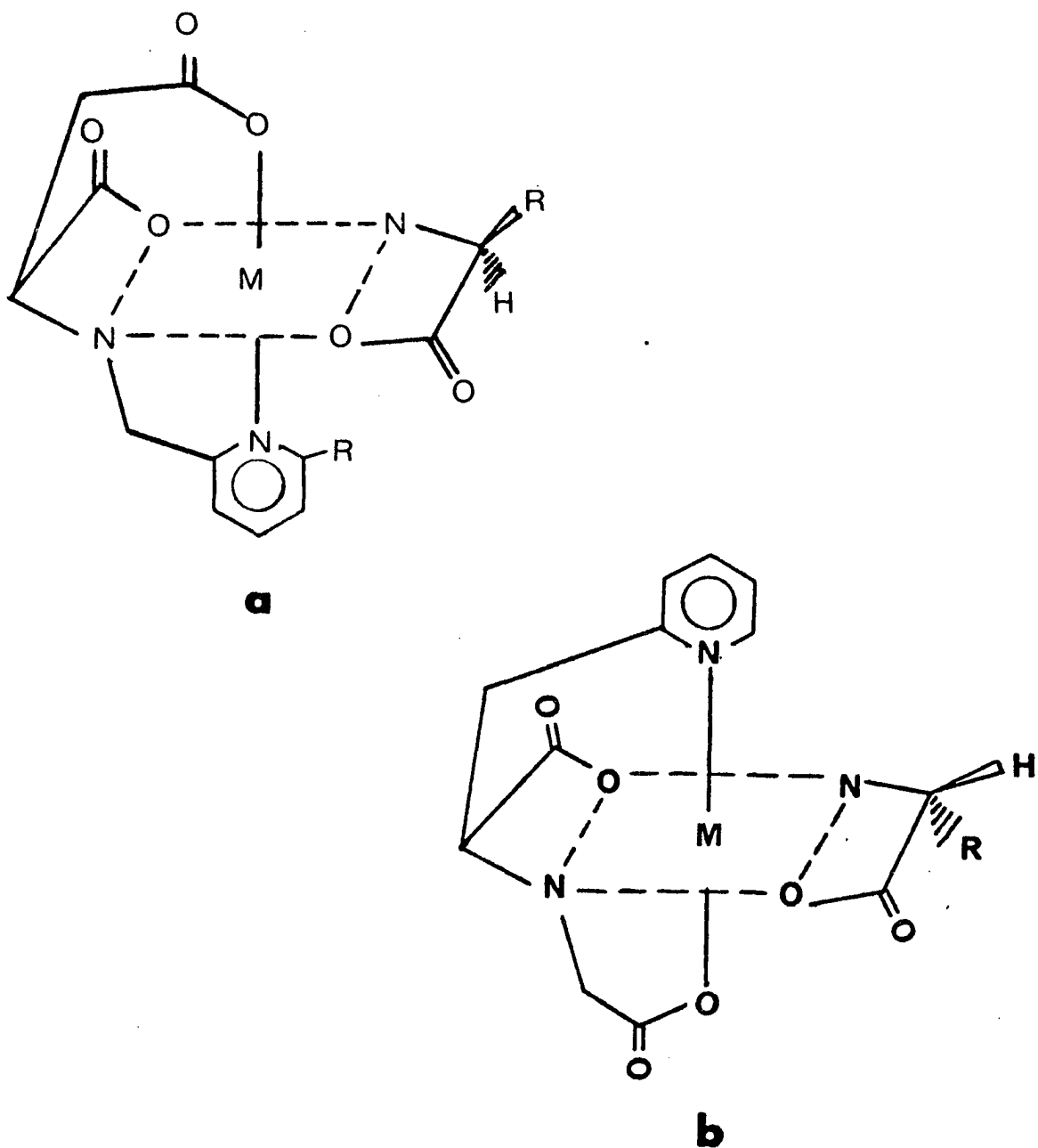


Figure 2. Proposed structures for a)  $R = H$ ,  $M(\text{PLASP})(\underline{L}\text{-AA})$  and  $R = \text{CH}_3$ ,  $M(\text{6MPLASP})(\underline{L}\text{-AA})$  and b)  $M(\text{N-Cm-L-Pyala})(\underline{D}\text{-AA})$

this was rationalized by the assumption that the mixed Ni(II) complexes have the structure shown in Figure 2b. In this structure the R-group of the L-amino acidate should interact sterically with the bulky pyridyl group and thus coordinate more weakly to the metal ion than a D-amino acidate.

In the discussion of these mixed ligand complexes only steric factors (interaction of bulky groups) were considered. However, other factors such as electronic and structural effects may also play a role in determining the overall geometry of these mixed ligand complexes. Electronic factors may be important in determining which mode of coordination, such as trans amino or amino trans to carboxylate, is preferred. Structural factors also may eliminate certain modes of coordination due to chelate ring or angular strain. Thus, our purpose was to examine the role of electronic, structural and steric factors on the overall geometry of these mixed ligand complexes.

In the present work the kinetically stable Co(III)-(Y)(AA) complexes, where Y is either PLASP<sup>2-</sup>, N-Cm-L-Pyala<sup>2-</sup> or N-Cm-L-Hist<sup>2-</sup> (Figure 1) and AA<sup>-</sup> is a bidentate amino acidate, were prepared. These Co(III)N<sub>3</sub>O<sub>3</sub> complexes were

characterized by various analytical techniques. The most valuable techniques were visible, circular dichroism,  $^{13}\text{C}$  nmr and  $^1\text{H}$  nmr spectroscopy and three dimensional X-ray crystallography. By comparing the structures of the various Co(III)(Y)(AA) complexes we hoped to establish trends in their structures and to understand factors which determine their overall geometries.

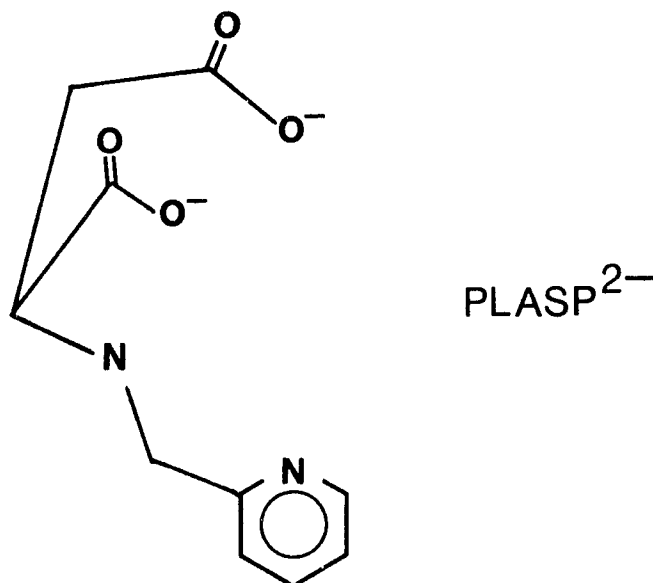
#### Explanation of Dissertation Format

The material in this dissertation is organized so that each section represents a manuscript suitable for publication. The numbering of figures and tables applies to only those contained within that section. The literature references cited in the General Introduction are given at the end under Literature Cited.

SECTION I. SYNTHESIS, SPECTRAL CHARACTERIZATION AND  
MOLECULAR STRUCTURE OF [N-(2-Pyridylmethyl)-  
L-aspartato][L-phenylalaninato]cobalt(III)-  
trihydrate, [Co(PLASP)(L-Phe)]·3H<sub>2</sub>O

## INTRODUCTION

Studies in this laboratory have shown that metal complexes of certain asymmetric tetradentate ligands exhibit stereoselective effects in coordinating optically active amino acids.<sup>1,2</sup> In order to better understand these effects, we have synthesized a series of mixed complexes of the type  $\text{Co}(\text{PLASP})^2-(\text{AA})$ , where  $\text{PLASP}^{2-}$  is the dianion of the tetradentate (N-2-pyridylmethyl)-L-aspartic acid ligand and  $\text{AA}^-$  is the anion of one of the



following amino acids: D or L-phenylalanine, D, D,L, or L-valine, L-alanine, L-threonine, L-proline, glycine and  $\alpha$ -aminoisobutyric acid.<sup>3</sup> Although there are four possible geometrical isomers (Figure 1) of these complexes, only

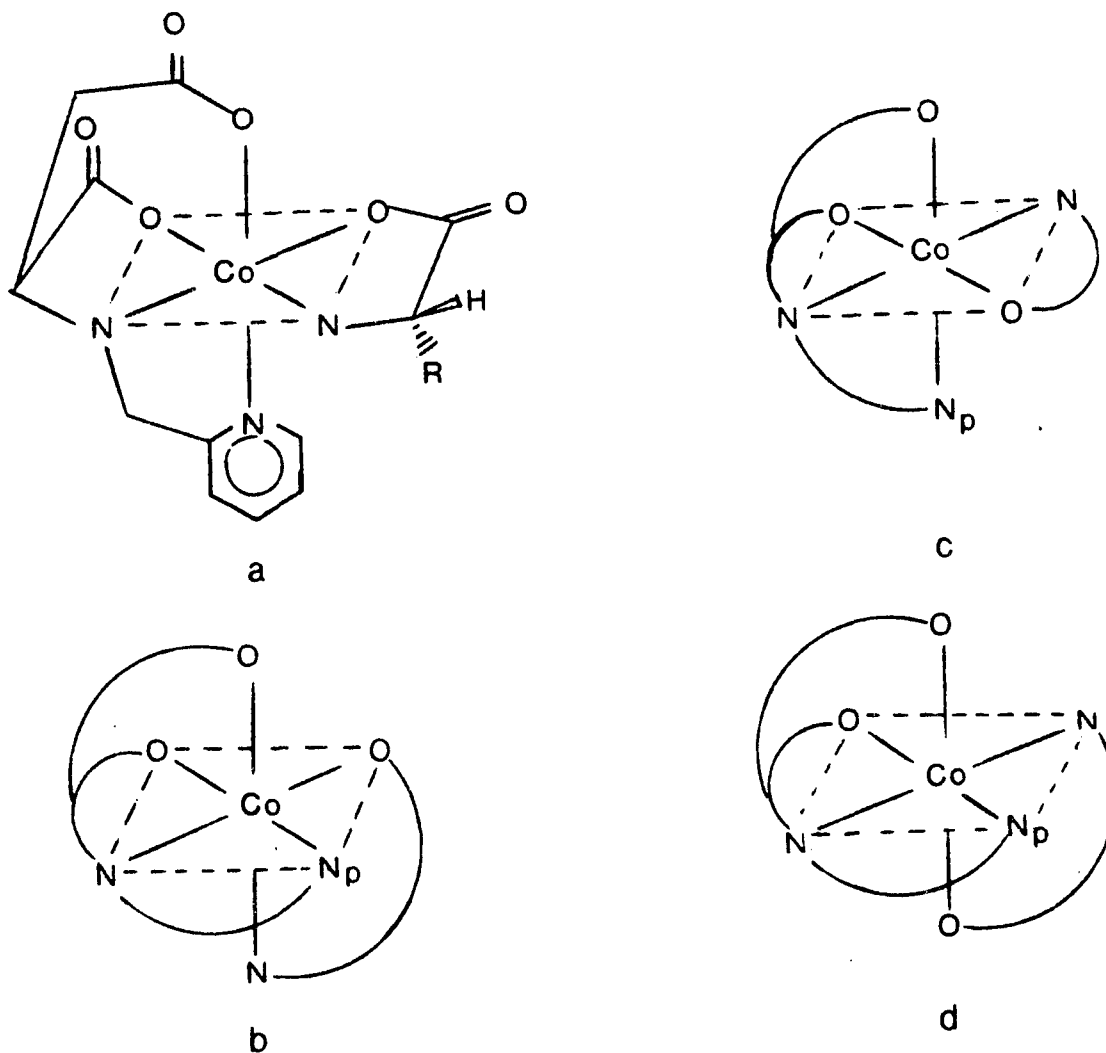


Figure 1. Four possible geometrical isomers of  $\text{Co(PLASP)(AA)}$ :  
 (a)  $\text{fac } \beta\text{-CO}_2^-$  trans to py, (b)  $\text{fac } \alpha\text{-CO}_2^-$  trans to py, (c)  $\text{mer } \beta\text{-CO}_2^-$  trans to py and (d)  $\text{mer } \alpha\text{-CO}_2^-$  trans to py



one was isolated for all the amino acids listed above. The visible spectra of these complexes, when compared to the spectra of various  $\text{Co(III)N}_3\text{O}_3$  complexes reported in the literature, support a facial arrangement of the oxygen (or nitrogen) atoms around the cobalt (Figures 1a and 1b).<sup>4-6</sup> Since the CD and  $^1\text{H}$  nmr spectra do not fully determine the type of facial isomer present, an X-ray structure analysis of  $[\text{Co(PLASP)(L-Phe)}] \cdot 3\text{H}_2\text{O}$  was undertaken. The synthesis and spectra of this complex are also reported herein.

## EXPERIMENTAL SECTION

Preparation of N-(2-pyridylmethyl)-L-aspartic acid, PLASPH<sub>2</sub> The synthesis given below is an improvement over that reported previously.<sup>1</sup> To a slurry of L-aspartic acid (53.2 g, 400 mmol) in 150 ml of water, 4N NaOH was added at room temperature until the pH reached 9.7-9.8. The pH increased to 10.1-10.2 after the solution was placed in an ice bath. Next a solution of 2-pyridine-carboxaldehyde (21.4 g, 200 mmol) in 20 ml of water was added dropwise over a period of 1 hour to give a pH of 9.6. After stirring for an additional hour, NaBH<sub>4</sub> (3.1 g, 80 mmol) dissolved in 20 ml water was added dropwise over 30 minutes. The pH of the solution was slowly brought back to 9.6 with 6N HCl. The solution was then stirred for 2 hours, and more NaBH<sub>4</sub> (3.1 g, 80 mmol) in 20 ml of water was added dropwise. After stirring overnight, the solution was brought to pH 3.2 with 6N HCl, and the unreacted aspartic acid was filtered off. The solution volume was reduced under vacuum until a solid formed. This solid was filtered; continued reduction of the filtrate gave additional fractions of solid. Each solid fraction was treated with 500-600 ml of boiling methanol and filtered. The methanol solutions were combined and taken to dryness

under vacuum. The resulting impure PLASPH<sub>2</sub> was dissolved in 300 ml of water and placed on a 3.6 X 60 cm column of Dowex 50W-X8 (50-100 mesh) ion exchange resin in the H<sup>+</sup> form. After washing the column with two liters of water, the product was eluted with 0.4N NH<sub>4</sub>OH, and 18 ml fractions were collected. The fractions with a pH between 3 and 4.5 were combined and reduced under vacuum to 100 ml. Next, 500 ml of absolute ethanol was added and the solution placed in a freezer at -10° C overnight. Twenty-three grams of product were obtained with another 2 g of product obtained by reducing the solution and adding absolute ethanol a second time. The total yield was 25 g (57%).

Preparation of [N-(2-pyridylmethyl)-L-aspartato]-  
[L-phenylalaninato]cobalt(III) trihydrate, [Co(PLASP)-  
(L-Phe)]·3H<sub>2</sub>O To a solution of N-(2-pyridylmethyl)-L-aspartic acid (2.24 g, 10 mmol) and NaOH (0.74 g, 18.5 mmol) in 30 ml of water, a solution of CoSO<sub>4</sub>·7H<sub>2</sub>O (2.81 g, 10 mmol) and 1.4 ml 30% H<sub>2</sub>O<sub>2</sub> was added. The resulting dark red-brown solution was stirred for 10 minutes, and a solution of L-phenylalanine (1.65 g, 10 mmol) and NaOH (0.16 g, 4 mmol) in 45 ml of water was added. The solution initially turned dark brown in color and slowly turned purple over a period of 1.5 hours. After stirring overnight, 1 ml of 30% H<sub>2</sub>O<sub>2</sub> in 10 ml of water was added to ensure

complete oxidation of the Co(II) to Co(III). This was followed by the addition of 2.5 ml of 1N H<sub>2</sub>SO<sub>4</sub>. The solution was heated to 45° C for 1 hour and filtered. The filtrate was carefully reduced under vacuum to a 50 ml volume. Half of this solution was placed on a 4.5 X 45 cm alumina column and eluted with water to give a brown band consisting of decomposition products and a red band containing the product. This red solution was reduced under vacuum to 100 ml and left standing for several days to give red-violet crystals suitable for X-ray analysis. The crystals were filtered and dried in vacuum. The yield of [Co(PLASP)-(L-Phe)]·3H<sub>2</sub>O was 16%. Anal. calcd. for [Co(PLASP)-(L-Phe)]·3H<sub>2</sub>O, C<sub>19</sub>H<sub>20</sub>N<sub>3</sub>O<sub>6</sub>Co·3H<sub>2</sub>O: C, 45.70; H, 5.21; N, 8.37. Found: C, 45.59; H, 5.33; N, 8.41.

Spectra The visible spectra were recorded in water at room temperature using a Jasco ORD/UV/CD-5 spectrophotometer. The <sup>1</sup>H nmr spectra were measured using a Varian Associates HA-100 spectrometer in 99.7% deuterium oxide vs t-butyl alcohol (δ 1.23) as an internal standard and trifluoroacetic acid as an external lock. Because of its low solubility in water, the <sup>1</sup>H nmr of [Co(PLASP)-(L-Phe)]·3H<sub>2</sub>O was accumulated using a Nicolet Instrument Corporation Model 535 Signal Averager. The chemical shifts are reported in ppm downfield from TMS.

Crystal data The crystals were obtained directly from the preparation in the form of red prismatic bars. A crystal with approximate dimensions of 0.1 X 0.2 X 0.4 mm was mounted on the end of a glass fiber, long dimension along the fiber axis, with epoxy glue and the fiber subsequently placed in a standard goniometer head. The goniometer was placed on an automatic four-circle X-ray diffractometer and three initial  $\omega$ -oscillation photographs were taken at various  $\chi$  and  $\phi$  settings using a Polaroid cassette. From these photographs, twelve independent reflections were selected and their coordinates<sup>5</sup> were input to the automatic indexing program ALICE.<sup>7</sup> The reduced cell and reduced cell scalars that resulted from ALICE indicated an orthorhombic crystal system. The  $\omega$ -oscillation photographs around each of the three axes subsequently taken verified the presence of mmm Laue symmetry. The observed layer line spacings agreed with the spacings predicted for the cell by the indexing program. A least-squares refinement of the lattice constants based on the  $\pm 2\theta$  measurements of 15 high-angle reflections on a previously aligned four-circle diffractometer (graphite-monochromated Mo K $_{\alpha}$  radiation,  $\lambda = 0.70954 \text{ \AA}$ ) at 25° C, yielded  $a = 9.821 (3)$ ,  $b = 23.069 (4)$ , and  $c = 9.564 (2) \text{ \AA}$ . The observed density is 1.5 g/cm<sup>3</sup> by the flotation method, and the calculated density is 1.53 g/cm<sup>3</sup>.

Collection and reduction of X-ray intensity data

Data were collected at room temperature using an automated four-circle diffractometer designed and built in the Ames Laboratory.<sup>8</sup> An  $\omega$  step-scan technique was used to measure all data within a  $2\theta$  sphere of  $50^\circ$  ( $\sin \theta/\lambda = 0.596 \text{ \AA}^{-1}$ ) in two octants. To check on the electronic and crystal stability, the intensities of three standard reflections were remeasured every 75 reflections. The intensities of these standard reflections did not vary significantly during the collection of 4445 reflections. Examination of the data revealed systematic extinctions for  $h00$ ,  $h = 2n + 1$ ,  $0k0$ ,  $k = 2n + 1$ , and  $00l$ ,  $l = 2n + 1$ , thus uniquely determining the space group to be  $P2_1^2 2_1 2_1$ .

The measured intensity data were corrected for Lorentz-polarization effects, but no absorption correction was made since the minimum and maximum transmission factors were 0.84 and 0.92 ( $\mu = 8.84 \text{ cm}^{-1}$ ). The estimated variance in each intensity was calculated by  $\sigma_I^2 = C_T + K_t C_B + (0.03 C_T)^2 + (0.03 C_B)^2$  where  $C_T$  and  $C_B$  represent the total and background count, respectively,  $K_t$  is a counting time constant, and the factor 0.03 represents an estimate of nonstatistical errors. The estimated standard deviations in the structure factors were calculated by the method of

finite differences.<sup>9</sup> Equivalent reflections were averaged and yielded 1,993 reflections with  $|F_o| > 3\sigma_{F_o}$  which were retained for use in subsequent calculations.

Solution and refinement The position of the cobalt atom was obtained by analysis of a sharpened three-dimensional Patterson function. The remaining atoms were found by successive structure factor<sup>10</sup> and electron density map calculations.<sup>11</sup> Before final refinement, it was observed that large reflections suffered from secondary extinctions effects. These effects were corrected by the approximation  $I_o' = I_o / (1 + gI_c)$ , where  $g$  was computed from seven of the largest reflections. The positional parameters for all the non-hydrogen atoms and their anisotropic thermal parameters were refined by a full-matrix least-squares procedure<sup>10</sup> minimizing the function  $\sum w(|F_o| - |F_c|)^2$ , where  $w = 1/\sigma_F^2$ , to a final conventional residual index of  $R = \sum ||F_o| - |F_c|| / \sum |F_o| = 0.059$ . The scattering factors used were those of Hanson, et al.,<sup>12</sup> modified for the real part of anomalous dispersion.<sup>13</sup>

The final positional and thermal parameters are given in Table I. The standard deviations were calculated from the inverse matrix of the final least-squares cycle.<sup>14</sup> Bond lengths and angles are given in Tables II and III.

Table I. Final atomic parameters

(a) Final positional parameters ( $\times 10^4$ ) and their estimated standard deviations (in parentheses)<sup>a</sup>

Atom	x	y	z
Co	4407 (1)	5126.4 (4)	5229 (1)
O1	5252 (6)	5575 (2)	6664 (6)
O2	6362 (7)	6408 (2)	6951 (7)
O3	3063 (5)	5712 (2)	4925 (6)
O4	2262 (7)	6580 (3)	4403 (9)
O5	3144 (5)	4771 (2)	6458 (5)
O6	1095 (5)	4373 (3)	6508 (7)
O7	5833 (10)	4273 (5)	1997 (14)
O8	-429 (8)	6354 (4)	4648 (9)
O9	7833 (10)	7230 (3)	5461 (11)
N1	5663 (7)	5505 (2)	3980 (7)
N2	5779 (6)	4550 (3)	5496 (6)
N3	3537 (6)	4686 (3)	3782 (7)
C1	5845 (8)	6019 (3)	6207 (9)
C2	5837 (8)	6101 (3)	4630 (10)
C3	4634 (9)	6468 (3)	4152 (10)
C4	3220 (9)	6246 (4)	4527 (10)
C5	7015 (8)	5188 (4)	3929 (11)
C6	6972 (7)	4658 (3)	4786 (10)
C7	8061 (9)	4286 (4)	4874 (12)
C8	7966 (10)	3802 (4)	5763 (11)
C9	6758 (10)	3709 (4)	6485 (10)
C10	5695 (9)	4087 (3)	6332 (9)

<sup>a</sup>The positional parameters are presented in fractional unit cell coordinates.



Table I. (continued)

Atom	x	y	z
C11	2107 (8)	4528 (3)	5860 (8)
C12	2169 (8)	4454 (3)	4285 (8)
C13	1904 (8)	3838 (3)	3797 (10)
C14	2922 (9)	3399 (3)	4291 (9)
C15	3933 (10)	3190 (4)	3353 (12)
C16	4883 (12)	2786 (5)	3781 (14)
C17	4879 (11)	2579 (4)	5098 (17)
C18	3881 (10)	2784 (4)	6079 (14)
C19	2929 (10)	3195 (4)	5658 (10)

(b) Final thermal parameters ( $\times 10^4$ ) and their estimated standard deviations (in parentheses)<sup>b</sup>

Atom	$\beta_{11}$	$\beta_{22}$	$\beta_{33}$	$\beta_{12}$	$\beta_{13}$	$\beta_{23}$
Co	54 (1)	9.0(0.2)	59 (1)	0 (0.3)	7 (1)	0.5(0.4)
O1	80 (7)	14 (1)	64 (6)	-5 (2)	-1 (5)	-1 (2)
O2	130 (9)	17 (1)	123 (9)	-21 (3)	-9 (8)	-10 (3)
O3	71 (6)	11 (1)	107 (8)	4 (2)	-3 (6)	5 (2)
O4	99 (8)	16 (1)	246 (15)	13 (3)	22 (10)	17 (4)
O5	55 (5)	16 (1)	60 (6)	-4 (2)	2 (5)	1 (2)
O6	56 (6)	26 (2)	104 (8)	-6 (3)	29 (6)	-4 (3)
O7	256 (18)	46 (3)	388 (25)	-13 (7)	-107 (19)	59 (8)

<sup>b</sup>The  $\beta_{ij}$  are defined by:  $T = \exp\{-(h^2\beta_{11} + k^2\beta_{22} + l^2\beta_{33} + 2hk\beta_{12} + 2hl\beta_{13} + 2kl\beta_{23})\}$ .

Table I. (continued)

Atom	$\beta_{11}$	$\beta_{22}$	$\beta_{33}$	$\beta_{12}$	$\beta_{13}$	$\beta_{23}$
O8	153 (10)	45 (2)	141 (11)	-22 (4)	-11 (11)	-6 (5)
O9	221 (13)	20 (2)	330 (20)	-13 (4)	76 (16)	8 (5)
N1	66 (7)	9 (1)	84 (8)	4 (3)	11 (8)	-1 (2)
N2	53 (7)	12 (1)	73 (8)	-3 (2)	-1 (6)	-2 (2)
N3	55 (7)	13 (1)	56 (7)	-7 (2)	5 (6)	-3 (2)
C1	61 (9)	14 (2)	76 (9)	1 (3)	-7 (8)	0 (3)
C2	76 (9)	11 (1)	93 (10)	-1 (3)	-1 (9)	-3 (3)
C3	90 (10)	13 (2)	103 (11)	-1 (3)	-10 (10)	5 (3)
C4	96 (10)	13 (2)	81 (11)	8 (3)	-3 (9)	1 (4)
C5	73 (9)	18 (2)	142 (13)	7 (4)	37 (10)	7 (4)
C6	55 (7)	14 (1)	93 (10)	4 (3)	-5 (9)	-6 (4)
C7	91 (10)	32 (2)	134 (14)	18 (4)	17 (12)	0 (5)
C8	85 (10)	18 (2)	127 (13)	14 (4)	-12 (10)	0 (4)
C9	114 (12)	15 (2)	93 (11)	4 (4)	-38 (11)	4 (4)
C10	87 (10)	11 (1)	93 (10)	6 (3)	-9 (10)	-3 (3)
C11	66 (9)	10 (1)	75 (9)	3 (3)	14 (8)	0 (3)
C12	48 (8)	14 (2)	57 (8)	1 (3)	5 (7)	0 (3)
C13	58 (8)	12 (1)	112 (11)	-5 (3)	-15 (9)	-4 (3)
C14	77 (9)	13 (2)	98 (11)	-7 (3)	11 (9)	-3 (3)
C15	112 (12)	20 (2)	162 (16)	2 (4)	45 (12)	-12 (5)
C16	125 (14)	20 (2)	206 (21)	10 (5)	27 (15)	-8 (6)
C17	136 (14)	16 (2)	220 (20)	7 (4)	1 (16)	-10 (6)
C18	98 (11)	19 (2)	213 (19)	-1 (4)	-24 (14)	12 (6)
C19	91 (10)	14 (2)	127 (13)	-6 (4)	-11 (10)	11 (4)

Table II. Interatomic distances ( $\text{\AA}$ ) and their estimated standard deviations (in parentheses)

Co-O1	1.909 (5)	C10-N2	1.34 (1)
Co-O3	1.911 (5)	C6-C7	1.37 (1)
Co-O5	1.896 (5)	C7-C8	1.41 (1)
Co-N1	1.926 (6)	C8-C9	1.39 (1)
Co-N2	1.910 (6)	C10-C9	1.37 (1)
Co-N3	1.919 (6)	C11-O5	1.295 (9)
C1-O1	1.257 (9)	C11-O6	1.225 (9)
C1-O2	1.253 (9)	C12-C11	1.52 (1)
C4-O3	1.298 (9)	C13-C12	1.52 (1)
C4-O4	1.22 (1)	C12-N3	1.523 (9)
C1-C2	1.52 (1)	C14-C13	1.50 (1)
C2-C3	1.52 (1)	C14-C15	1.42 (1)
C2-N1	1.518 (9)	C14-C19	1.39 (1)
C5-N1	1.52 (1)	C15-C16	1.38 (1)
C3-C4	1.52 (1)	C16-C17	1.34 (2)
C5-C6	1.47 (1)	C17-C18	1.44 (2)
C6-N2	1.377 (9)	C18-C19	1.39 (1)
O4-O8	2.70 (1)	O7-N3	2.98 (1)
O2-O9	2.78 (1)	O7 <sup>a</sup> -O8 <sup>b</sup>	2.70 (1)
O9-O4 <sup>c</sup>	2.808 (1)	O8 <sup>d</sup> -O9	2.76 (1)
O6-N1 <sup>e</sup>	2.98 (1)		

<sup>a</sup>Symmetry operation  $x, y, 1 + z$ .

<sup>b</sup>Symmetry operation  $1/2 - x, 1 - y, 1/2 + z$ .

<sup>c</sup>Symmetry operation  $1/2 + x, 1 1/2 - y, 1 - z$ .

<sup>d</sup>Symmetry operation  $1 + x, y, z$ .

<sup>e</sup>Symmetry operation  $1/2 - x, 1 - y, 1/2 + z$ .

Table III. Bond angles (deg) and their estimated standard deviations (in parentheses)

O1-Co-O3	91.5 (2)	N1-C2-C3	107.1 (7)
O1-Co-O5	94.2 (2)	C1-C2-C3	111.8 (7)
O1-Co-N1	85.5 (2)	C2-C3-C4	116.6 (7)
O1-Co-N2	88.6 (2)	O3-C4-O4	122.4 (8)
O3-Co-O5	87.0 (2)	O3-C4-C3	119.9 (7)
O3-Co-N1	91.6 (2)	O4-C4-C3	117.7 (7)
O3-Co-N3	87.5 (3)	N1-C5-C6	110.9 (6)
O5-Co-N2	94.5 (3)	N2-C6-C5	116.7 (7)
O5-Co-N3	85.8 (2)	N2-C6-C7	121.2 (8)
N1-Co-N2	86.9 (3)	C5-C6-C7	122.1 (8)
N1-Co-N3	94.5 (3)	C6-C7-C8	118.8 (9)
N2-Co-N3	92.4 (3)	C7-C8-C9	118.6 (8)
O1-Co-N3	179.0 (3)	C8-C9-C10	120.0 (8)
O3-Co-N2	178.5 (3)	C9-C10-N2	121.7 (8)
O5-Co-N1	178.5 (3)	O5-C11-O6	122.8 (7)
Co-O1-C1	113.2 (5)	O5-C11-C12	117.1 (7)
Co-O3-C4	129.2 (5)	O6-C11-C12	120.1 (8)
Co-O5-C11	115.3 (5)	N3-C12-C11	108.1 (7)
Co-N1-C2	103.2 (5)	N3-C12-C13	112.4 (6)
Co-N1-C5	111.2 (5)	C11-C12-C13	113.8 (7)
Co-N2-C10	126.3 (5)	C12-C13-C14	114.9 (7)
Co-N2-C6	114.1 (5)	C13-C14-C15	119.7 (8)
Co-N3-C12	110.5 (5)	C13-C14-C19	121.9 (8)
C2-N1-C5	110.6 (6)	C15-C14-C19	118.4 (9)
C6-N2-C10	119.5 (7)	C14-C15-C16	121 (1)
O1-C1-O2	125.1 (8)	C15-C16-C17	121 (1)
O1-C1-C2	116.3 (7)	C16-C17-C18	120 (1)
O2-C1-C2	118.5 (8)	C17-C18-C19	120 (1)
N1-C2-C1	107.1 (7)	C14-C19-C18	120 (1)

## RESULTS AND DISCUSSION

Description and discussion of the structure The crystal structure of  $[\text{Co}(\text{PLASP})(\underline{\text{L}}\text{-Phe})] \cdot 3\text{H}_2\text{O}$  consists of discrete molecules having a slightly distorted octahedral coordination geometry around the cobalt atom. All three waters (07, 08, 09) of hydration provide crystalline stability by forming strong hydrogen bonds between complexes in neighboring unit cells and asymmetric units. The various hydrogen bonds are given in Table II. Strong interactions occur between the carboxylate oxygen, 02, the water molecule, 09, and the carboxylate oxygen, 04, of a neighboring asymmetric unit  $(1/2 + x, 1/2 - y, 1 - z)$ . Other hydrogen bonding interactions connecting various asymmetric units involve a series of three hydrogen bonds such as  $04(1 + x, y, z) \cdots 08(1 + x, y, z) \cdots 09 \cdots 02$ . Additional crystalline stability is provided by the weaker hydrogen bond between 06 and N1 of an adjacent unit  $(1/2 - x, 1 - y, 1/2 + z)$ . The atoms are labeled as shown in Figure 2. A stereographic view of the unit cell and adjacent moieties of  $[\text{Co}(\text{PLASP}) - (\underline{\text{L}}\text{-Phe})] \cdot 3\text{H}_2\text{O}$  is presented in Figure 3.

The coordination about the cobalt atom can be considered to be facial, since the three carboxylate oxygens (01, 03, 05) occupy one triangular face of the coordination

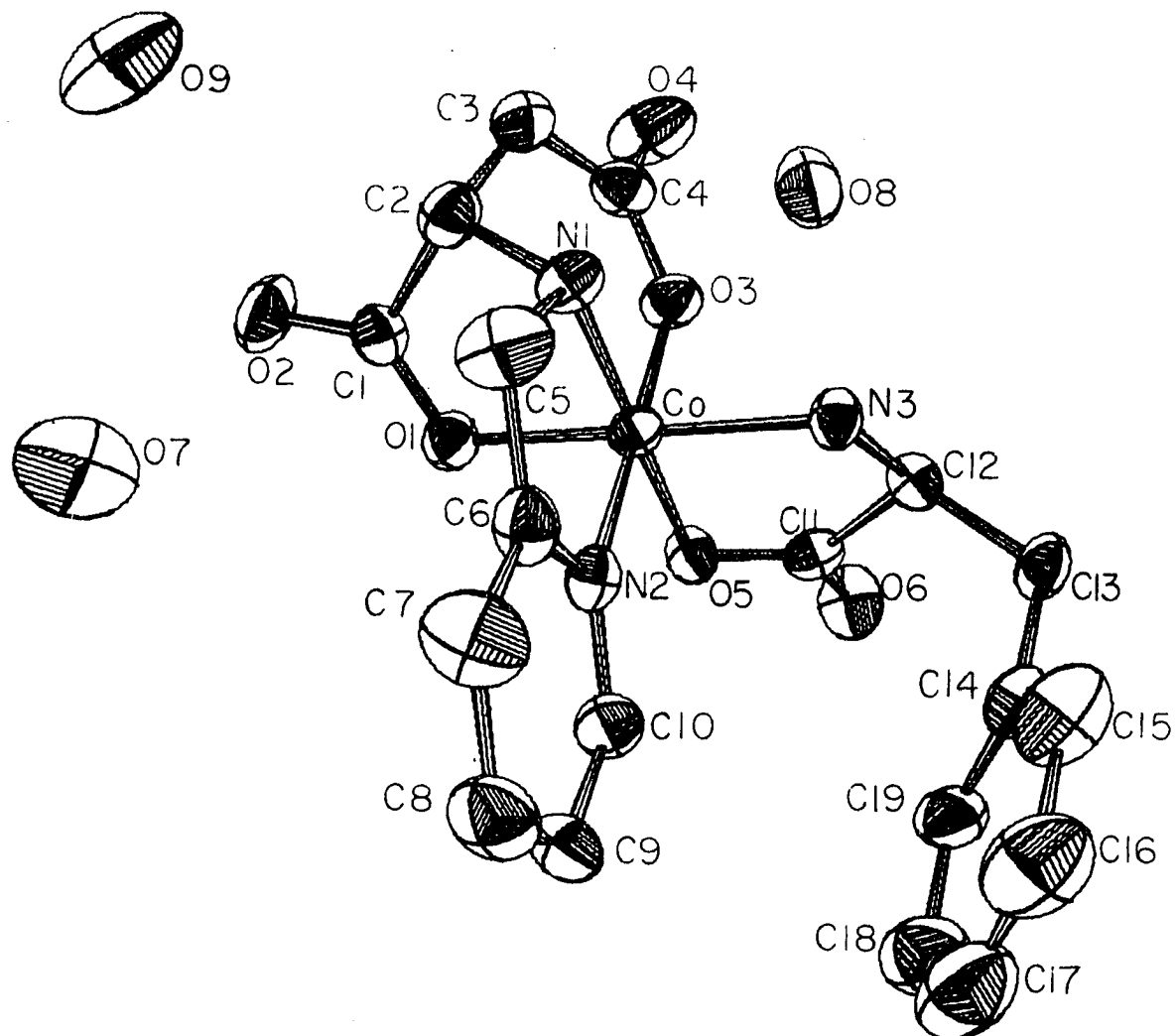


Figure 2. Structure of  $[\text{Co}(\text{PLASP})(\underline{\text{L}}\text{-Phe})] \cdot 3\text{H}_2\text{O}$

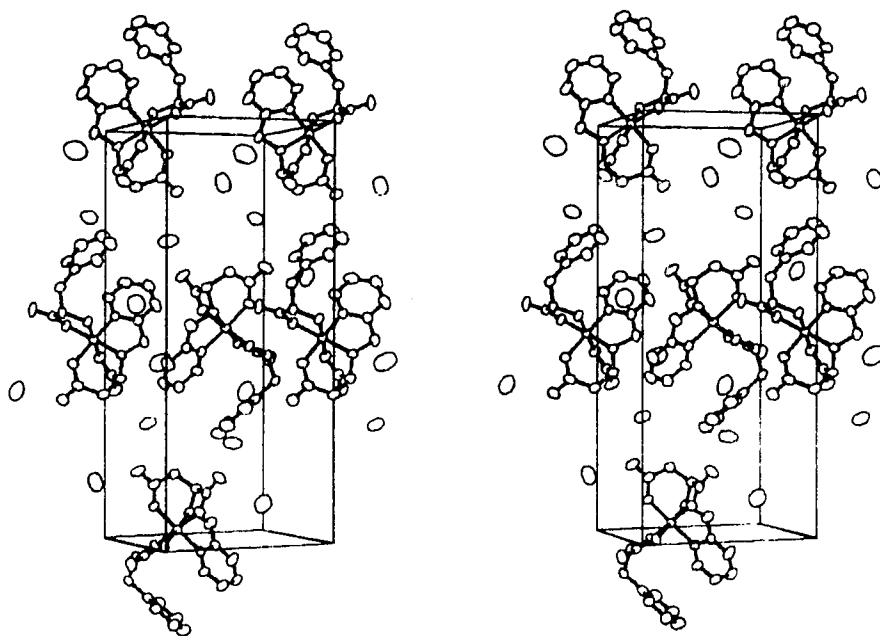


Figure 3. Stereoscopic view of the unit cell with the a axis horizontal and the b axis vertical

octahedron, and the three nitrogen atoms (N1, N2, N3) occupy another face. The L-aspartic acid portion of the PLASP<sup>2-</sup> ligand is facially coordinated to the cobalt atom through its  $\alpha$ -amino nitrogen (N1),  $\alpha$ -carboxylate oxygen (O1) and  $\beta$ -carboxylate oxygen (O3). This mode of coordination is similar to that found for various bis-L-aspartato cobalt(III) complexes previously reported in the literature.<sup>15,16</sup> The N-2-pyridylmethyl group is attached to the cobalt atom through the pyridine nitrogen (N2) and occupies a position trans to the  $\beta$ -carboxylate oxygen (O3). The bidentate amino acid, L-phenylalanine, occupies the two remaining coordination sites about the cobalt atom. The  $\alpha$ -amino nitrogen (N3) of phenylalanine is coordinated to the cobalt in a position trans to the  $\alpha$ -carboxylate oxygen (O1) of PLASP<sup>2-</sup>, and its  $\alpha$ -carboxylate oxygen (O5) is attached trans to the secondary nitrogen (N1) of the PLASP<sup>2-</sup> ligand. The absolute configuration about the cobalt atom was assigned by using optically active amino acids of known configuration in the synthesis of the complex.

The bond distances observed within the PLASP<sup>2-</sup> and L-Phe<sup>-</sup> ligands are comparable to average values found in structures of other complexes containing aspartic acid,<sup>15,16</sup>



phenylalanine,<sup>17</sup> and pyridine<sup>18-20</sup> ligands. For the  $\beta$ -carboxylate of PLASP<sup>2-</sup> and the  $\alpha$ -carboxylate of L-Phe<sup>-</sup>, two different C-O bond distances are observed. The C-O distances (C4-O3 = 1.298(9) Å, C11-O5 = 1.295(9) Å) for the coordinated oxygen atoms are significantly longer than those (C4-O4 = 1.22(1) Å, C11-O6 = 1.225(9) Å) for the uncoordinated "carbonyl-type" oxygen atoms, as observed in other cobalt(III) complexes containing coordinated amino acids.<sup>21-25</sup> On the other hand, the C-O distances of both the coordinated (C1-O1 = 1.257(9) Å) and the uncoordinated (C1-O2 = 1.253(9) Å) oxygen atoms appear to be equal in the  $\alpha$ -carboxylate group of PLASP<sup>2-</sup>. This has been noted before in the literature.<sup>26</sup>

The bond distances Co-N1 (1.926(6) Å), Co-N3 (1.919(6) Å), Co-O1 (1.909(5) Å), Co-O3 (1.911(5) Å) and Co-O5 (1.896(5) Å) are similar to the cobalt secondary amino nitrogen,<sup>21,24,27-30</sup> cobalt primary amino nitrogen,<sup>31-34</sup> and cobalt carboxylate oxygen<sup>15,16,21-29,31-35</sup> distances found in other cobalt(III) complexes containing polyamines, amino acids, and amino polycarboxylates. The cobalt pyridine bond distance (Co-N2 = 1.910(6) Å) compares closely with the Co(III)-N(sp<sup>2</sup>) distances reported for other Co(III) complexes containing coordinated pyridine and imidazole.<sup>20,24,34</sup>

The deviations of the bond angles around the cobalt atom from ideal octahedral geometry range from  $1.5^\circ$  to  $4.5^\circ$ . The greatest deviations from  $90^\circ$  occur for the angles contained in the three five-membered chelate rings, O1-Co-N1,  $85.5(2)^\circ$ , N1-Co-N2,  $86.9(3)^\circ$  and O5-Co-N3,  $85.8(2)^\circ$ , and the angles in the same plane as a five-membered ring, N1-Co-N3,  $94.5(3)^\circ$ , O1-Co-O5,  $94.2(2)^\circ$  and O5-Co-N2,  $94.5(3)^\circ$ . The O-Co-N bond angles of the five-membered "glycinate-type" rings are consistent with angles reported for other Co(III) amino acid complexes.<sup>15-35</sup> The smallest angular deviation from ideal geometry is for the O1-Co-O3 ( $91.5(2)^\circ$ ) angle contained in the six-membered ring of the PLASP<sup>2-</sup> ligand, and this value is consistent with those reported for Co(III)bis-aspartato complexes.<sup>15,16</sup>

The largest deviation of the cobalt atom out of a coordination plane occurs for the O1-O5-N1-N3 plane. The cobalt atom is displaced  $0.02 \overset{\circ}{\text{Å}}$  out of this plane toward the pyridine nitrogen, N2 (Plane 1, Table IV). Also the distance from the cobalt to the plane defined by the pyridine ring is  $0.045 \overset{\circ}{\text{Å}}$ , and is somewhat shorter than the distances reported previously.<sup>25</sup> The coordination plane, O3-N1-N2-O5-Co, and the pyridine plane, N2-C6-C7-C8-C9-C10 (Plane 2, Table IV), are nearly parallel as

Table IV. Equations of least-squares planes<sup>a</sup>

Atom	D <sup>b</sup>	Atom	D
Plane 1: O1-O5-N1-N3			
$0.6535 X + 0.7414 Y - 0.1524 Z - 5.1979 = 0$			
Co	-0.0204	C1	0.4416
O1	-0.0038	C2	0.8186
O5	0.0038	C3	2.2862
N1	0.0037	C4	2.7593
N3	-0.0038	C11	0.3408
N2	-1.9250	C12	0.4040
		C13	-0.4084
Plane 2: (pyridine ring) C6-C7-C8-C9-C10-N2			
$0.3482 X + 0.5403 Y + 0.7660 Z - 11.70 = 0$			
N2	-0.0078	N1	0.0322
C5	0.0620	C10	-0.0011
C6	0.0146	Co	0.0453
C7	-0.0122	O3	0.0934
C8	0.0033	O5	0.0713
C9	0.0032		
Plane 3: O5-C11-O6-C12			
$-0.4144 X + 0.9013 Y - 0.1260 Z - 7.8600 = 0$			
Co	0.3751	O6	0.0031
O5	0.0028	C12	0.0023
C11	-0.0083	N3	-0.0113

<sup>a</sup>Planes are defined as  $C_1X + C_2Y + C_3Z + C_4 = 0$  where X, Y, and Z are Cartesian coordinates.

<sup>b</sup>D is the distance (Å) of the given atom from the fitted plane.

Table IV. (continued)

---

Atom	D	Atom	D
Plane 4: (phenyl ring) C14-C19			
$0.6169 X + 0.7373 Y + 0.2755 Z - 8.6903 = 0$			
C13	-0.0087	C17	-0.0048
C14	-0.0084	C18	-0.0023
C15	0.0014	C19	0.0089
C16	0.0052		

---

demonstrated by the small dihedral angle of  $1.60^\circ$  between these two planes. Additional evidence of the near parallelism of the pyridine and O3-N1-N2-O5-Co planes is the small deviation of N1 ( $0.03 \text{ \AA}$ ), C5 ( $0.06 \text{ \AA}$ ), O3 ( $0.09 \text{ \AA}$ ), and O5 ( $0.07 \text{ \AA}$ ) out of the plane defined by the pyridine (Plane 2, Table IV).

The five-membered glycinate ring of the PLASP<sup>2-</sup> ligand is in an asymmetric-envelope conformation with the  $\beta$ -carbon (C3) in an axial position as shown in Figure 4a. The torsional angle, N1-C2-C1-O1, of  $24.6^\circ$  falls within the  $0-30^\circ$  range observed for other coordinated amino acids.<sup>36</sup>

In addition to the asymmetric carbons in the ligands, the coordination of the PLASP<sup>2-</sup> ligand to the cobalt atom gives rise to an asymmetric secondary nitrogen, N1, which has the R absolute configuration. The configuration of the PLASP<sup>2-</sup> chelate rings seems to produce little angular strain in the C2-N1-C5 bond angle ( $110.6(6)^\circ$ ), which is close to the ideal tetrahedral value of  $109.5^\circ$ . This nearly ideal bond angle may possibly be used to explain why the pyridine coordinates trans to the  $\beta$ -COO<sup>-</sup> group of PLASP<sup>2-</sup> instead of in the somewhat more strained position trans to the  $\alpha$ -COO<sup>-</sup> group of PLASP<sup>2-</sup>. This angular strain has been noted before for Co(III) complexes

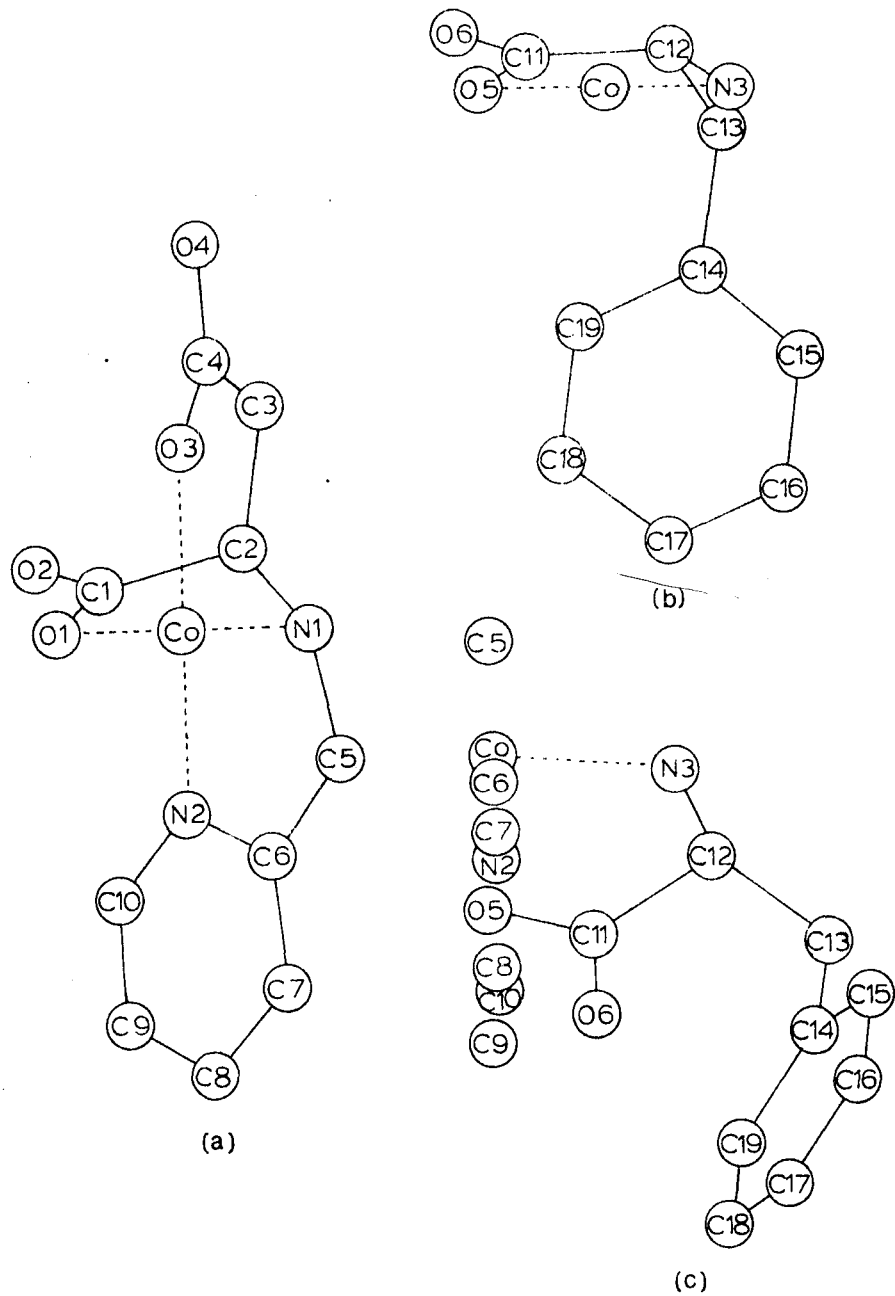


Figure 4. Projections of various parts of  $[\text{Co}(\text{PLASP})-(\text{L-Phe})]\cdot 3\text{H}_2\text{O}$ : (a)  $\text{PLASP}^{2-}$ , (b)  $\text{L-Phe}^-$  chelate ring and (c) the pyridine and phenyl rings as viewed parallel to the pyridine ring

containing polydentate chelates, such as iminodiacetic acid and ethylenediaminetetraacetic acid.<sup>21,29</sup>

The five-membered ring of the phenylalanine ligand is also coordinated to the cobalt atom in an asymmetric envelope configuration. This is shown in Figure 4b. The  $\alpha$ -carbon, C12, is displaced out of the N1-N3-Co-O1-O5 plane in a direction away from the pyridine ring. This displacement of the  $\alpha$ -carbon along with the bending of the chelate ring, puts the phenyl R group in an equatorial position as opposed to an axial position with reference to the N1-N3-Co-O1-O5 plane. The atoms of the phenylalanine ligand (O5, C11, O6, C12, N3) are nearly planar, as demonstrated by a torsional angle of  $1.43^\circ$  (N3-C12-C11-O5 angle) and the fact that N3 deviates only  $0.01 \text{ \AA}$  out of the O5-O6-C11-C12 plane (Plane 3, Table IV). The phenyl group of the phenylalanine ligand is planar with the largest deviation from planarity being  $0.009 \text{ \AA}$  (Plane 4, Table IV). The dihedral angle between the planes defined by the pyridine and phenyl rings is  $34.5^\circ$  and the closest distance between the two rings is  $3.46(1) \text{ \AA}$  (for C17...C9). The phenylalanine ligand does not appear to interact sterically with any part of the PLASP<sup>2-</sup> ligand. The spacial relationship between the pyridine and phenyl rings is shown in Figure 4c.

Discussion of spectra In the  $^1\text{H}$  nmr spectrum of the free ligand, PLASPH<sub>2</sub>, the  $\alpha$ -proton of the aspartic acid portion of the molecule occurs as a triplet centered at  $\delta$  4.03, and the  $\beta$ -protons of the aspartic acid portion occur as a doublet centered at  $\delta$  3.01. The methylene protons of the pyridylmethyl group occur as a singlet centered at  $\delta$  4.50, while the pyridyl protons occur as a doublet centered at  $\delta$  8.62 for the ortho proton, a triplet centered at  $\delta$  8.01 for the para proton and an overlapping doublet and triplet at  $\delta$  7.65-7.48 for the two meta protons.

The accumulated spectrum of the  $[\text{Co}(\text{PLASP})(\underline{\text{L}}\text{-Phe})] \cdot 3\text{H}_2\text{O}$  complex in D<sub>2</sub>O at room temperature, gives a multiplet centered at  $\delta$  7.47 for the pyridyl meta protons, a doublet centered at  $\delta$  7.87 for the ortho proton, a triplet centered at  $\delta$  8.00 for the pyridyl para proton, a multiplet at  $\delta$  7.24 for the phenyl protons and overlapping multiplets at  $\delta$  3.1 for the  $\beta$ -PLASP<sup>2-</sup> and  $\beta$ - $\underline{\text{L}}$ -Phe<sup>-</sup> protons. The methylene protons of the pyridylmethyl fragment occur as two doublets centered at  $\delta$  4.48 and 5.29, with a coupling constant of 18 Hz. The  $\alpha$ -proton of  $\underline{\text{L}}$ -Phe<sup>-</sup> occurs as a multiplet centered at  $\delta$  4.10 while the  $\alpha$ -proton of PLASP<sup>2-</sup> occurs as a multiplet at  $\delta$  3.93.



The  $^1\text{H}$  nmr spectrum of the Co complex supports a facial geometry around the cobalt ion. The splitting of the methylene protons of the pyridylmethyl group from a singlet into two doublets shows that the chemical environments on both sides of the plane formed by the coordinated  $-\text{NH}-\text{CH}_2-\text{Py}$  group in the complex are different (i.e. on one side is a coordinated nitrogen and on the other is an oxygen).

The visible spectrum is given in Figure 5. The visible spectrum for the complex shows two symmetrical peaks at 371 nm ( $\epsilon = 138 \text{ cm}^{-1}\text{M}^{-1}$ ) and 513 nm ( $\epsilon = 226 \text{ cm}^{-1}\text{M}^{-1}$ ). This spectrum is very similar to those of facial  $\text{Co(III)N}_3\text{O}_3$  complexes of amino acids and their derivatives reported previously in the literature.<sup>4,5,6</sup>

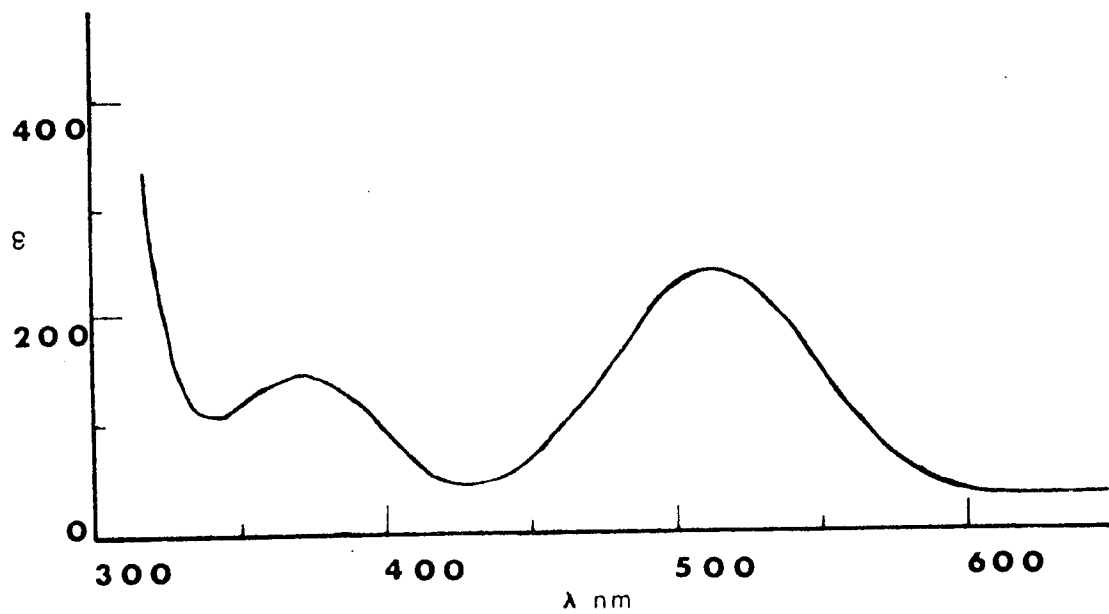


Figure 5. Visible spectrum of [Co(PLASP)(L-Phe)]·3H<sub>2</sub>O

## CONCLUSION

Attempts to prepare the other isomers of Co(PLASP) (AA) complexes (Figures lb, lc, and ld) by other synthetic routes,<sup>3</sup> have given only the facial isomer in which the pyridine is coordinated trans to the  $\beta$ -CO<sub>2</sub><sup>-</sup> group (Figure la). This may be due to a combination of electronic, structural and steric factors. If the PLASP<sup>2-</sup> ligand is considered first, there are two ways the pyridine nitrogen can coordinate as shown in Figures la and lb. The difference in electronic factors between these two sites should be small, since the pyridine is coordinated trans to a CO<sub>2</sub><sup>-</sup> group in both cases. Structurally these two sites are not equivalent. It has been noted before that polydentate ligands such as <sup>-</sup>O<sub>2</sub>C-CH<sub>2</sub>-NH-CH<sub>2</sub>-CO<sub>2</sub><sup>-</sup>, IMDA<sup>2-</sup>, can coordinate in two ways.<sup>21, 29, 35</sup> In the facial mode, the glycinate chelate rings are 90° to each other, and there is very little strain in the C-N-C angle. In the meridional mode the glycinate chelate rings are in the same plane. This type of coordination causes considerable strain in the C-N-C angle. Thus, coordination of the pyridine trans to the  $\beta$ -CO<sub>2</sub><sup>-</sup> group in Co(PLASP) (L-Phe) likewise gives the

least strain at N1 and allows the rigid chelate ring Co-N1-C5-C6-N2 (along with the entire pyridine ring) to be planar.

If the coordination of the phenylalaninate ligand is considered next, there are two ways it can coordinate as shown in Figures 1a and 1c. Coordination as in Figure 1a would be electronically favored since the amino group is trans to oxygen (the carboxylate group). It has been noted before<sup>6, 37, 38</sup> that amino groups avoid coordinating trans to each other, which would favor the structure in Figure 1a over that in 1c. Additional support for facial coordination is given in an earlier theoretical account of bonding in transition metal complexes which states that the most stable isomer for low spin- $d^6$   $ML_3L_3'$  complexes should be facial.<sup>39</sup> This appears to be the case in complexes where no steric interaction is evident. Also, coordination as in Figure 1a is sterically favored since the  $\alpha$ -carbon of the phenylalaninate chelate ring is pointing up and away from the pyridine ring. This configuration of the  $L$ -Phe<sup>-</sup> ring is determined by the bulky R group,  $-CH_2-\phi$ , which would favor the equatorial rather than axial position.

## REFERENCES

1. Nakon, R.; Rechani, P. R.; Angelici, R. J. Inorg. Chem. 1973, 12, 2431.
2. Bedell, S. A.; Rechani, P. R.; Angelici, R. J.; Nakon, R. Inorg. Chem. 1977, 16, 972.
3. Meiske, L. A.; Angelici, R. J.; Jacobson, R. A., Abstract of the 14th Midwest Regional ACS Meeting, Oct., 1978.
4. Douglas, B. E.; Yamada, S. Inorg. Chem. 1965, 4, 1561.
5. Denning, R. G.; Piper, T. S. Inorg. Chem. 1966, 5, 1056.
6. Watabe, M.; Onuki, K.; Yoshikawa, S. Bull. Chem. Soc. Japan 1975, 48, 687; Bull. Chem. Soc. Japan 1976, 49, 1845.
7. Jacobson, R. A. J. Appl. Cryst. 1976, 9, 115.
8. Rohrbaugh, W. J.; Jacobson, R. A. Inorg. Chem. 1974, 13, 2535.
9. Lawton, S. L.; Jacobson, R. A. Inorg. Chem. 1968, 7, 2124.
10. Busing, W. R.; Martin, K. O.; Levy, H. A. "ORFLS, A Fortran Crystallographic Least Squares Program", U. S. Atomic Energy Commission Report ORNL-TM-305. Oak Ridge National Laboratory, Oak Ridge, Tenn., 1962.
11. Hubbard, C. A.; Quicksall, C. O.; Jacobson, R. A. "The Fast Fourier Algorithm and the Programs ALFF, ALFFDP, ALFFPROJ, ALFFT and FRIEDEL", U. S. Atomic Energy Commission Report IS-2625. Iowa State University and Institute for Atomic Research, Ames, Iowa, 1971.
12. Hanson, H. P.; Herman, F.; Lea, J. D.; Skillman, S. Acta Crystallogr. 1960, 17, 1040.

13. Templeton, D. H. "International Tables for X-ray Crystallography", The Kynock Press: Birmingham, England, 1962; Vol. III, Table 3.3.2C, p. 215-216.
14. Busing, W. R.; Martin, K. O.; Levy, H. A. "ORFFE, A Fortran Crystallographic Function and Error Program", U. S. Atomic Energy Commission Report ORNL-TM-306. Oak Ridge National Laboratory, Oak Ridge, Tenn., 1964.
15. Oonishi, I.; Shibata, M.; Marumo, F.; Saito, Y. Acta Crystallogr. 1973, B29, 2448.
16. Oonishi, I.; Sato, S.; Saito, Y. Acta Crystallogr. 1975, B31, 1318.
17. van der Helm, D.; Lawson, M. B.; Enwell, E. L. Acta Crystallogr. 1971, B27, 2411.
18. Loiseleur, H. Acta Crystallogr. 1972, B28, 816.
19. Stälin, W.; Oswald, H. R. Acta Crystallogr. 1971, B27, 1368.
20. Reimann, C. W.; Zocchi, M.; Mighell, A. B.; Santoro, A. Acta Crystallogr. 1971, B27, 2111.
21. Halloran, L. J.; Caputo, R. E.; Willett, R. D.; Legg, J. I. Inorg. Chem. 1975, 14, 1762.
22. Anderson, B. F.; Buckingham, D. A.; Gainsford, G. J.; Robertson, G. B.; Sargeson, A. M. Inorg. Chem. 1975, 14, 1658.
23. Liu, C. F.; Ibers, J. A. Inorg. Chem. 1969, 8, 1911.
24. Voss, K. E.; Angelici, R. J.; Jacobson, R. A. Inorg. Chem. 1978, 17, 1922.
25. Ebner, S. R.; Angelici, R. J.; Jacobson, R. A. Inorg. Chem. 1979, 18, 765.
26. Watson, W. H.; Johnson, D. R.; Celap, M. B.; Kamberi, B. Inorg. Chim. Acta 1972, 6, 591.

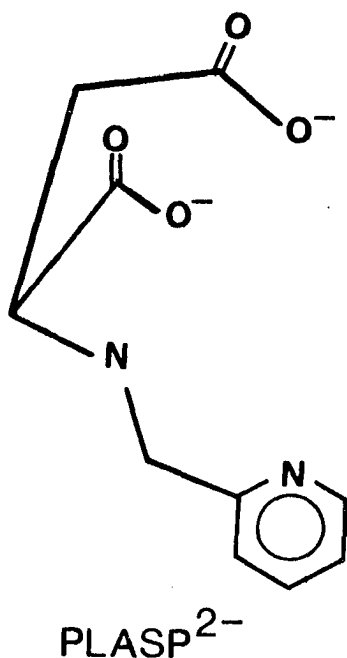
27. Buckingham, D. A.; Cresswell, P. J.; Dellaca, R. J.; Dwyer, M.; Gainsford, G. J.; Marzilli, L. G.; Maxwell, I. E.; Robinson, W. T.; Sargeson, A. M.; Turnbull, K. R. J. Am. Chem. Soc. 1974, 96, 1713.
28. Svetich, G. W.; Voge, A. A.; Brushmiller, J. G.; Berends, E. A. J. Chem. Soc., Chem. Commun. 1972, 701.
29. Weakliem, H. A.; Hoard, J. L. J. Am. Chem. Soc. 1959, 81, 549.
30. Freeman, H. C.; Marzilli, L. G.; Maxwell, I. E. Inorg. Chem. 1970, 9, 2408.
31. Barnet, M. T.; Freeman, H. C.; Buckingham, D. A.; Hsu, I.; van der Helm, D. Chem. Commun. 1970, 367.
32. Herak, R.; Prelesnik, B.; Manojlovic-Muir, L.; Muir, K. W. Acta Crystallogr. 1974, B30, 229.
33. Gillard, R. D.; Payne, N. C.; Robertson, G. B. J. Chem. Soc. A. 1970, 2579.
34. Thorup, N. Acta Crystallogr. 1975, A31, S142; Acta Chem. Scand. 1977, A31, 203.
35. Corradi, A. B.; Palmieri, C. G.; Nardelli, M.; Pellinghelli, M. A.; Tani, M. E. V. J. Chem. Soc., Dalton Trans. 1973, 655.
36. Hawkins, C. J. "Absolute Configuration of Metal Complexes", Wiley-Interscience: New York, N.Y., 1971, p. 94.
37. Watabe, M.; Zama, M.; Yoshikawa, S. Bull. Chem. Soc. Japan 1978, 51, 1354.
38. Ebner, S. R.; Angelici, R. J. submitted for publication to Inorg. Chem.
39. Burdett, J. K. Adv. Inorg. Chem. Radiochem. 1978, 21, 113.

SECTION II. SYNTHESIS AND SPECTRAL CHARACTERIZATION OF  
THE MIXED LIGAND COMPLEXES, [N-(2-Pyridyl-  
methyl)-L-aspartato][amino acidato]cobalt(III),  
Co(PLASP)(AA)



## INTRODUCTION

Nickel(II) and copper(II) complexes of N-(2-pyridyl-methyl)-L-aspartate, PLASP<sup>2-</sup>, stereoselectively coordinate optically active amino acidates, AA<sup>-</sup>, in forming M(PLASP)(AA)<sup>-</sup> complexes.<sup>1</sup> In order to investigate the



structure of mixed complexes containing PLASP<sup>2-</sup> and AA<sup>-</sup> ligands, the kinetically inert cobalt(III) complexes of the type Co(PLASP)(AA) were prepared. In the present study, AA<sup>-</sup> is one of the following amino acidates: glycinate (Gly<sup>-</sup>),  $\alpha$ -aminoisobutyrate ( $\alpha$ -AIBA<sup>-</sup>), L-alaninate (L-Ala<sup>-</sup>), L-threoninate (L-Thr<sup>-</sup>), L-prolinate (L-Pro<sup>-</sup>), D or L or D,L-valinate (Val<sup>-</sup>), D or L-asparaginate (AsN<sup>-</sup>) and D or L-phenylalaninate (Phe<sup>-</sup>).

Previously we determined the X-ray diffraction structure of the complex,  $[\text{Co}(\text{PLASP})(\underline{\text{L}}\text{-Phe})] \cdot 3\text{H}_2\text{O}$ .<sup>2</sup> This  $\text{Co}(\text{III})\text{N}_3\text{O}_3$  complex was found to have a facial structure in which the three coordinated oxygen (or nitrogen) atoms occupy one triangular face of the coordination octahedron, and the pyridyl group of  $\text{PLASP}^{2-}$  is coordinated trans to the  $\beta\text{-CO}_2^-$  group of  $\text{PLASP}^{2-}$  (Figure 1a).<sup>2</sup> We proposed that this geometry was due to a combination of electronic, structural and steric factors. It was of interest to prepare other  $\text{Co}(\text{PLASP})(\text{AA})$  complexes to establish their geometries and to seek trends in their UV, visible, CD, and nmr spectra.

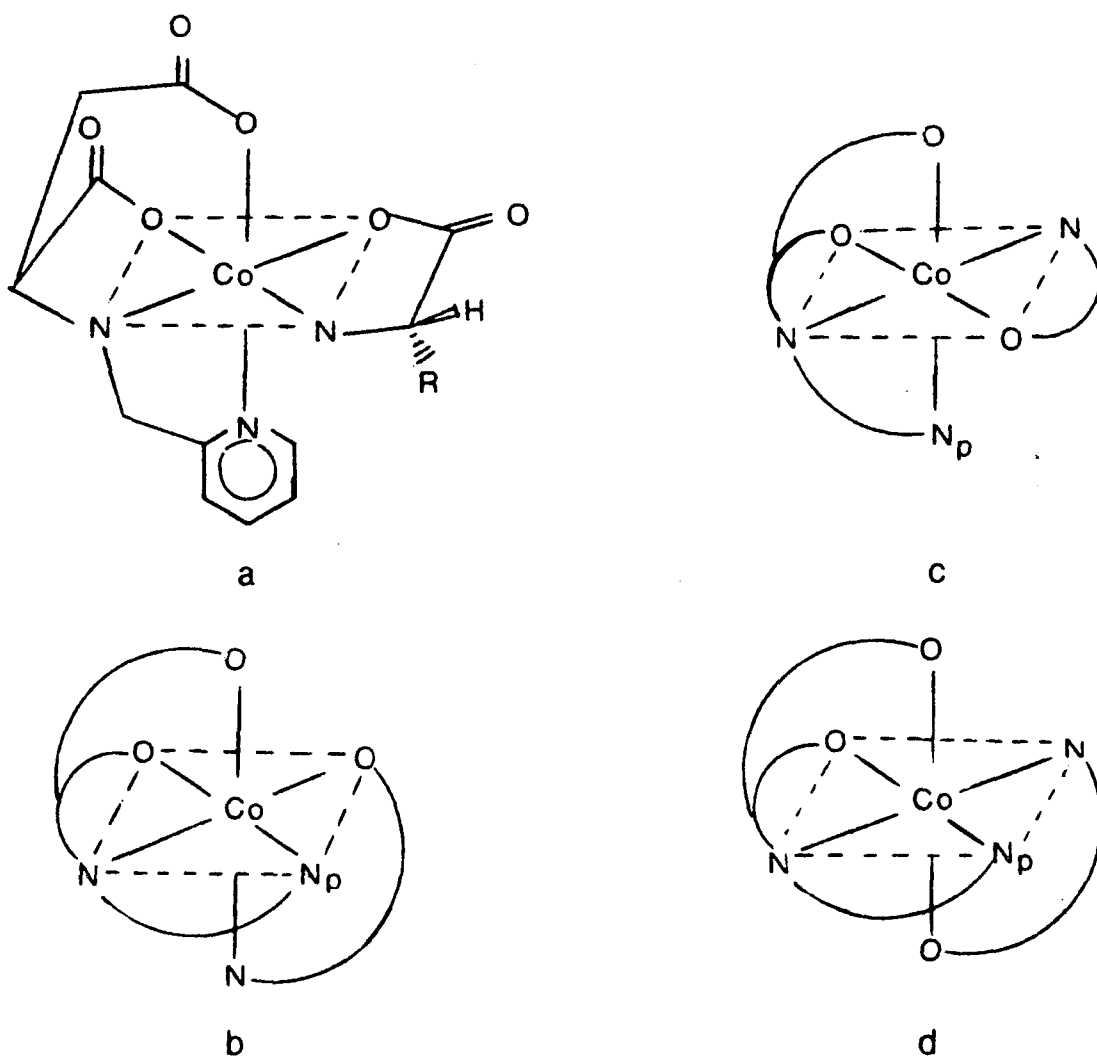


Figure 1. The four possible isomers of  $\text{Co(PLASP)(L-AA)}$  complexes, a)  $\text{fac } \beta\text{-CO}_2^-$ , b)  $\text{fac } \alpha\text{-CO}_2^-$ , c)  $\text{mer } \beta\text{-CO}_2^-$  and d)  $\text{mer } \alpha\text{-CO}_2^-$

## EXPERIMENTAL SECTION

Materials All amino acids were purchased from Aldrich and Eastman Kodak and were used without further purification. The ligand, PLASPH<sub>2</sub>, was prepared as previously reported.<sup>2</sup>

Preparation of the [N-(2-pyridylmethyl)-L-aspartato]-[amino acidato]cobalt(III), Co(PLASP)(AA), complexes The method of preparation and purification (see below) of each Co(PLASP)(AA) complex is given in Table I. Elemental analyses and yields of each product are also given in that table.

Method A This procedure in which excess hydrogen peroxide is used to oxidize Co(II) to Co(III) in the presence of PLASP<sup>2-</sup> and AA<sup>-</sup> has been described previously.<sup>2</sup> All reactions were carried out using 10 mmol PLASP<sup>2-</sup>, 10 mmol AA<sup>-</sup>, and 10 mmol CoSO<sub>4</sub>·7H<sub>2</sub>O except in the preparation of [Co(PLASP)(L-Thr)]·1 1/2H<sub>2</sub>O which was carried out using 5 mmol each of PLASP<sup>2-</sup>, AA<sup>-</sup> and CoSO<sub>4</sub>·7H<sub>2</sub>O. All products were purified using column chromatography on either aluminum oxide (acidic or neutral) or Dowex 50W-X8 in the Na<sup>+</sup> form. A typical column size was 2.5 x 60 cm. The solvent used for purification on alumina was either water or a water-ethanol mixture,

Table I. Syntheses, purification and elemental analysis of Co(PLASP) (AA) complexes

Complex	Method of Preparation	Column Support	Chromatography Solvent	% Yield
[Co(PLASP) (Gly)]	A	Neutral Alumina	$\frac{50}{50}$ $\frac{\text{MeOH}}{\text{H}_2\text{O}}$	9
[Co(PLASP) ( <u>L</u> -Ala)]	A	Neutral Alumina	H <sub>2</sub> O	19
[Co(PLASP) ( $\alpha$ -AIBA)] · H <sub>2</sub> O	A	Neutral Alumina	$\frac{50}{50}$ $\frac{\text{EtOH}}{\text{H}_2\text{O}}$	18
[Co(PLASP) ( <u>L</u> -Thr)] · 1 1/2H <sub>2</sub> O	A	Neutral Alumina	$\frac{40}{60}$ $\frac{\text{EtOH}}{\text{H}_2\text{O}}$	18
[Co(PLASP) ( <u>L</u> -Pro)] · 1 1/2H <sub>2</sub> O	A	Dowex	H <sub>2</sub> O	26
	D	Dowex	H <sub>2</sub> O	40
[Co(PLASP) ( <u>L</u> -Val)]	A	Neutral Alumina	$\frac{40}{60}$ $\frac{\text{EtOH}}{\text{H}_2\text{O}}$	34
	B	Acidic Alumina	$\frac{40}{60}$ $\frac{\text{EtOH}}{\text{H}_2\text{O}}$	14
[Co(PLASP) ( <u>D</u> -Val)]	A	Neutral Alumina	$\frac{40}{60}$ $\frac{\text{EtOH}}{\text{H}_2\text{O}}$	9
[Co(PLASP) ( <u>D</u> , <u>L</u> -Val)]	A	Neutral Alumina	$\frac{40}{60}$ $\frac{\text{EtOH}}{\text{H}_2\text{O}}$	30
	C	Dowex	H <sub>2</sub> O	33
[Co(PLASP) ( <u>L</u> -AsN)] · H <sub>2</sub> O	D	Dowex	H <sub>2</sub> O	36
[Co(PLASP) ( <u>D</u> -AsN)] · 1/2H <sub>2</sub> O	D	Dowex	H <sub>2</sub> O	11
[Co(PLASP) ( <u>L</u> -Phe)] · 3H <sub>2</sub> O	A	Neutral Alumina	H <sub>2</sub> O	18
[Co(PLASP) ( <u>D</u> -Phe)] · 2H <sub>2</sub> O	A	Neutral Alumina	H <sub>2</sub> O	8

Formula		%C	%H	%N
$C_{12}H_{14}N_3O_6Co$	Theory	40.57	3.94	11.83
	Found	40.76	4.17	11.83
$C_{13}H_{16}N_3O_6Co$	Theory	42.29	4.34	11.39
	Found	42.18	4.51	11.40
$C_{14}H_{18}N_3O_6Co \cdot 1H_2O$	Theory	41.91	4.99	10.48
	Found	42.15	5.22	10.35
$C_{14}H_{18}N_3O_7Co \cdot 1 \frac{1}{2}H_2O$	Theory	39.45	4.93	9.86
	Found	39.57	4.77	9.81
$C_{15}H_{18}N_3O_6Co \cdot 1 \frac{1}{2}H_2O$	Theory	42.66	4.98	9.95
	Found	42.38	5.19	9.90
$C_{15}H_{20}N_3O_6Co$	Theory	45.35	5.04	10.58
	Found	45.41	4.90	10.60
$C_{15}H_{20}N_3O_6Co$	Theory	45.35	5.04	10.58
	Found	45.16	5.10	10.52
$C_{15}H_{20}N_3O_6Co$	Theory	45.35	5.04	10.58
	Found	44.91	5.24	10.26
$C_{14}H_{17}N_4O_7Co \cdot H_2O$	Theory	39.08	4.42	13.03
	Found	39.09	4.57	13.04
$C_{14}H_{17}N_4O_7Co \cdot 1 \frac{1}{2}H_2O$	Theory	39.91	4.27	13.30
	Found	40.08	4.51	13.19
$C_{19}H_{20}N_3O_6Co \cdot 3H_2O$	Theory	45.70	5.21	8.41
	Found	45.59	5.33	8.37
$C_{19}H_{20}N_3O_6Co \cdot 2H_2O$	Theory	47.41	4.99	8.73
	Found	47.26	4.15	8.69

while water was used as the solvent for purifications on Dowex 50W-X8. The product was the second band eluted from the columns and was preceded by a brown band containing decomposition products, unreacted ligands, and salts. The product isolated by column chromatography was further purified by dissolving the complex in a minimum of water and adding a volume of methanol or ethanol equal to 4-5 times the volume of water to force precipitation. The complexes  $[\text{Co}(\text{PLASP})(\underline{\text{L}}\text{-Phe})] \cdot 3\text{H}_2\text{O}$ ,  $[\text{Co}(\text{PLASP})(\underline{\text{D}}\text{-Phe})] \cdot 2\text{H}_2\text{O}$  and  $[\text{Co}(\text{PLASP})(\underline{\text{L}}\text{-Ala})]$  were purified in either of two ways. The first was by recrystallization from water of the reddish solid obtained by concentrating the reaction mixture under vacuum. The second was by column chromatography. The complex  $[\text{Co}(\text{PLASP})(\underline{\text{L}}\text{-Phe})] \cdot \text{H}_2\text{O}$  was precipitated by dissolving the  $[\text{Co}(\text{PLASP})(\underline{\text{L}}\text{-Phe})] \cdot 3\text{H}_2\text{O}$  complex in water and then adding a volume of ethanol equal to 4-5 times the volume of water. Anal. calcd. for  $\text{C}_{19}\text{H}_{20}\text{N}_3\text{O}_6\text{Co} \cdot \text{H}_2\text{O}$ : C, 49.25; H, 4.75; N, 9.07. Found: C, 49.13; H, 4.73; N, 9.01.

Method B, Preparation of  $[\text{Co}(\text{PLASP})(\underline{\text{L}}\text{-Val})]$

The  $\text{PLASPH}_2$  (1.12 g, 5 mmol),  $\underline{\text{L}}\text{-ValH}$  (0.89 g, 5 mmol),  $\text{Na}_3[\text{Co}(\text{CO}_3)_3] \cdot 3\text{H}_2\text{O}$  (1.82 g, 5 mmol) and activated carbon were placed in a flask, and 50 ml of water was added. The solution began foaming, and a purple color became

visible. Next, 15 ml of 1N H<sub>2</sub>SO<sub>4</sub> was added, and more foaming occurred. The solution was stirred overnight, filtered, and reduced in vacuum to 3-5 ml. This solution was placed on an acidic alumina column (2.5 x 65 cm) and eluted with 40:60 EtOH:H<sub>2</sub>O. The large reddish-pink band containing the product was collected, concentrated to 1-2 ml, and 125 ml of methanol was added to precipitate the product.

Method C, Preparation of [Co(PLASP)(D,L-Val)]

The PLASPH<sub>2</sub> (0.56 g, 2.5 mmol), D,L-ValH (0.30 g, 2.5 mmol), CoSO<sub>4</sub>·7H<sub>2</sub>O (0.70 g, 2.5 mmol), and 5 ml of 1N NaOH were dissolved in 50 ml of water, and PbO<sub>2</sub> (0.35 g, 1.5 mmol) was added. The solution was heated (50-60°) for 1 hour. Next 2.5 ml of 1N H<sub>2</sub>SO<sub>4</sub> was added, and the solution was filtered. The solution was concentrated under reduced pressure to 1-2 ml and placed on a column (1.9 x 40 cm) of Dowex 50W-X8 in the Na<sup>+</sup> form. The first band eluted from the column contained decomposition and anionic products. The second reddish-pink band containing the product was collected, reduced to ~5 ml and 100 ml of ethanol was added to force out the product.

Method D The ligands, PLASPH<sub>2</sub> (0.56 g, 2.5 mmol) and AAH (2.5 mmol), and CoSO<sub>4</sub>·7H<sub>2</sub>O (0.70 g, 2.5 mmol) were placed in 10 ml of water. Next, 7.5 ml of 1N NaOH was



added to give a brown solution of pH 9. The solution was stirred for 5 minutes and activated carbon (0.1 g) was added. Then a solution of  $K_2S_2O_8$  (0.4 g, 1.5 mmol) in 15 ml of water was added. The reaction mixture was heated for 1 hour at  $\sim 60^\circ C$  and filtered to give a deep purple solution. The solution was reduced to 5-10 ml and placed on a column (2.5 x 65 cm) of Dowex 50W-X8 in the  $Na^+$  form. The first band off the column contains anionic and decomposition products while the second reddish-pink band contains the desired product. This second band was collected and reduced to  $\sim 5$  ml. The product was precipitated by addition of ethanol. Separation of the two diastereomers,  $Co(PLASP)(\underline{L}\text{-AsN})$  and  $Co(PLASP)(\underline{D}\text{-AsN})$  was achieved by placing the reaction mixture (after reduction to 5-10 ml) on a Dowex 50W-X8 column in the  $Na^+$  form. Upon elution with water, three bands formed with the first band off the column containing decomposition and anionic products, the second containing the  $[Co(PLASP)(\underline{L}\text{-AsN})]\cdot H_2O$  diastereomer and the third band containing the  $[Co(PLASP)(\underline{D}\text{-AsN})]\cdot 1/2H_2O$  diastereomer.

Spectra Visible and CD spectra were recorded in water at room temperature using a Jasco ORD/UV/CD-5 spectrophotometer. The  $^1H$  nmr spectra were recorded in

99.7% deuterium oxide at room temperature on a Jeol FX90Q Fourier transform nmr spectrometer, using *t*-butyl alcohol ( $\delta$  1.23) as an internal standard. The peak positions are given in ppm downfield from TMS. The  $^{13}\text{C}$  nmr spectra also were recorded at room temperature on the above nmr spectrometer in either 99.7% deuterium oxide or 70%  $\text{H}_3\text{PO}_4$  (aqueous), using 1,4-dioxane (67.0 ppm downfield from TMS) as an internal standard.

## RESULTS AND DISCUSSION

Figure 1 shows the four possible geometric isomers of the Co(PLASP)(L-AA) complex. The structures in Figures 1a and 1b have a facial arrangement of oxygen atoms. Reversing the coordination of the amino acidate, AA<sup>-</sup>, in Figures 1a and 1b, gives the two meridional isomers shown in Figures 1c and 1d. The four isomers in Figure 1 are denoted as fac β-CO<sub>2</sub><sup>-</sup>, fac α-CO<sub>2</sub><sup>-</sup>, mer β-CO<sub>2</sub><sup>-</sup> and mer α-CO<sub>2</sub><sup>-</sup> with the terms β-CO<sub>2</sub><sup>-</sup> and α-CO<sub>2</sub><sup>-</sup> being used to denote which CO<sub>2</sub><sup>-</sup> group of PLASP<sup>2-</sup> is coordinated trans to the pyridyl group.

Visible spectra of the Co(PLASP)(AA) complexes

The visible spectrum of [Co(PLASP)(α-AIBA)]·H<sub>2</sub>O in water is shown in Figure 2 and is characteristic of the other Co(PLASP)(AA) visible spectra whose maxima are listed in Table II. The visible spectra of these Co(PLASP)(AA) complexes (with their two symmetrical peaks at 513 ± 4 nm and 370 ± 3 nm) are comparable to various facial Co(III)N<sub>3</sub>O<sub>3</sub> complexes containing amino acidates reported previously.<sup>3, 4, 5</sup> Since the absorption maxima and extinction coefficients for the complexes listed in Table II are so similar, the arrangement of the ligands around the Co(III) in all of

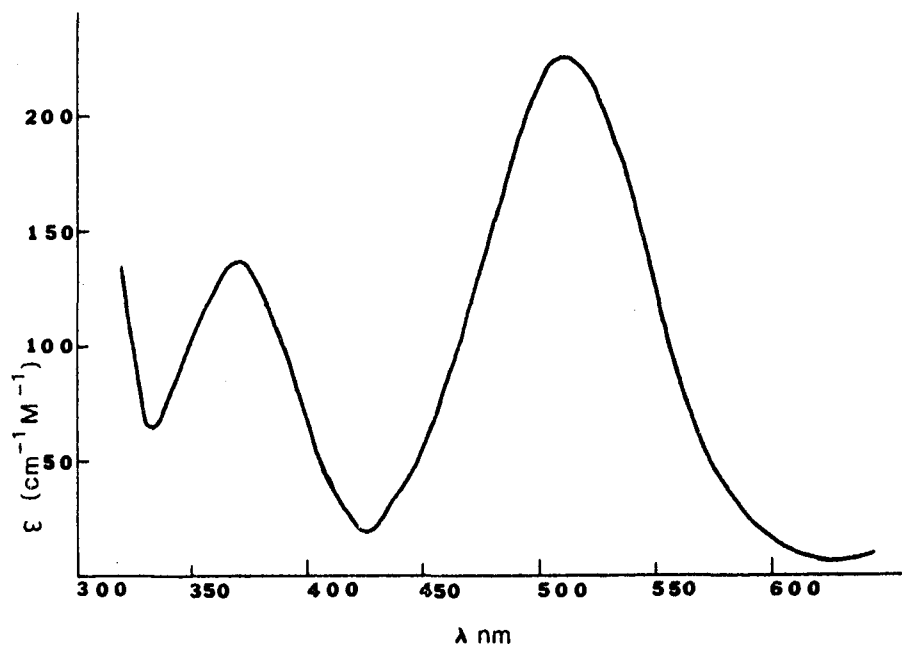


Figure 2. Visible spectrum of [Co(PLASP)(α-AIBA)]·H<sub>2</sub>O in water

Table II. Visible absorption maxima for Co(PLASP) (AA) complexes in water

Compound	$\lambda$ (nm)	$\epsilon$ ( $\text{cm}^{-1}\text{M}^{-1}$ )	$\lambda$ (nm)	$\epsilon$ ( $\text{cm}^{-1}\text{M}^{-1}$ )
[Co (PLASP) (Gly) ]	515	223	370	137
[Co (PLASP) ( <u>L</u> -Ala) ]	512	230	370	146
[Co (PLASP) ( $\alpha$ -AIBA) ] $\cdot$ H <sub>2</sub> O	511	222	370	136
[Co (PLASP) ( <u>L</u> -Thr) ] $\cdot$ 1 1/2H <sub>2</sub> O	511	233	368	134
[Co (PLASP) ( <u>L</u> -Pro) ] $\cdot$ 1 1/2H <sub>2</sub> O	517	211	373	138
[Co (PLASP) ( <u>L</u> -Val) ]	510	229	368	132
[Co (PLASP) ( <u>D</u> -Val) ]	513	230	371	137
[Co (PLASP) ( <u>D</u> , <u>L</u> -Val) ]	513	201	370	120
[Co (PLASP) ( <u>L</u> -AsN) ] $\cdot$ H <sub>2</sub> O	513	199	371	122
[Co (PLASP) ( <u>D</u> -AsN) ] $\cdot$ 1/2H <sub>2</sub> O	513	220	371	128
[Co (PLASP) ( <u>L</u> -Phe) ] $\cdot$ H <sub>2</sub> O	513	228	369	138
[Co (PLASP) ( <u>L</u> -Phe) ] $\cdot$ 3H <sub>2</sub> O	512	226	368	142
[Co (PLASP) ( <u>D</u> -Phe) ] $\cdot$ 2H <sub>2</sub> O	512	232	369	136

these complexes is probably the same. This is consistent with  $^{13}\text{C}$  nmr studies of these complexes which show the  $^{13}\text{C}$  chemical shifts of the coordinated ligand  $\text{PLASP}^{2-}$  to remain nearly identical in all of the  $\text{Co}(\text{PLASP})(\text{AA})$  complexes (see below). Therefore, based on the visible and  $^{13}\text{C}$  nmr spectra of the  $\text{Co}(\text{PLASP})(\text{AA})$  complexes and the previously reported X-ray structure<sup>2</sup> of  $[\text{Co}(\text{PLASP})(\text{L-Phe})]\cdot 3\text{H}_2\text{O}$ , all of the complexes listed in Table II are assigned the facial structure in which the pyridine is coordinated trans to the  $\beta\text{-CO}_2^-$  group of  $\text{PLASP}^{2-}$  (Figure 1a). Further evidence for this assignment is given by the circular dichroism spectra of the complexes and will be considered next.

Circular dichroism spectra of the  $\text{Co}(\text{PLASP})(\text{AA})$  complexes The circular dichroism spectra of the various  $\text{Co}(\text{PLASP})(\text{AA})$  complexes in water are shown in Figures 3-5, and the numerical values for their minima and maxima are given in Table III. Each circular dichroism spectrum can be divided into two major bands, with band I occurring in the 485 to 560 nm range and band II occurring from 330 to 385 nm; these bands occur in the regions of the visible spectrum where these complexes absorb.

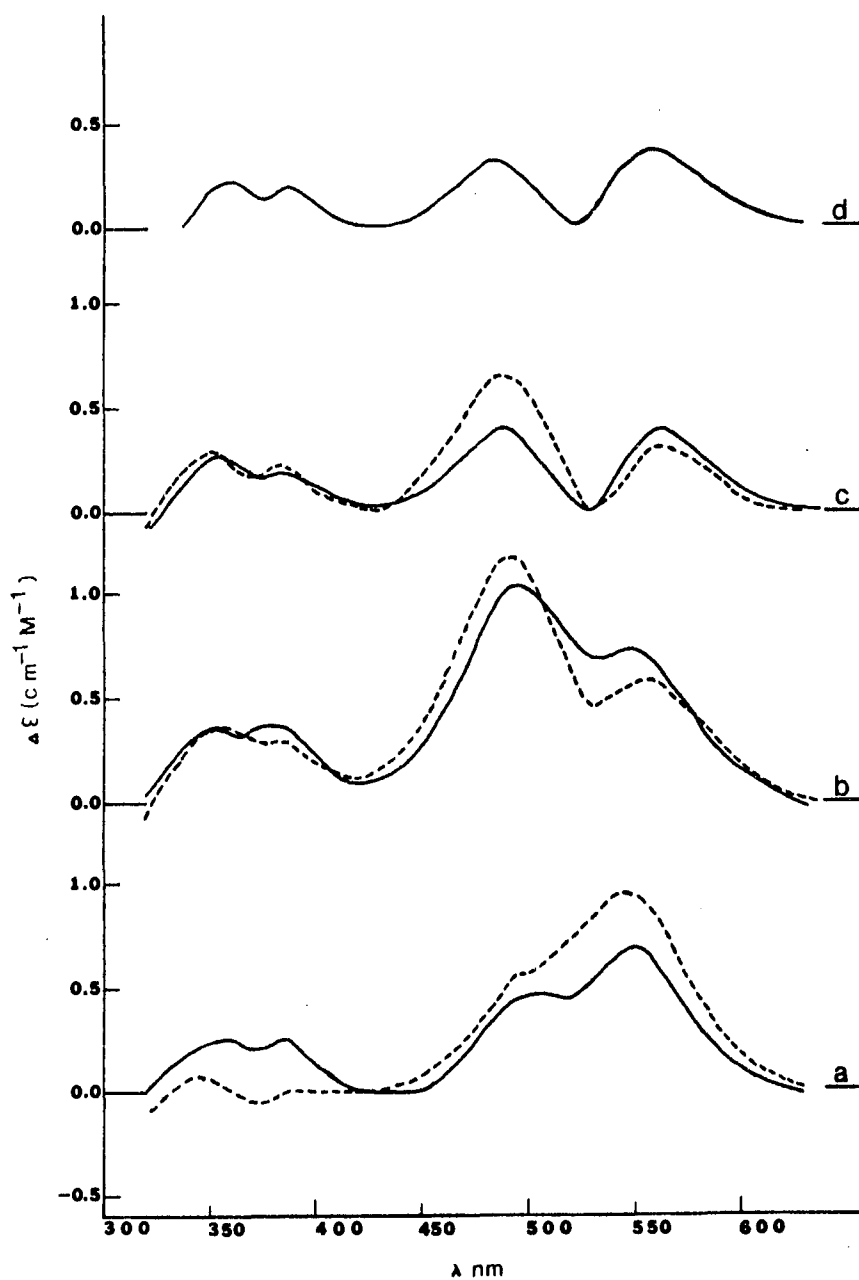


Figure 3. CD spectra for a)  $[\text{Co}(\text{PLASP})(\text{Gly})]$  (----) and  $[\text{Co}(\text{PLASP})(\underline{\text{L}}\text{-Ala})]$  (—), b)  $[\text{Co}(\text{PLASP})(\underline{\text{L}}\text{-Pro})] \cdot 1 \frac{1}{2}\text{H}_2\text{O}$  (----) and  $[\text{Co}(\text{PLASP})(\underline{\text{L}}\text{-Asn})] \cdot \text{H}_2\text{O}$  (—), c)  $[\text{Co}(\text{PLASP})(\underline{\text{L}}\text{-Val})]$  (----) and  $[\text{Co}(\text{PLASP})(\underline{\text{L}}\text{-Thr})] \cdot 1 \frac{1}{2}\text{H}_2\text{O}$  (—) and d)  $[\text{Co}(\text{PLASP})(\underline{\text{L}}\text{-Phe})] \cdot 3\text{H}_2\text{O}$  (—)

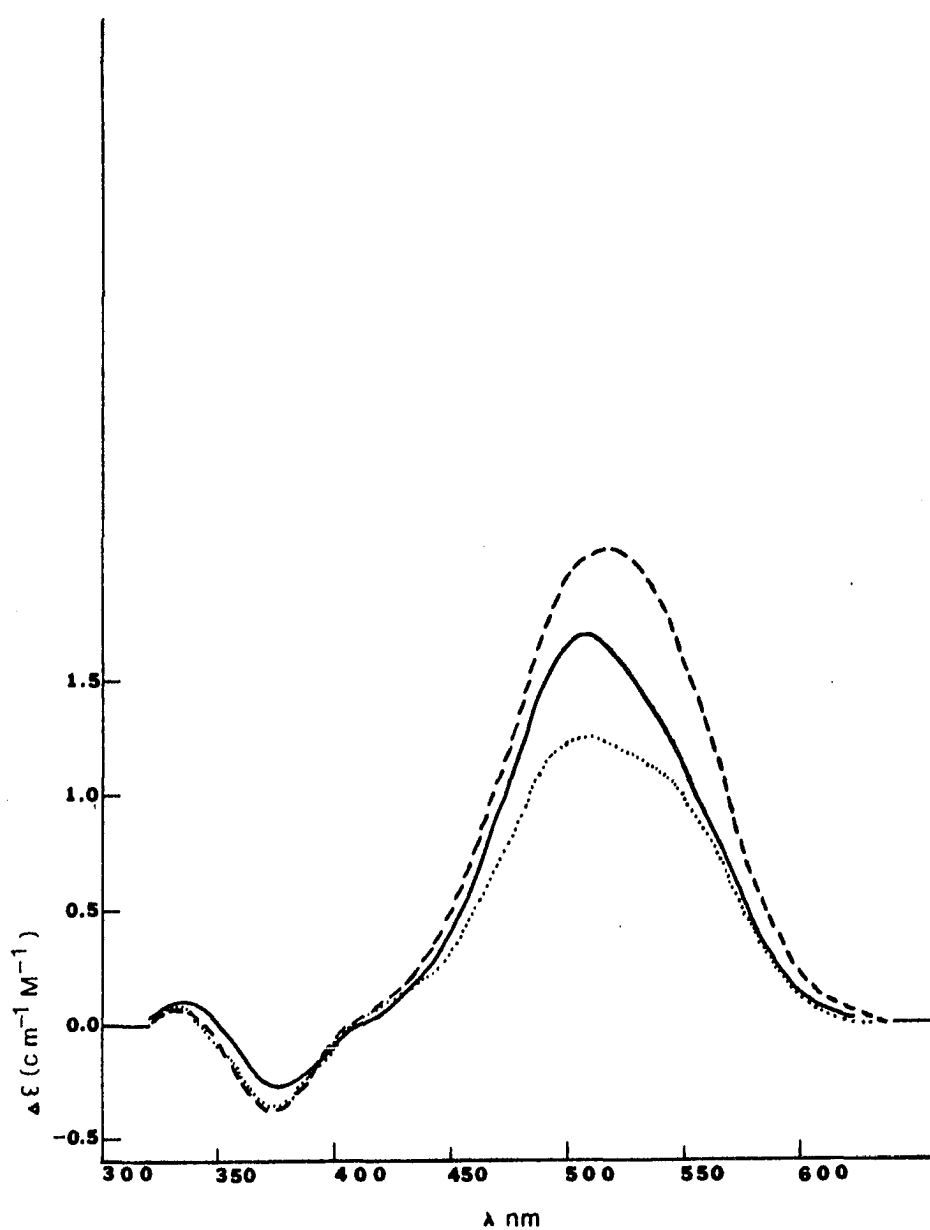


Figure 4. CD spectra for  $[\text{Co}(\text{PLASP})(\underline{\text{D}}\text{-Val})]$  (----),  $[\text{Co}(\text{PLASP})(\underline{\text{D}}\text{-Phe})] \cdot 2\text{H}_2\text{O}$  (—) and  $[\text{Co}(\text{PLASP})(\underline{\text{D}}\text{-AsN})] \cdot 1/2\text{H}_2\text{O}$  (.....)



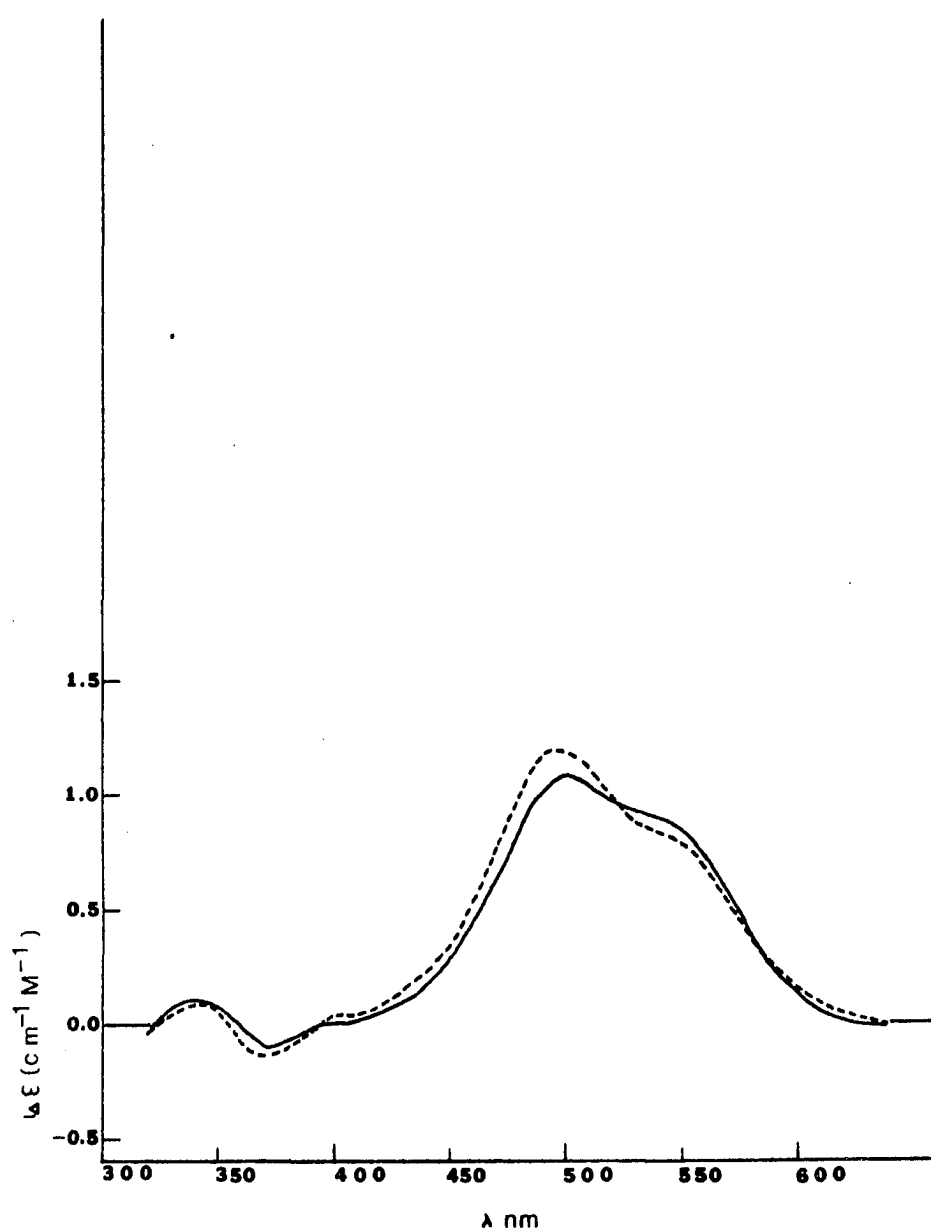


Figure 5. CD spectra for  $[\text{Co(PLASP)(}\alpha\text{-AIBA)}] \cdot \text{H}_2\text{O}$  (----) and  $[\text{Co(PLASP)(D,L-Val)}]$  (—)

Table III. Circular dichroism maxima and minima for Co(PLASP)(AA) complexes in water

Complex	Band I				Band II			
	$\lambda_{nm}$	$\Delta\epsilon^a$	$\lambda_{nm}$	$\Delta\epsilon$	$\lambda_{nm}$	$\Delta\epsilon$	$\lambda_{nm}$	$\Delta\epsilon$
[Co(PLASP)(Gly)]	544	+0.94	495	+0.56	370	-0.06	345	+0.07
[Co(PLASP)( <u>L</u> -Ala)]	546	+0.68	500	+0.46	375	+0.25	359	+0.25
[Co(PLASP)( $\alpha$ -AIBA)] $\cdot$ H <sub>2</sub> O	545	+0.81	495	+1.17	370	-0.13	340	+0.09
[Co(PLASP)( <u>L</u> -Thr)] $\cdot$ 1 1/2H <sub>2</sub> O	560	+0.38	486	+0.39	382	+0.19	355	+0.26
[Co(PLASP)( <u>L</u> -Pro)] $\cdot$ 1 1/2H <sub>2</sub> O	555	+0.58	490	+1.16	385	+0.29	358	+0.36
[Co(PLASP)( <u>L</u> -Val)]	560	+0.31	488	+0.63	380	+0.18	355	+0.25
[Co(PLASP)( <u>D</u> -Val)]			520	+2.07	372	-0.38	332	+0.06
[Co(PLASP)( <u>D</u> , <u>L</u> -Val)]	538	+0.91	500	+1.08	375	-0.10	340	+0.11
[Co(PLASP)( <u>L</u> -AsN)] $\cdot$ H <sub>2</sub> O	545	+0.70	495	+1.01	375	+0.36	355	+0.34
[Co(PLASP)( <u>D</u> -AsN)] $\cdot$ 1/2H <sub>2</sub> O			504	+1.24	375	-0.41	332	+0.08
[Co(PLASP)( <u>L</u> -Phe)] $\cdot$ 3H <sub>2</sub> O	560	+0.36	485	+0.31	385	+0.18	360	+0.20
[Co(PLASP)( <u>D</u> -Phe)] $\cdot$ 2H <sub>2</sub> O			505	+1.68	375	-0.27	338	+0.10

<sup>a</sup>Units for  $\Delta\epsilon$  are (cm<sup>-1</sup>M<sup>-1</sup>).

Based upon the general shapes of bands I and II, the CD spectra of the Co(PLASP)(AA) complexes can be divided into three groups. The first group contains the Co(PLASP)(L-AA) and Co(PLASP)(Gly) complexes; their CD spectra are shown in Figure 3. For these complexes both bands I and II consist of two positive peaks, with the exception of band II of the glycinate complex which has a small negative and a small positive peak. The intensities of the peaks in band I vary considerably from one L-amino acidate to another, while the intensities of the peaks in band II remain fairly constant.

The second group consists of the Co(PLASP)(D-AA) complexes (Figure 4), in which band I is a single broad positive peak which also varies in intensity from one D-amino acidate to another. Band II consists of a small positive peak and a larger negative peak which, as in the case of the L-AA<sup>-</sup> complexes, does not vary greatly in intensity from one D-AA<sup>-</sup> to another.

Band I of the third group, containing only [Co(PLASP)-( $\alpha$ -AIBA)] $\cdot$ H<sub>2</sub>O and Co(PLASP)(D,L-Val) (Figure 5), consists of two positive peaks which are similar to those of band I of the L-AA<sup>-</sup> complexes. However, band II which is similar to band II of the D-AA<sup>-</sup> complexes (Figure 4) consists of

a negative and a positive peak. Since the Co(PLASP)(AA) complexes in the three groups mentioned above have the same basic structures, differing only at the  $\alpha$ -carbon of the amino acidate, differences in their CD peak intensities and shapes must be related to the differences at the  $\alpha$ -carbon of the amino acidates.

Previous work by various authors has shown that CD spectra of several cobalt(III) complexes containing optically active ligands can be separated into a configurational effect (the contribution to the CD spectrum from the spatial position of the chelate rings) and a vicinal effect (the contribution from an asymmetric ligand).<sup>4,6-10</sup> Similar arguments may be applied here to explain the differences in the CD spectra of the Co(PLASP)(AA) complexes. These spectra for the Co(PLASP)(AA) complexes should be resolvable into a Y contribution, where Y is the effect on the CD associated with a change in the optical activity of (or substitution at) the amino acidate  $\alpha$ -carbon, and an X contribution, where X is the effect on the CD associated with the rest of the complex.

Thus the value of  $\Delta\epsilon$  at a given wavelength in the CD spectrum of a Co(PLASP)(AA) complex may be expressed as follows:

$$X + Y_{\underline{D}} \text{ or } \underline{L} = \text{CD}[\text{Co}(\text{PLASP})(\underline{D}\text{- or } \underline{L}\text{-AA})] \quad (1)$$

If it is assumed that  $Y_{\underline{D}} = -Y_{\underline{L}}$ , then

$$X = \frac{\text{CD}[\text{Co}(\text{PLASP})(\underline{L}\text{-AA})] + \text{CD}[\text{Co}(\text{PLASP})(\underline{D}\text{-AA})]}{2} \quad (2)$$

Using CD data for pairs of  $\text{Co}(\text{PLASP})(\underline{D}\text{-AA})$  and  $\text{Co}(\text{PLASP})(\underline{L}\text{-AA})$  complexes, X values have been calculated for complexes where  $\text{AA}^- = \text{Val}^-$ ,  $\text{Phe}^-$ , and  $\text{AsN}^-$ .

The above treatment implies that X values for all  $\text{Co}(\text{PLASP})(\text{AA})$  complexes should be the same. That this is substantially the case is shown in Figure 6. From eq. 2, it follows that the CD spectrum of  $\text{Co}(\text{PLASP})(\underline{D}, \underline{L}\text{-Val})$  should also be the same as that of the calculated X values. This is verified in Figure 5. The presence of equal amounts of diastereomers in the  $\text{Co}(\text{PLASP})(\underline{D}, \underline{L}\text{-Val})$  complex is confirmed by its proton nmr spectrum (see below). Finally, it should be noted that the CD spectrum of the complex  $\text{Co}(\text{PLASP})(\alpha\text{-AIBA})$  containing a non-optically active amino acidate is essentially the same as that of  $\text{Co}(\text{PLASP})(\underline{D}, \underline{L}\text{-Val})$  (Figure 5) and that of the calculated X terms (Figure 6). These results support the assumption that the X contribution is essentially the same in all of these complexes.

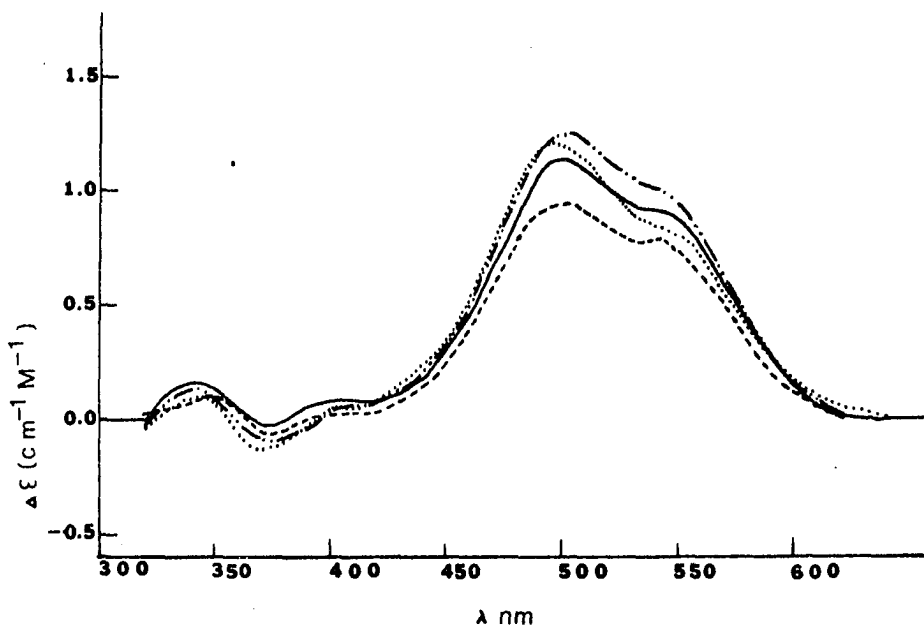


Figure 6. CD spectrum for  $[\text{Co}(\text{PLASP})(\alpha\text{-AIBA})]\cdot\text{H}_2\text{O}$  (.....) and calculated X terms from  $\{[\text{Co}(\text{PLASP})(\underline{\text{L}}\text{-Val})] + [\text{Co}(\text{PLASP})(\underline{\text{D}}\text{-Val})]\}/2$  (-.-.-),  $\{[\text{Co}(\text{PLASP})(\underline{\text{L}}\text{-AsN})]\cdot\text{H}_2\text{O} + [\text{Co}(\text{PLASP})(\underline{\text{D}}\text{-AsN})]\cdot 1/2\text{H}_2\text{O}\}/2$  (—) and  $\{[\text{Co}(\text{PLASP})(\underline{\text{L}}\text{-Phe})]\cdot 3\text{H}_2\text{O} + [\text{Co}(\text{PLASP})(\underline{\text{D}}\text{-Phe})]\cdot 2\text{H}_2\text{O}\}/2$  (----)

The Y terms, however, depend, as expected, upon the chirality and the nature of the R group at the optically active amino acidate  $\alpha$ -carbon. These factors are also important for determining the geometry of the  $AA^-$  chelate ring.

In order to accommodate a bulky R-group in the favorable equatorial position, an L-amino acidate should adopt the conformation shown in Figure 7a, while a D-amino acidate should adopt the conformation shown in Figure 7b. It should be noted that the L-Phe $^-$  chelate ring in solid  $[Co(PLASP)(\underline{L}\text{-Phe})] \cdot 3H_2O$  adopts the conformation shown in Figure 7a.<sup>2</sup> If the amino acidate has two groups of the same size attached to the  $\alpha$ -carbon as in  $\alpha$ -aminoisobutyrate ( $H_2NC(CH_3)_2CO_2^-$ ), the amino acidate could either adopt a planar conformation as in Figure 7c or equilibrate between the two structures in Figures 7a and 7b. Thus, the observed CD spectrum for  $Co(PLASP)(\alpha\text{-AIBA})$  should be a good approximation for X since the Y contribution will be either averaged to zero due to equilibration between the two structures in Figures 7a and 7b or zero due to the planar (no net Y) nature of the  $\alpha\text{-AIBA}^-$  chelate ring. This appears to be a reasonable approximation since, as noted above, the CD spectrum of the  $\alpha\text{-AIBA}^-$  complex is essentially the same

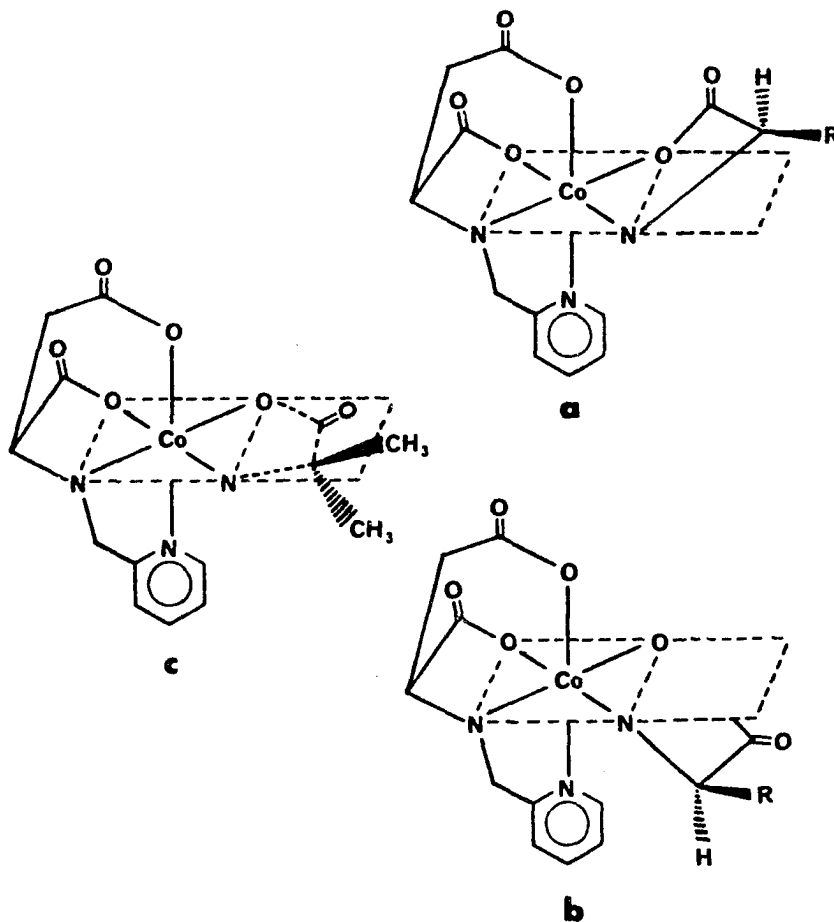


Figure 7. Possible  $AA^-$  chelate ring conformations in  
 a)  $Co(PLASP)(\underline{L}\text{-AA})$ , b)  $Co(PLASP)(\underline{D}\text{-AA})$   
 and c)  $Co(PLASP)(\alpha\text{-AIBA})$  complexes



as that of the Co(PLASP)(D,L-Val) complex and that of the calculated X terms.

Calculations of the Y terms for the Val<sup>-</sup>, Phe<sup>-</sup>, and AsN<sup>-</sup> diastereomers using eq. 1 and assuming X is equal to the observed CD spectrum of the [Co(PLASP)-( $\alpha$ -AIBA)] complex are given in Figure 8. Examination of these curves shows that to a first approximation, the assumption that  $Y_{\underline{D}} = -Y_{\underline{L}}$  in formulating eq. 2 is valid. Since the degree of bending of an L-amino acidate chelate ring from the coordination plane as in Figure 7a should be equal but opposite in direction to a D-amino acidate chelate ring as in Figure 7b, Y may represent the contribution of the amino acidate chelate ring bending to the overall CD spectrum. It should be noted that if any steric interaction or hydrogen bonding is present in one diastereomer (such as Co(PLASP)(L-AA)) and not in the other (such as Co(PLASP)(D-AA)), then  $Y_{\underline{D}}$  may not be equal to  $-Y_{\underline{L}}$ . This may occur in the Co(PLASP)(D and L-AsN<sup>-</sup>) complexes where the  $\beta$ -amide group is polar and capable of hydrogen bonding with other polar groups of the complex.

In addition to Y terms calculated from eqs. 1 and 2 for complexes with AA<sup>-</sup> = Val<sup>-</sup>, Phe<sup>-</sup>, and AsN<sup>-</sup>, these terms were also calculated for L-Ala<sup>-</sup>, L-Pro<sup>-</sup>, L-Thr<sup>-</sup>, and Gly<sup>-</sup> using eq. 1 assuming the X terms to be equal to the CD

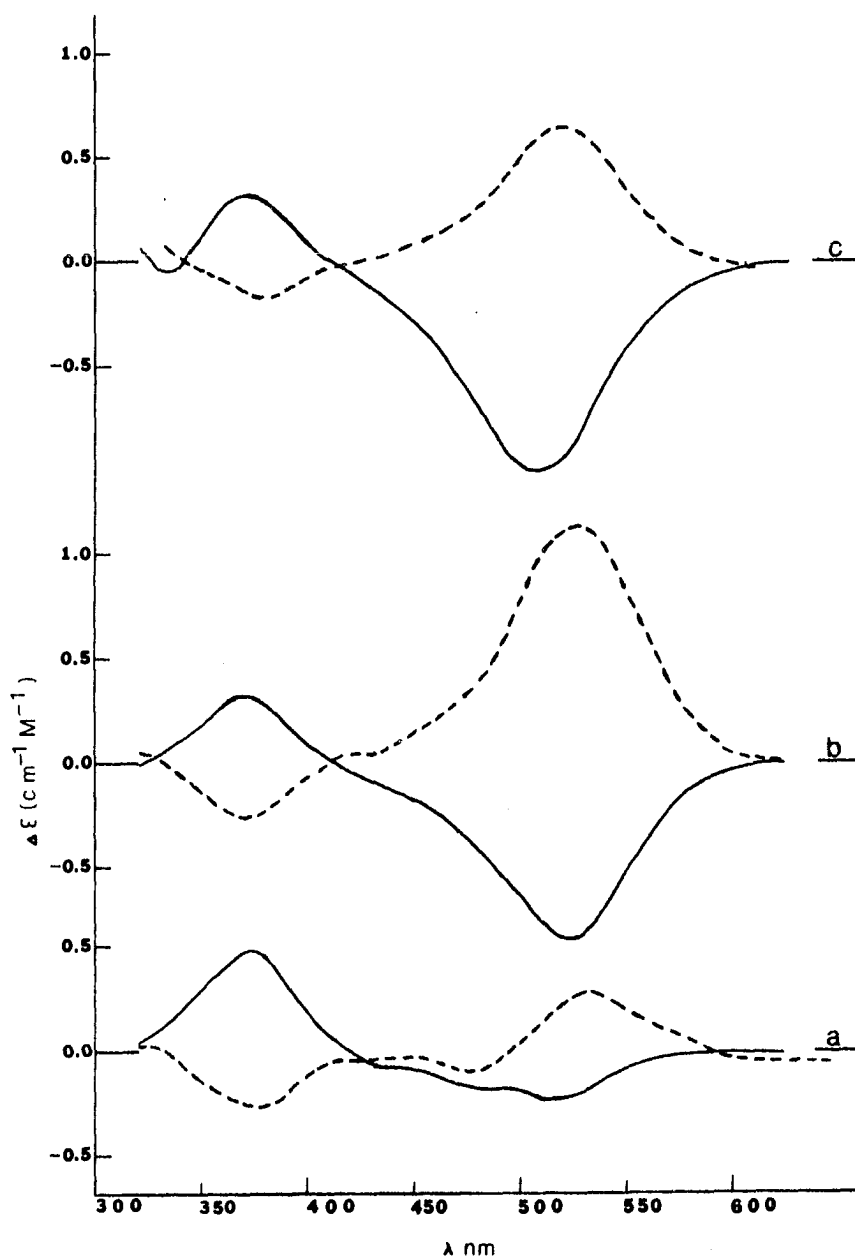


Figure 8. Y terms calculated by  $[\text{Co}(\text{PLASP})(\text{AA})]^-$ -  
 $[\text{Co}(\text{PLASP})(\alpha\text{-AIBA})] \cdot \text{H}_2\text{O}$  for a)  $\underline{\text{D}}\text{-Asn}^-$  (----)  
 and  $\underline{\text{L}}\text{-Asn}^-$  (—), b)  $\underline{\text{D}}\text{-Val}^-$  (----) and  $\underline{\text{L}}\text{-Val}^-$   
 (—) and c)  $\underline{\text{D}}\text{-Phe}^-$  (----) and  $\underline{\text{L}}\text{-Phe}^-$  (—)

spectrum of  $\text{Co(PLASP)}(\alpha\text{-AIBA})$ ; these Y terms are shown in Figure 9. The basic shape of the Y curves of all the  $\text{Co(PLASP)}(\underline{\text{L}}\text{-AA})$  complexes is essentially the same (Figures 8 and 9). This conclusion also includes the non-optically active  $\text{Gly}^-$ , which suggests that the  $\text{Gly}^-$  chelate ring has the conformation adopted by the  $\underline{\text{L}}$ -amino acidates (Figure 7a). It also indicates that the  $\text{AA}^-$  ligand need not be optically active in order to contribute a Y term to the spectrum. This suggests that it is the chelate ring conformation which is important in determining the magnitude of Y in the  $\text{Co(PLASP)}(\text{AA})$  complexes. Further evidence for the conformation (or bending) of the chelate rings is given in the discussion of the  $^1\text{H}$  nmr spectra of the  $\text{Co(PLASP)}(\text{AA})$  complexes.

$^1\text{H}$  nmr spectra of the  $\text{Co(PLASP)}(\text{AA})$  complexes      The  $^1\text{H}$  nmr spectra of the various  $\text{Co(PLASP)}(\text{AA})$  complexes and  $\text{PLASPH}_2$  in 99.7% deuterium oxide are given in Table IV. By comparing  $^1\text{H}$  nmr spectra of the various complexes given in Table IV, the proton chemical shifts of the coordinated  $\text{PLASP}^{2-}$  ligand (with the exception of the ortho pyridyl proton which will be considered later) are nearly identical and are not affected by the amino acidate present in the complex.

In general the  $\alpha$ -proton of the coordinated  $\text{PLASP}^{2-}$  occurs as a quartet at  $\delta$  3.95 while the  $\beta$ -methylene protons

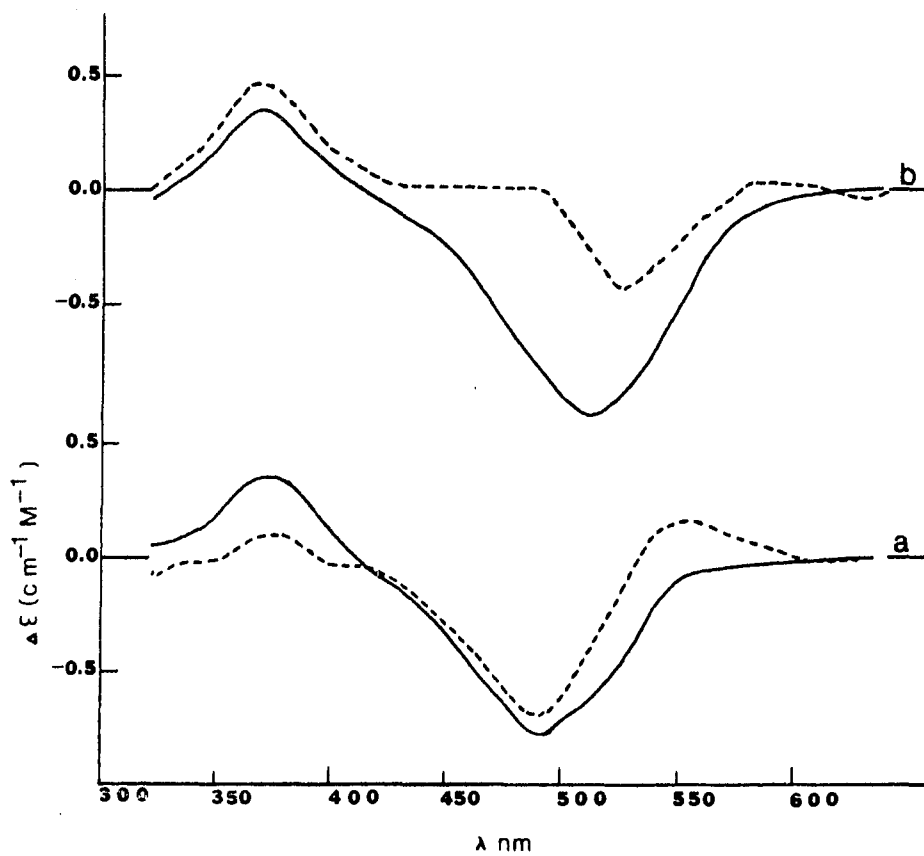


Figure 9. Y terms calculated by  $[\text{Co}(\text{PLASP})(\text{AA})]^-$ -  
 $[\text{Co}(\text{PLASP})(\alpha\text{-AIBA})] \cdot \text{H}_2\text{O}$  for a) Gly<sup>-</sup> (----)  
 and L-Ala<sup>-</sup> (—) and b) L-Pro<sup>-</sup> (----) and  
 L-Thr<sup>-</sup> (—)

Table IV. The  $^1\text{H}$  chemical shifts of various  $\text{Co}(\text{PLASP})(\text{AA})$  complexes and  $\text{PLASPH}_2$  in 99.7%  $\text{D}_2\text{O}^{\text{a}}$

$\text{AA}^-$	$\text{PLASP}^{2-}$						$\text{AA}^-$		
	$\delta$ $\alpha\text{-H}$	$\delta$ $\beta\text{-H}^{\text{b}}$	$\delta$ $\text{-CH}_2\text{-py}^{\text{c}}$	$\delta$ $\underline{\text{o}}\text{-py}$	$\delta$ $\underline{\text{m}}\text{-py}$	$\delta$ $\underline{\text{p}}\text{-py}$	$\delta$ $\alpha\text{-H}$	$\delta$ $\beta\text{-H}$	$\delta$ $\gamma\text{-H}$
$\alpha\text{-AIBA}^-$	3.95q	3.07m	5.21d 4.48d	8.21d	7.60m	8.07t		1.23s 1.51s	
$\text{Gly}^-$	3.94q	3.08m	5.19d 4.46d	8.24d	7.60m	8.08t	3.61d <sup>d</sup> 3.27d		
$\underline{\text{L}}\text{-Val}^-$	3.95q	3.07m	5.24d 4.48d	8.21d	7.59m	8.07t	3.69d	2.27m	0.94d 0.70d
$\underline{\text{D}}\text{-Val}^-$	3.94q	3.06m	5.24d 4.51d	8.11d	7.60m	8.07t	3.36d	2.30m	0.96d 0.89d
$\underline{\text{D}}, \underline{\text{L}}\text{-Val}^-$	3.94m	3.06m	5.24d 4.49d 4.47d	8.20d 8.11d	7.58m	8.06t	3.68d 3.36d	2.27m	0.95d <sup>e</sup> 0.70d <sup>e</sup> 0.88d
$\underline{\text{L}}\text{-Pro}^-$	3.97q	3.09m	5.31d 4.52d	8.29d	7.64m	8.10t	4.18m	2.9- 1.2m <sup>f</sup>	
$\underline{\text{L}}\text{-Thr}^-$	3.97q	3.09m	5.23d 4.42d	8.18d	7.56m	8.04t	3.63d	4.36m	1.20d
$\underline{\text{L}}\text{-AsN}^-$	3.94m	3.09m	5.21d 4.46d	8.29d	7.56m	8.06t	3.94m	2.85d	
$\underline{\text{D}}\text{-AsN}^-$	3.94q	3.07m	5.23d 4.48d	8.18d	7.60m	8.08t	3.69q	2.84m	

<u>L</u> -Phe <sup>-</sup>	3.93q	3.1m	5.29d 4.48d	7.87d	7.47m	8.00t	4.1m	3.1m	7.24m <sup>g</sup>
<u>D</u> -Phe <sup>-</sup>	3.91q	3.1m	5.30d 4.44d	8.19d	7.52m	8.04t	3.65	3.4m	7.34m <sup>g</sup>
PLASPH <sub>2</sub>	4.03t	3.01d	4.50s	8.62d	7.56m	8.01t			

<sup>a</sup>The center of each peak (or peaks) is given and the multiplicity is given by s = singlet, d = doublet, t = triplet, q = quartet and m = multiplet.

<sup>b</sup>The multiplet consists of two overlapping AB quartets.

<sup>c</sup>The coupling constant for the doublets given in this column is 18 Hz.

<sup>d</sup>J = 17 Hz.

<sup>e</sup>The relative areas for the  $\gamma$ -methyl groups are a total of 3 for the doublets at 0.96 and 0.88 and 1 for the doublet at 0.70. The coupling constant for each doublet is 7 Hz.

<sup>f</sup>This region includes the  $\beta$ ,  $\gamma$  and  $\delta$  protons of the proline ligand.

<sup>g</sup>The peak given is for all the phenyl protons of the phenylalaninate ligand.

occur as two overlapping quartets (arising from an ABX pattern) centered at  $\delta$  3.1. The pyridylmethylene protons appear as two doublets centered at  $\delta$  5.25 and 4.46 with a coupling constant of 18 Hz. This coupling constant is similar to those reported for the methylene protons of cobalt(III) complexes containing ligands such as  $\text{O}_2\text{C}-\text{CH}_2-\text{NH}-\text{CH}_2-\text{CO}_2^-$ ,  $\text{IMDA}^{2-}$ .<sup>10,11</sup> The pyridyl protons of the coordinated  $\text{PLASP}^{2-}$  exhibit a complex pattern (Figure 10) which is similar to the splitting observed for 2-picoline.<sup>12</sup> The meta protons occur as a multiplet (an overlapping doublet and triplet) centered at  $\delta$  7.5-7.6 while the para proton occurs as a triplet centered at  $\delta$  8.05. The ortho proton occurs as a doublet whose position varies from  $\delta$  7.87 to 8.29.

A comparison of the chemical shifts for the ortho pyridyl protons in Figure 10 reveals that the shifts of the various D-amino acidate complexes remain fairly constant ( $\delta$  8.11-8.19) while the shifts of certain L-amino acidate complexes are slightly deshielded when compared to the D-amino acidates; also the shifts of the L-amino acidate complexes do not remain constant ( $\delta$  8.29-7.87). These differences in chemical shifts for all the complexes can be accounted for if the direction of chelate ring bending and the size and type of R-group are considered. In the D-analogs (Figure 7b) the chelate ring is bent downward and

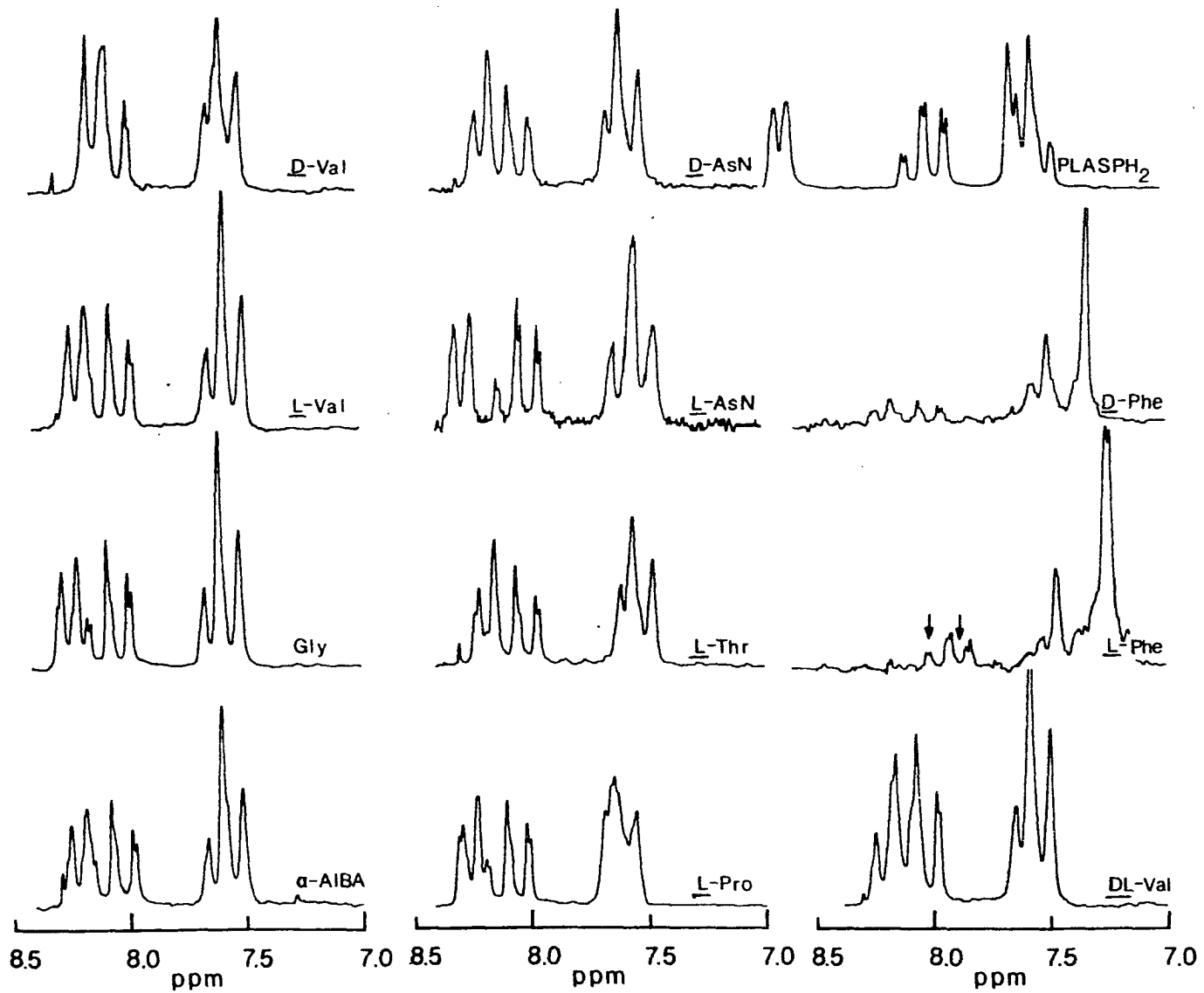


Figure 10. Proton nmr for the pyridyl protons of PLASPH<sub>2</sub> and various Co(PLASP)(AA) complexes in 99.7% D<sub>2</sub>O



toward the ortho proton while in the L-analogs (Figure 7a) the chelate ring is bent upward and away from the ortho proton. Thus the  $\alpha$ -carboxylate of the amino acidate is closer to the ortho proton in the D-analogs giving rise to a greater amount of shielding relative to the L-amino acidates. The variation in the chemical shift of the ortho proton in the L-amino acidate complexes may be attributed to the presence of a bulky R-group in the vicinity of the ortho pyridyl proton. The shielding of the ortho pyridyl proton in the L-Phe<sup>-</sup> complex presumably is due to the orientation of the phenyl group which has been shown by an X-ray structure to be in a shielding position in the solid state.

Although the PLASP<sup>2-</sup> protons (with the exception of the ortho pyridyl proton) in the different Co(PLASP)(AA) complexes do not vary, there are considerable differences in the chemical shifts of the amino acidate protons of the enantiomers of Val<sup>-</sup>, Asn<sup>-</sup> and Phe<sup>-</sup>, of the glycinate protons, and of the  $\alpha$ -AIBA<sup>-</sup> methyl protons. In general, the  $\alpha$ -protons of the L-amino acidates occur at lower fields than those of the D-analogs. This is presumably due to the positioning of the  $\alpha$ -protons of the D-amino acidates over the pyridine  $\pi$  cloud. Likewise the glycinate proton at  $\delta$  3.27 and the methyl group of  $\alpha$ -AIBA<sup>-</sup> at  $\delta$  1.23 can be assigned to those protons pointing over

the pyridyl ring while the glycinate proton at  $\delta$  3.61 and the  $\alpha$ -AIBA<sup>-</sup> methyl at  $\delta$  1.51 can be assigned to those directed away from the pyridine group. Although a similar trend is not seen for the  $\beta$ -protons of the amino acidates, the  $\gamma$ -protons of L-Val<sup>-</sup> and the phenyl protons of L-Phe<sup>-</sup> are upfield from their D-analogs. Both L-Val<sup>-</sup> and D-Val<sup>-</sup> have a  $\gamma$ -methyl group at  $\delta$  0.95 but in L-Val<sup>-</sup> (which has its R group near the pyridyl ring) the second  $\gamma$ -methyl group is shielded ( $\delta$  0.70) more than the corresponding  $\gamma$ -methyl group ( $\delta$  0.89) of D-Val<sup>-</sup> (which has its R group away from the pyridyl ring). This trend is the same for L-Phe<sup>-</sup> where the phenyl group is close to the pyridyl ring and thus shielded ( $\delta$  7.24) when compared to the D-Phe<sup>-</sup> phenyl group ( $\delta$  7.34). The smaller difference in chemical shifts between the  $\gamma$ -protons of D and L-Val<sup>-</sup> as compared to their  $\alpha$ -proton difference is presumably due to the greater distance from the pyridyl ring to these  $\gamma$ -protons.

<sup>13</sup>C nmr spectra of the Co(PLASP)(AA) complexes      The

<sup>13</sup>C nmr spectra for PLASPH<sub>2</sub>, PLASPNa<sub>2</sub> and the various Co(PLASP)(AA) complexes in D<sub>2</sub>O and 70% H<sub>3</sub>PO<sub>4</sub> are given in Table V. The chemical shifts of the PLASP<sup>2-</sup> portion of the complex remain constant in all complexes and do not seem to be affected by the type of amino acidate used. This is consistent with assigning the same structure

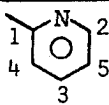
Table V.  $^{13}\text{C}$  nmr of the Co(PLASP)(AA) complexes in  $\text{D}_2\text{O}^{\text{a}}$ 

Complex	PLASP $^{2-}$				
	$\alpha\text{-CO}_2^-$	$\beta\text{-CO}_2^-$	$\alpha\text{-C}$	$\beta\text{-C}$	py-C-N
[Co(PLASP)(Gly)]	183.1	177.0	68.4	59.0	37.8
[Co(PLASP)( $\alpha$ -AIBA)] $\cdot\text{H}_2\text{O}$	183.0	176.8	68.5	59.2	38.0
[Co(PLASP)( <u>L</u> -Thr)] $\cdot 1\ 1/2\text{H}_2\text{O}$	183.0	177.0	68.5	59.2	37.7
[Co(PLASP)( <u>L</u> -Pro)] $\cdot 1\ 1/2\text{H}_2\text{O}$	183.0	176.9	68.6	59.1	38.0
[Co(PLASP)( <u>L</u> -Val)]	183.0	176.9	68.5	59.2	37.9
[Co(PLASP)( <u>D</u> -Val)]	183.1	176.6	68.4	59.2	38.0
[Co(PLASP)( <u>D</u> , <u>L</u> -Val)]	183.0 183.2	177.0 176.7	68.5	59.2	37.9
[Co(PLASP)( <u>L</u> -AsN)]	183.2	177.1	68.5	59.1	37.9
[Co(PLASP)( <u>D</u> -AsN)]	183.3	176.9	68.4	59.1	37.9
[Co(PLASP)( $\alpha$ -AIBA)] $\cdot\text{H}_2\text{O}^{\text{b}}$	183.1	180.4	67.5	59.4	36.8
[Co(PLASP)( <u>L</u> -Ala)] $^{\text{b}}$	183.1	180.7	67.6	59.4	36.6
[Co(PLASP)( <u>L</u> -Phe)] $\cdot 3\text{H}_2\text{O}^{\text{b}}$	183.3	180.2	67.9		38.7
[Co(PLASP)( <u>D</u> -Phe)] $\cdot 2\text{H}_2\text{O}^{\text{b}}$	182.9	180.5	67.6		37.3
PLASPH $_2$	174.8	172.4	58.5	50.5	34.7
PLASPNa $_2$	181.2	180.1	61.5	52.6	41.8

<sup>a</sup>The chemical shifts are given downfield from TMS with dioxane used as an internal reference at 67.0 ppm.

<sup>b</sup>In 70%  $\text{H}_3\text{PO}_4$  (aqueous).

<sup>c</sup>Phenyl ring carbon resonances.

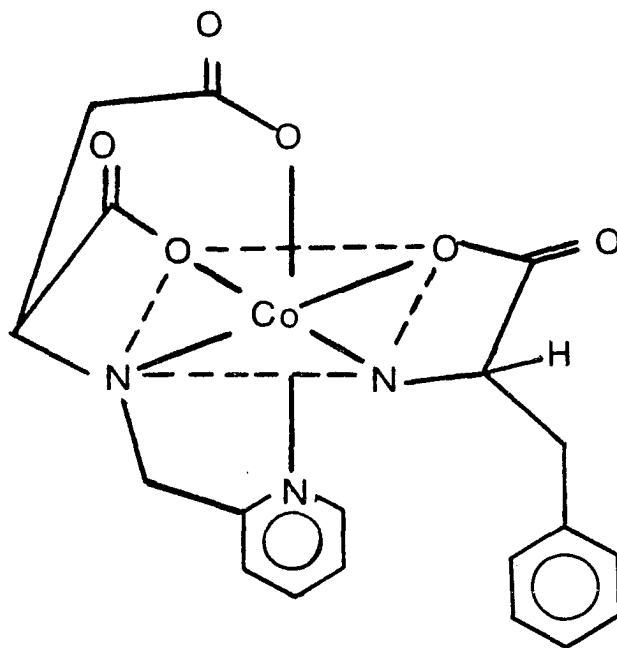
PLASP <sup>2-</sup>					AA <sup>-</sup>			
					$\alpha$ -CO <sub>2</sub> <sup>-</sup>	$\alpha$ -C	$\beta$ -C	$\gamma$ -C
1	2	3	4	5				
165.2	150.1	141.6	126.0	122.9	185.6	46.8		
165.4	149.6	141.6	126.1	123.1	189.9	61.4	27.6 27.5	
165.3	150.2	141.5	125.6	122.5	184.8	66.8	63.7	18.8
164.7	149.8	141.7	126.3	123.6	187.1	66.3	50.0	29.3 26.0
165.5	149.7	141.6	126.0	122.8	186.0	63.9	30.2	18.1 15.7
165.4	149.7	141.5	126.1	123.1	186.1	63.4	30.0	18.6 16.0
165.5				122.9	186.0	63.7	30.2	18.0 18.5
165.4	149.7	141.5	126.0	123.1	186.1	63.4	29.9	15.7 15.9
165.0	150.9	141.5	125.4	122.5	185.0	54.9	35.6	175.2
165.4	149.9	141.6	126.2	123.1	185.0	55.3	37.6	174.8
164.9	149.7	142.9	127.2	123.9	191.0	63.0	27.8 27.3	
164.6	149.8	142.9	127.4	123.9	188.1	55.2	18.5	
164.7	150.0	142.7	127.4	123.8	187.1			135.2 <sup>C</sup> 129.8
163.9	148.6	141.9	127.1	123.4	186.3			134.1 <sup>C</sup> 130.2
150.1	148.9	140.2	125.4	125.2				
157.9	148.8	138.6	123.6	123.4				

(Figure 1a) to all the various Co(PLASP)(AA) complexes isolated. The  $\alpha$ -CO<sub>2</sub><sup>-</sup> carbon resonances of the chelated PLASP<sup>2-</sup> ligand in D<sub>2</sub>O were observed to fall in the range 183.0-183.3 ppm while the  $\beta$ -CO<sub>2</sub><sup>-</sup> carbon resonances fall in the range 176.6-177.1 ppm. The  $\alpha$ -carbon resonances occur in the range 68.4-68.5 ppm and the  $\beta$ -carbon resonances occur at 59.0-59.2 ppm. The above assignments are consistent with the chemical shifts for cobalt complexes containing aspartic acid previously reported.<sup>13,14</sup> The pyridylmethyl carbons fall in the range 37.7-38.0 ppm while the pyridyl carbons range from 122.5-165.5 ppm and are assigned further in Table V. Spectra of the less soluble complexes containing Ala<sup>-</sup> and Phe<sup>-</sup> were obtained in 70% H<sub>3</sub>PO<sub>4</sub> and are similar to the <sup>13</sup>C spectra of the more soluble complexes in D<sub>2</sub>O. The largest difference occurs in the chemical shift of the  $\beta$ -CO<sub>2</sub><sup>-</sup> carbon of the PLASP<sup>2-</sup> ligand. This change in the  $\beta$ -CO<sub>2</sub><sup>-</sup> carbon resonance may be due to some protonation of the  $\beta$ -CO<sub>2</sub><sup>-</sup> group by the H<sub>3</sub>PO<sub>4</sub> solvent.

The  $\alpha$ -CO<sub>2</sub><sup>-</sup> and  $\alpha$ -carbon resonances of the coordinated amino acidates vary considerably and range from 184.8-189.9 ppm and 46.8-66.8 ppm, respectively, and agree with previous reported values for chelated  $\alpha$ -amino acidates.<sup>15</sup> The  $\beta$  and  $\gamma$  (or phenyl) carbons are assigned in Table V and also agree with previously reported values.<sup>16</sup>

## CONCLUSION

In a previous paper we reported the crystal structure for  $[\text{Co}(\text{PLASP})(\underline{\text{L}}\text{-Phe})] \cdot 3\text{H}_2\text{O}$  (shown below) and suggested that this facial  $\text{Co}(\text{III})\text{N}_3\text{O}_3$  structure was due to a



favorable combination of electronic, structural and steric factors.<sup>2</sup> The coordination of the tetradentate  $\text{PLASP}^{2-}$  ligand with its pyridyl group trans to the  $\beta\text{-CO}_2^-$  group of  $\text{PLASP}^{2-}$  gives the least strained bond angle around the secondary amino nitrogen and thus is presumably favored structurally over the more strained structures (Figures 1b and 1d) in which the pyridyl group is trans

to the  $\alpha$ -CO<sub>2</sub><sup>-</sup> group of PLASP<sup>2-</sup>. There were results in the literature to suggest that coordination of the L-Phe<sup>-</sup> amino acidate to give a facial isomer is electronically favored over a meridional Co(III)N<sub>3</sub>O<sub>3</sub> structure. Finally it was suggested that coordination of the L-Phe<sup>-</sup> ligand was sterically favored when compared to a D-amino acidate since the  $\alpha$ -carbon of the L-Phe<sup>-</sup> chelate ring is pointing up and away from the pyridyl ring.

From the present study, it appears that the D or L configuration of the amino acidate does not play a large role in determining the overall geometry of the Co(PLASP)(AA) complexes since the same isomer (Figure 1a) was isolated for both enantiomers of Val<sup>-</sup>, Phe<sup>-</sup> and AsN<sup>-</sup>. Thus, only electronic and structural factors seem to have a major role in determining the overall geometry of the Co(PLASP)(AA) complexes.

## REFERENCES

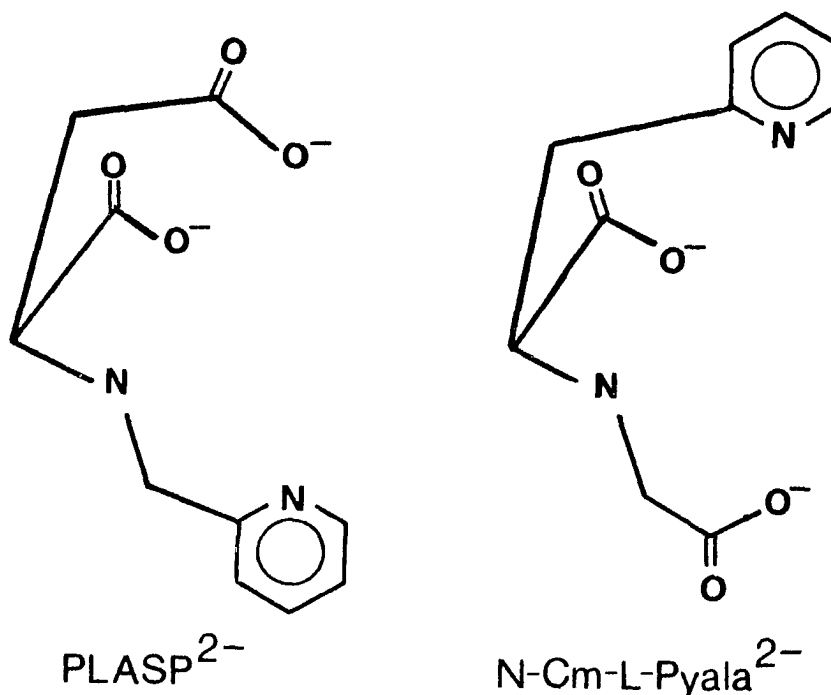
1. Nakon, R.; Rechani, P. R.; Angelici, R. J. Inorg. Chem. 1973, 12, 2431.
2. Meiske, L. A.; Jacobson, R. A.; Angelici, R. J. submitted for publication to Inorg. Chem.
3. Watabe, M.; Onuki, K.; Yoshikawa, S. Bull. Chem. Soc. Japan 1975, 48, 687.
4. Douglas, B. E.; Yamada, S. Inorg. Chem. 1965, 4, 1561.
5. Denning, R. G.; Piper, T. S. Inorg. Chem. 1966, 5, 1056.
6. Koine, N.; Sakota, N.; Hidaka, J.; Shimura, Y. Bull. Chem. Soc. Japan 1969, 42, 1583.
7. Koine, N.; Sakota, N.; Hidaka, J.; Shimura, Y. Bull. Chem. Soc. Japan 1970, 43, 1737.
8. Koine, N.; Sakota, N.; Hidaka, J.; Shimura, Y. Inorg. Chem. 1973, 12, 859.
9. Liu, C. T.; Douglas, B. E. Inorg. Chem. 1964, 3, 1356.
10. Legg, J. I.; Cooke, D. W. Inorg. Chem. 1966, 5, 594.
11. Legg, J. I.; Cooke, D. W.; Douglas, B. E. Inorg. Chem. 1967, 6, 700.
12. Pouchet, C. J.; Campbell, J. R. "Aldrich Library of NMR Spectra", Aldrich Chemical Company, Inc., Milwaukee, Wisconsin, 1974; 9, 2B.
13. Ama, T.; Yasui, T. Chemistry Letters 1974, 1295.
14. Yasui, T.; Ama, T. Bull. Chem. Soc. Japan 1975, 48, 3171.
15. Ama, T.; Yasui, T. Bull. Chem. Soc. Japan 1976, 49, 472.
16. Horsley, W.; Sternlicht, H.; Cohen, J. S. J. Am. Chem. Soc. 1970, 92, 680.



SECTION III. SYNTHESIS AND SPECTRAL CHARACTERIZATION OF  
fac- AND mer-[N-Carboxymethyl-L- $\beta$ -(2-pyridyl)-  
 $\alpha$ -alaninato] [D-threoninato]cobalt(III),  
Co(N-Cm-L-Pyala) (D-Thr) AND THE MOLECULAR  
STRUCTURE OF THE mer- ISOMER

## INTRODUCTION

Metal complexes of the two asymmetric tetradentate ligands, N-(2-pyridylmethyl)-L-aspartate (PLASP<sup>2-</sup>) and N-carboxymethyl-L-β-(2-pyridyl)-α-alaninate (N-Cm-L-Pyala<sup>2-</sup>) (see below), exhibit stereoselective effects in coordinating



optically active amino acidates (AA<sup>-</sup>).<sup>1,2</sup> Stereoselectivity has also been found in the formation of their Co(III) complexes. Thus the only isolated isomer of the Co(PLASP)-(AA) complexes is a facial isomer in which the pyridine nitrogen is coordinated trans to the β-carboxylate group of the PLASP<sup>2-</sup> ligand.<sup>3,4</sup> This coordination geometry was

ascribed to a combination of electronic, structural and steric factors. In order to investigate these factors further, a series of mixed complexes of the type  $\text{Co}(\text{N-Cm-L-Pyala})(\text{AA})$ , where  $\text{N-Cm-L-Pyala}^{2-}$  is shown above and  $\text{AA}^-$  is a potentially bidentate amino acidate, was prepared.

Comparison of the two ligands,  $\text{PLASP}^{2-}$  and  $\text{N-Cm-L-Pyala}^{2-}$  (see above) shows that the pyridyl and  $\beta\text{-CO}_2^-$  groups of  $\text{PLASP}^{2-}$  are interchanged in the  $\text{N-Cm-L-Pyala}^{2-}$  ligands. In view of the relatively minor structural differences between these ligands, it was of interest to compare the structures of the  $\text{Co}(\text{III})$  complexes for the purpose of understanding the factors which contribute to the formation of the observed  $\text{Co}(\text{III})$  complex isomers. For this reason, isomers of  $\text{Co}(\text{N-Cm-L-Pyala})(\text{AA})$  (Figure 1) were prepared and structurally characterized for comparison with the analogous  $\text{Co}(\text{PLASP})(\text{AA})$  and other related  $\text{Co}(\text{III})\text{N}_3\text{O}_3$  complexes.<sup>3-7</sup>

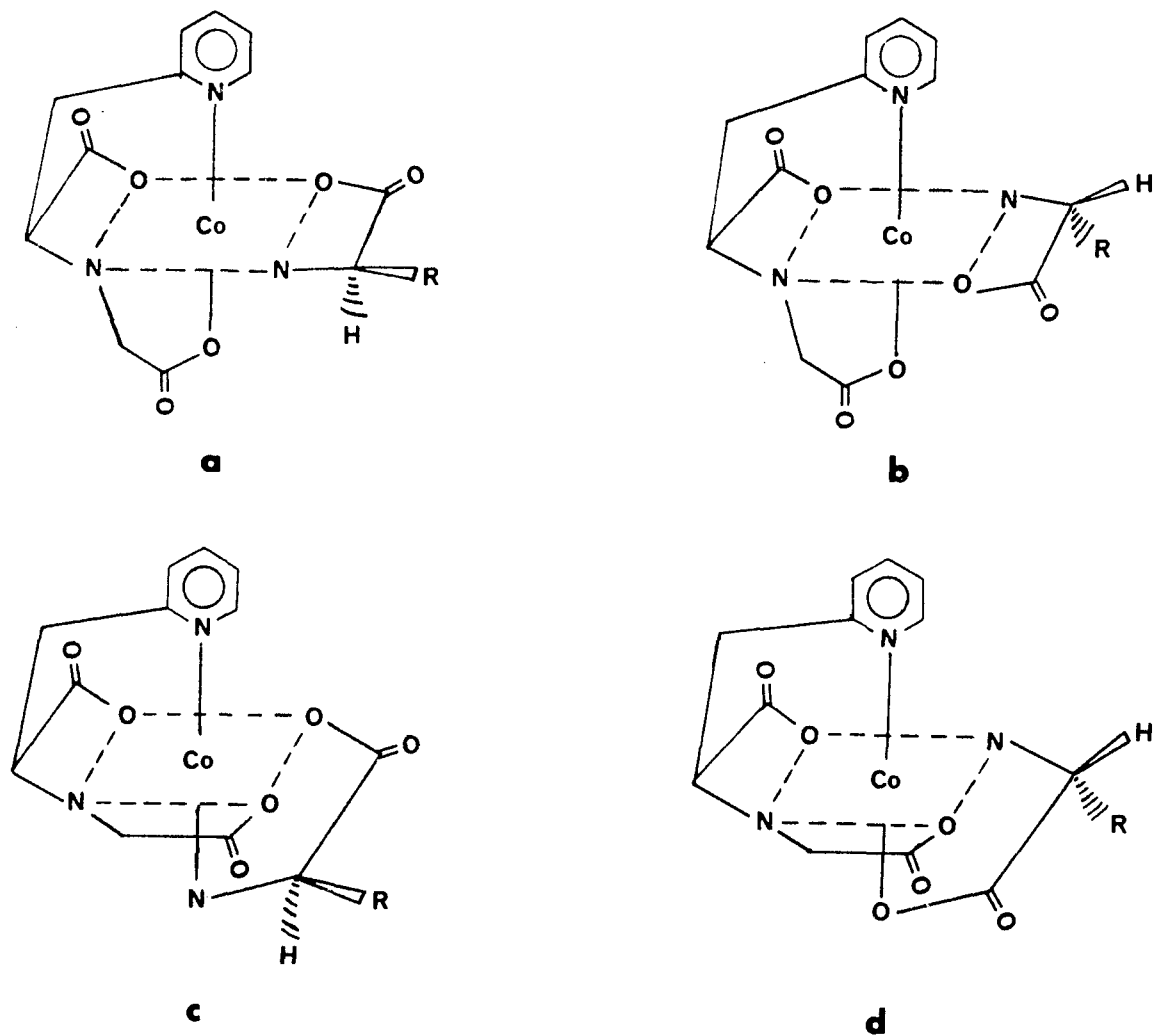


Figure 1. The four possible isomers of  $\text{Co}(\text{N-Cm-L-Pyala})-(\text{D-AA})$ : a) fac, b) mer  $\text{N-Cm-CO}_2^-$ , c) mer  $\text{AA}^-$  amino and d) mer  $\text{AA}^- \text{CO}_2^-$

## EXPERIMENTAL SECTION

Purification of N-carboxymethyl-L-β-(2-pyridyl)-α-alanine, N-Cm-L-PyalaH<sub>2</sub> The ligand, N-Cm-L-PyalaH<sub>2</sub>, was prepared as previously reported.<sup>2</sup> Its purification was performed by ion exchange chromatography using Dowex 50W-X8 (50-100 mesh) in the H<sup>+</sup> form in a manner similar to that described previously for N-(2-pyridylmethyl)-L-aspartic acid.<sup>4</sup> Fractions with pH values between 2.8 and 4.0 were combined and reduced to near dryness. Absolute ethanol was added to precipitate additional product, and the resulting slurry was filtered. The product, N-Cm-L-PyalaH<sub>2</sub>, was identified by comparing its melting point and <sup>1</sup>H nmr spectrum to those previously reported.<sup>2</sup>

Preparation of fac-[N-carboxymethyl-L-β-(2-pyridyl)-α-alaninato] [D-threoninato]cobalt(III)·monohydrate, fac-[Co(N-Cm-L-Pyala) (D-Thr)]·H<sub>2</sub>O, and mer-[N-carboxymethyl-L-β-(2-pyridyl)-α-alaninato] [D-threoninato]cobalt(III).

hemihydrate, [Co(N-Cm-L-Pyala) (D-Thr)]·1/2H<sub>2</sub>O To an aqueous solution containing D-threonine (0.30 g, 2.5 mmol), N-Cm-L-PyalaH<sub>2</sub> (0.56 g, 2.5 mmol) and 6 ml of 1.0 N NaOH in 20 ml of water was added a solution of CoSO<sub>4</sub>·7H<sub>2</sub>O (0.70 g, 2.5 mmol) and 3 ml of 5% H<sub>2</sub>O<sub>2</sub> (aqueous) in 15 ml of water. The reaction mixture was stirred overnight at room temperature

to give a purple solution. This solution was filtered and reduced to ~10 ml in vacuum giving a reddish pink precipitate which was later identified as the facial isomer. The facial isomer was filtered off, and the remaining solution was placed on a column (1.7 x 55 cm) of acidic alumina (120 ml). The column was eluted with 40:60 EtOH:H<sub>2</sub>O to give two bands. The purple meridional isomer along with other impurities was not adsorbed on the column and eluted as band I. The less soluble facial isomer was retained on the column and slowly moved down the column as band II. Band II was reduced to near dryness in vacuum yielding the facial isomer as a reddish pink solid which was removed by filtration and washed with 95% ethanol. Band I was reduced to dryness in vacuum, dissolved in 3-4 ml of water, loaded on a column (1.5 x 65 cm) of Dowex 50W-X8 (100-200 mesh) in the Na<sup>+</sup> form and eluted with water to give two bands. The first was light brown and contained decomposition products along with Na<sub>2</sub>SO<sub>4</sub>. The second band which contained the purple meridional isomer was reduced to dryness in vacuum and dissolved in 2 ml of H<sub>2</sub>O. The solution was filtered through glass wool into a 10 mm nmr tube. Upon standing for several days crystals began to form. These

were filtered and found to be suitable for X-ray analysis. A second batch of crystals was obtained by addition of 95% EtOH to the filtrate. The total yield of the facial isomer was 145 mg (15%) and of the meridional isomer 56 mg (6%). Anal. calcd. for fac-[Co(N-Cm-L-Pyala)(D-Thr)]·H<sub>2</sub>O, C<sub>14</sub>H<sub>18</sub>N<sub>3</sub>O<sub>7</sub>Co·H<sub>2</sub>O: C, 40.30; H, 4.80; N, 10.07. Found: C, 40.36; H, 5.14; N, 10.05. Anal. calcd for mer-[Co(N-Cm-L-Pyala)(D-Thr)]·1/2H<sub>2</sub>O, C<sub>14</sub>H<sub>18</sub>N<sub>3</sub>O<sub>7</sub>Co·1/2H<sub>2</sub>O: C, 41.19; H, 4.66; N, 10.30. Found: C, 41.87; H, 4.79; N, 10.30.

Spectra Visible and circular dichroism spectra were recorded in water at room temperature using a Jasco ORD/UV/CD-5 spectrophotometer. Proton nmr spectra of the meridional and facial isomers and the free ligand, N-Cm-L-PyalaH<sub>2</sub>, were recorded at room temperature on a Jeol FX-90Q spectrometer in 99.7% deuterium oxide with t-butyl alcohol ( $\delta$  1.23 ppm) as an internal reference and deuterium as an internal lock. The peak positions ( $\delta$ ) are given in ppm downfield from TMS.

Crystal data The crystals were obtained as red-violet elongated hexagonal plates in the manner described above. A crystal of approximate dimensions 0.08 x 0.2 x 0.25 mm ( $\mu = .11.4 \text{ cm}^{-1}$ ) was mounted on a glass fiber. The fiber was then positioned on a goniometer head and

three preliminary  $\omega$ -oscillation photographs were taken at various  $\chi$  and  $\phi$  settings on an automated four-circle diffractometer. From these photographs 10 independent reflections were selected and their coordinates were input to the automatic indexing program ALICE.<sup>8</sup> The resulting reduced cell and reduced cell scalars indicated  $P2_1$  (monoclinic) symmetry which was subsequently verified by three axial  $\omega$ -oscillation photographs. The layer spacings observed in these photographs agreed within experimental error with those predicted for this cell by the indexing program. The lattice constants were determined by least-squares refinement based on the  $\pm 2\sigma$  measurements of 12 high-angle reflections on a previously aligned diffractometer (Mo- $K_{\alpha}$  radiation,  $\lambda = 0.70954 \text{ \AA}$ ) at 27° C. The constants are  $a = 10.350(4)$ ,  $b = 10.339(4)$ ,  $c = 15.340(6)$ ,  $\beta = 92.98(5)$ ,  $V = 1639(1) \text{ \AA}^3$  and  $Z = 4$ . The observed density is  $1.6 \text{ g/cm}^3$  by the flotation method and the calculated density using the above cell constants is  $1.65 \text{ g/cm}^3$ .

Collection and reduction of X-ray intensity data The data were collected at 27° C with an automated four-circle diffractometer (using graphite-monochromated Mo- $K_{\alpha}$  radiation) designed and built at Ames Laboratory and previously described



by Rohrbaugh and Jacobson.<sup>9</sup> All the data (3468 reflections) in the  $hkl$  and  $\bar{h}\bar{k}l$  octants within a  $2\sigma$  sphere of  $50^\circ$  ( $\sin \theta/\lambda = 0.596 \text{ \AA}^{-1}$ ) were measured using an  $\omega$  step-scan technique.

To assure electronic and crystal stability, the intensities of three standard reflections were measured after every seventy-five reflections. These standard reflections did not change significantly throughout the entire data collection period. Examination of the data revealed systematic absences of the  $0k0$  reflections for  $k = 2n + 1$ , thus uniquely defining the space group as  $P2_1$ .

The measured intensity data were corrected for Lorentz and polarization effects. Since a scan around the goniometer axis showed all measured intensities to be within 6%, no absorption corrections were made on the measured intensity data.

The estimated variance in each intensity was calculated by  $\sigma_I^2 = C_T + K_t C_B + (0.03C_T)^2 + (0.03C_B)^2$ , where  $C_T$  and  $C_B$  represent total and background count, respectively,  $K_t$  is a counting time constant, and the factor 0.03 represents an estimate of nonstatistical errors. The estimated standard deviations in the structure factor amplitudes were calculated by the method of finite differences.<sup>10</sup> Of the 3468 reflections collected, 3285 independent reflections had  $I_o \geq 3\sigma_I$  and were used in the structure solution and refinement.

Solution and refinement of the structure The positions of the two cobalt atoms in the asymmetric unit were obtained by analysis of a sharpened three-dimensional Patterson function. The remaining atoms were found by successive structure factor<sup>11</sup> and electron density map calculations.<sup>12</sup> The positional parameters for all non-hydrogen atoms and their anisotropic thermal parameters were refined by a block matrix least squares procedure<sup>13</sup> to a weighted R factor of .085. The final refinement of parameters was by a full matrix least squares procedure,<sup>11</sup> minimizing the function  $\sum w (|F_o| - |F_c|)^2$ , where  $w = 1/\sigma_F^2$ , to a conventional discrepancy factor of  $R = \sum ||F_o| - |F_c|| / \sum |F_o| = 0.084$ . The scattering factors were those of Hanson et al.,<sup>14</sup> modified for the real and imaginary parts of anomalous dispersion.<sup>15</sup>

The solution and refinement of the structure were completed without attempting to refine the absolute configuration of the ligands. The configurations of chiral atoms in the complex were based on the known configurations of N-Cm-L-PyalaH<sub>2</sub><sup>1</sup> and D-threonine used in the synthesis of the complex.

The final positional and thermal parameters are given in Table I. The standard deviations were calculated from the inverse matrix of the final least squares cycle.<sup>16</sup> Bond lengths and angles are given in Tables II and III.

Table I. Final atomic parameters

(a) Final positional parameters ( $\times 10^4$ ) and their standard deviations (in parentheses)<sup>a</sup>

	<u>x</u>	<u>y</u>	<u>z</u>
Co1 <sup>b</sup>	1596 (1)	0	4115.3 (7)
O11	1543 (5)	1804 (5)	4272 (4)
O12	1360 (6)	3273 (6)	5329 (4)
O13	1548 (6)	-1835 (6)	4069 (4)
O14	1293 (6)	-3529 (5)	4936 (5)
O15	2113 (5)	135 (6)	2950 (3)
O16	1449 (7)	753 (10)	1611 (4)
OT1	-1324 (9)	-889 (9)	2063 (7)
N11	1020 (7)	-134 (7)	5275 (4)
N12	3397 (6)	-41 (8)	4596 (4)
N13	-142 (7)	123 (7)	3573 (4)
C10	1451 (8)	2133 (8)	5077 (6)
C11	1530 (8)	1051 (9)	5748 (6)
C12	2955 (9)	855 (10)	6053 (6)
C13	3853 (8)	439 (9)	5364 (5)
C14	5159 (8)	467 (11)	5576 (6)
C15	6045 (9)	-26 (12)	5007 (7)
C16	5579 (9)	-526 (11)	4213 (6)
C17	4267 (8)	-549 (9)	4024 (6)
C18	1350 (9)	-1448 (8)	5609 (6)

<sup>a</sup>The positional parameters are presented in fractional unit cell coordinates.

<sup>b</sup>The y positional parameter was not varied.

Table I. (continued)

---

	<u>x</u>	<u>y</u>	<u>z</u>
C19	1393 (8)	-2352 (9)	4817 (6)
CT1	1245 (9)	552 (10)	2369 (6)
CT2	-69 (9)	791 (9)	2728 (5)
CT3	-1232 (10)	489 (11)	2091 (6)
CT4	-2432 (10)	1091 (13)	2403 (8)
OH1	4082 (8)	888 (7)	1224 (5)
Co2	4394 (1)	472 (1)	8741.2 (7)
O21	3945 (6)	1903 (6)	8031 (4)
O22	4646 (7)	3893 (7)	7776 (4)
O23	4952 (6)	859 (6)	9333 (4)
O24	6656 (7)	1351 (7)	1.0423 (5)
O25	3186 (6)	578 (6)	8082 (4)
O26	1098 (7)	746 (9)	7704 (5)
OT2	686 (7)	205 (10)	8964 (6)
N21	5532 (7)	1592 (7)	9412 (4)
N22	5839 (7)	-11 (8)	8009 (4)
N23	2917 (7)	866 (8)	9432 (5)
C20	4745 (9)	2847 (9)	8148 (5)
C21	5939 (8)	2574 (8)	8767 (5)
C22	7005 (9)	2108 (8)	8215 (6)
C23	6833 (8)	770 (8)	7807 (5)
C24	7741 (9)	365 (10)	7233 (6)
C25	7709 (11)	880 (11)	6912 (7)
C26	6723 (11)	1718 (10)	7156 (7)
C27	5785 (10)	1222 (10)	7697 (6)
C28	6524 (9)	810 (8)	9893 (6)
C29	6039 (9)	565 (9)	9978 (6)

---

Table I. (continued)

	<u>x</u>	<u>y</u>	<u>z</u>
CT5	1989 (9)	299 (9)	8184 (6)
CT6	1682 (9)	616 (10)	8903 (6)
CT7	621 (8)	172 (11)	9472 (6)
CT8	842 (13)	1164 (13)	9852 (8)

(b) Final thermal parameters ( $\times 10^4$ ) and their estimated standard deviations (in parentheses)<sup>c</sup>

	$\beta_{11}$	$\beta_{22}$	$\beta_{33}$	$\beta_{12}$	$\beta_{13}$	$\beta_{23}$
Co1	44.8(9)	37.0(9)	20.1(4)	-2.6(8)	-5.2(5)	-0.6(6)
O11	57(6)	34(5)	29(3)	-2(4)	-5(3)	3(3)
O12	63(6)	41(6)	44(3)	-2(5)	2(4)	-10(3)
O13	66(6)	53(6)	31(3)	2(5)	-5(3)	-8(3)
O14	61(6)	29(5)	54(4)	-1(5)	-2(4)	6(3)
O15	65(5)	71(6)	21(2)	7(5)	-8(3)	-4(3)
O16	98(8)	211(13)	21(3)	2(9)	-6(4)	18(5)
OT1	136(11)	93(9)	111(7)	11(9)	-76(7)	-45(7)
N11	64(7)	33(6)	26(3)	-9(6)	-6(4)	0(4)
N12	56(6)	62(6)	20(3)	-4(7)	-3(3)	-9(4)
N13	67(6)	52(7)	25(3)	-12(6)	-6(4)	13(4)
C10	35(8)	48(8)	31(4)	0(6)	-2(4)	3(5)
C11	48(7)	48(8)	27(4)	-2(7)	-3(4)	2(5)

<sup>c</sup>The  $\beta_{ij}$  are defined by  $T = \exp\{-(h^2\beta_{11} + k^2\beta_{22} + l^2\beta_{33} + 2hk\beta_{12} + 2hl\beta_{13} + 2kl\beta_{23})\}$ .

Table I. (continued)

	$\beta_{11}$	$\beta_{22}$	$\beta_{33}$	$\beta_{12}$	$\beta_{13}$	$\beta_{23}$
C12	59(8)	73(10)	29(4)	0(8)	-9(5)	2(5)
C13	55(7)	53(7)	26(3)	-3(7)	-4(4)	8(5)
C14	41(7)	101(10)	40(4)	-1(8)	-8(5)	-1(6)
C15	54(8)	94(10)	50(5)	3(10)	-3(5)	10(7)
C16	53(8)	104(11)	37(5)	5(8)	-4(5)	11(6)
C17	54(8)	71(9)	35(4)	-7(7)	2(5)	-6(5)
C18	69(9)	41(7)	28(4)	-2(7)	-2(5)	0(4)
C19	47(9)	56(9)	34(4)	-1(7)	-5(5)	0(5)
CT1	85(9)	64(8)	29(4)	-7(9)	-5(5)	-5(6)
CT2	69(8)	72(11)	22(3)	-10(8)	-9(4)	-2(5)
CT3	80(10)	93(10)	38(4)	-14(10)	-30(6)	-3(6)
CT4	62(9)	125(14)	62(6)	-6(10)	-30(7)	21(8)
OH1	136(9)	79(7)	42(3)	13(7)	0(5)	0(4)
Co2	62(1)	41.4(9)	21.9(4)	-1.2(9)	-2.2(5)	-2.6(6)
O21	68(6)	63(6)	27(3)	-13(5)	-13(3)	-1(3)
O22	102(8)	62(7)	39(3)	15(6)	-9(4)	21(4)
O23	82(7)	50(6)	33(3)	-4(6)	10(4)	0(3)
O24	109(8)	61(6)	43(3)	25(6)	-6(4)	22(4)
O25	85(7)	70(6)	32(3)	-3(6)	-1(4)	-11(4)
O26	90(8)	139(10)	42(3)	-12(8)	-21(4)	-30(5)
OT2	84(7)	174(14)	72(5)	-4(9)	-22(5)	-8(7)
N21	52(7)	44(6)	22(3)	9(5)	-3(4)	5(3)
N22	89(7)	42(6)	20(3)	0(7)	0(4)	1(4)
N23	51(6)	78(8)	32(3)	0(6)	-5(4)	-10(4)
C20	71(9)	54(9)	23(3)	14(8)	0(4)	-1(5)
C21	67(8)	36(7)	21(3)	3(6)	-4(4)	4(4)
C22	70(9)	47(8)	27(4)	6(7)	1(5)	-6(5)

Table I. (continued)

	$\beta_{11}$	$\beta_{22}$	$\beta_{33}$	$\beta_{12}$	$\beta_{13}$	$\beta_{23}$
C23	42(7)	61(10)	25(4)	12(7)	-3(4)	7(5)
C24	73(9)	77(10)	30(4)	9(8)	-4(5)	-7(5)
C25	93(11)	89(11)	37(5)	26(10)	5(6)	-8(6)
C26	105(12)	88(11)	35(4)	29(10)	0(6)	-11(6)
C27	114(11)	57(9)	30(4)	20(9)	2(6)	-7(5)
C28	77(9)	34(9)	31(4)	6(7)	-7(5)	8(5)
C29	76(10)	53(8)	25(4)	7(8)	0(5)	9(4)
CT5	83(10)	69(11)	28(4)	-20(8)	-11(5)	0(5)
CT6	62(8)	81(10)	33(4)	10(8)	-7(5)	-15(6)
CT7	48(8)	124(15)	42(4)	8(10)	-10(5)	7(7)
CT8	139(15)	96(13)	50(6)	-15(12)	2(8)	21(8)

Table II. Bond distances in Å for mer-[Co(N-Cm-L-Pyala)-  
(D-Thr)]·1/2H<sub>2</sub>O and their estimated standard  
deviations (in parentheses)

Co1-O11	1.882 (6)	Co2-O21	1.881 (6)
Co1-O13	1.900 (6)	Co2-O23	1.906 (6)
Co1-O15	1.898 (5)	Co2-O25	1.907 (6)
Co1-N11	1.911 (7)	Co2-N21	1.913 (7)
Co1-N12	1.970 (6)	Co2-N22	1.981 (7)
Co1-N13	1.946 (7)	Co2-N23	1.948 (8)
C10-O11	1.29 (1)	C20-O21	1.29 (1)
C10-O12	1.25 (1)	C20-O22	1.22 (1)
C19-O13	1.28 (1)	C29-O23	1.32 (1)
C19-O14	1.24 (1)	C29-O24	1.22 (1)
CT1-O15	1.30 (1)	CT5-O25	1.29 (1)
CT1-O16	1.21 (1)	CT5-O26	1.24 (1)
CT3-OT1	1.43 (1)	CT7-OT2	1.44 (1)
C10-C11	1.52 (1)	C20-C21	1.54 (1)
C11-C12	1.54 (1)	C21-C22	1.50 (1)
C11-N11	1.51 (1)	C21-N21	1.49 (1)
C12-C13	1.51 (1)	C22-C23	1.53 (1)
C13-C14	1.37 (1)	C23-C24	1.39 (1)
C13-N12	1.34 (1)	C23-N22	1.36 (1)
C14-C15	1.40 (1)	C24-C25	1.38 (1)
C15-C16	1.39 (1)	C25-C26	1.40 (1)
C16-C17	1.37 (1)	C26-C27	1.41 (1)
C17-N12	1.39 (1)	C27-N22	1.34 (1)
C18-C19	1.54 (1)	C28-C29	1.52 (1)
C18-N11	1.49 (1)	C28-N21	1.47 (1)



Table II. (continued)

---

CT1-CT2	1.51 (1)	CT5-CT6	1.50 (1)
CT2-CT3	1.54 (1)	CT6-CT7	1.51 (1)
CT2-N13	1.47 (1)	CT6-N23	1.50 (1)
CT3-CT4	1.49 (2)	CT7-CT8	1.51 (2)
OH1-O16	2.82 (1)	O26-CT8	3.35 (1)
OH1-N23 <sup>a</sup>	2.95 (1)	O26-OT2	2.78 (1)
N13-CT4	3.07 (1)	N23-CT8	3.09 (1)
N13-OT1	2.77 (1)		

---

<sup>a</sup>Symmetry operation  $x, y, 1 - z$ .

Table III. Bond angles in degrees for mer-[Co(N-Cm-L-Pyala)-(D-Thr)]·1/2H<sub>2</sub>O and their estimated standard deviations (in parentheses)

	Molecule 1	Molecule 2
O1-Co-O3	173.8 (3)	174.2 (3)
O1-Co-O5	93.4 (3)	90.3 (3)
O1-Co-N1	86.6 (3)	87.9 (3)
O1-Co-N2	90.4 (3)	92.4 (3)
O1-Co-N3	87.6 (3)	88.5 (3)
O3-Co-O5	92.6 (3)	95.5 (3)
O3-Co-N1	87.3 (3)	86.3 (3)
O3-Co-N2	90.9 (3)	88.1 (3)
O3-Co-N3	91.5 (3)	91.4 (3)
O5-Co-N1	178.2 (3)	176.9 (3)
O5-Co-N2	92.7 (3)	92.8 (3)
O5-Co-N3	83.8 (3)	84.0 (3)
N1-Co-N2	89.1 (3)	89.8 (3)
N1-Co-N3	94.4 (3)	93.4 (3)
N2-Co-N3	175.8 (3)	176.7 (3)
Co-O1-CO	112.9 (5)	112.2 (5)
Co-O3-C9	112.7 (6)	112.7 (6)
Co-O5-CT1	116.7 (5)	
Co-O5-CT5		114.6 (6)
Co-N1-C1	105.7 (5)	104.0 (5)
Co-N1-C8	108.1 (5)	109.3 (5)
Co-N2-C3	127.1 (6)	125.7 (6)
Co-N2-C7	113.8 (5)	114.8 (7)
Co-N3-CT2	108.6 (5)	
Co-N3-CT6		109.9 (5)

Table III. (continued)

	Molecule 1	Molecule 2
O1-CO-O2	123.9 (8)	124.6 (8)
O1-CO-C1	116.7 (7)	115.9 (7)
O2-CO-C1	119.3 (8)	119.5 (8)
O3-C9-O4	123.8 (9)	122.9 (9)
O3-C9-C8	117.7 (8)	116.6 (8)
O4-C9-C8	118.5 (8)	120.4 (8)
O5-CT1-O6	124.4 (9)	
O5-CT5-O6		122.2 (9)
O5-CT1-CT2	113.9 (7)	
O5-CT5-CT6		118.2 (8)
O6-CT1-CT2	121.7 (8)	
O6-CT5-CT6		119.6 (9)
N1-C1-CO	105.6 (6)	106.7 (7)
N1-C1-C2	110.2 (7)	113.3 (7)
N1-C8-C9	107.4 (7)	109.4 (7)
N2-C3-C2	121.4 (7)	121.3 (7)
N2-C3-C4	120.8 (8)	120.8 (8)
N2-C7-C6	121.7 (8)	122 (1)
N3-CT2-CT1	109.4 (7)	
N3-CT6-CT5		107.4 (7)
N3-CT2-CT3	112.8 (8)	
N3-CT6-CT7		111.3 (7)
CO-C1-C2	108.7 (7)	107.4 (7)
C1-N1-C8	120.7 (6)	119.4 (7)
C1-C2-C3	116.2 (7)	116.6 (7)
C2-C3-C4	117.6 (8)	117.8 (8)

Table III. (continued)

	Molecule 1	Molecule 2
C3-C4-C5	121.0 (9)	120.4 (9)
C3-N2-C7	118.9 (7)	119.5 (8)
C4-C5-C6	118.3 (8)	119.0 (9)
C5-C6-C7	119.2 (9)	117.8 (9)
CT1-CT2-CT3	115.0 (8)	
CT5-CT6-CT7		114.9 (9)
CT2-CT3-CT4	110.3 (9)	
CT6-CT7-CT8		113.6 (9)
CT2-CT3-OT1	105.7 (8)	
CT6-CT7-OT2		108.5 (8)
CT4-CT3-OT1	112 (1)	
CT8-CT7-OT2		110 (1)

## RESULTS AND DISCUSSION

Description and discussion of the structure Each asymmetric unit of the crystal contains two molecules of (N-carboxymethyl-L- $\beta$ -(2-pyridyl)- $\alpha$ -alaninato) (D-threoninato)-cobalt(III) and one molecule of water. In each complex molecule, the cobalt atom is octahedrally coordinated to three oxygen and three nitrogen atoms (Figure 2). Since the bond distances and angles listed in Tables II and III do not differ significantly for the two complex molecules, only those for molecule 1 will be discussed below. The digits 1 or 2 directly following either Co, O, N or C refer to molecule 1 or molecule 2 in the asymmetric unit.

The coordination around the cobalt atom is considered to be meridional since the three carboxylate oxygens (O11, O13, O15) lie in a plane which is perpendicular to the plane of the three nitrogens (N11, N12, N13). The L- $\beta$ -(2-pyridyl)- $\alpha$ -alaninate fragment of N-Cm-L-Pyala<sup>2-</sup> is facially coordinated to the cobalt through its  $\alpha$ -carboxylate oxygen (O11), its secondary  $\alpha$ -amino nitrogen (N11) and its pyridine nitrogen (N12) in a manner similar to that reported for the bis[D- $\beta$ -(2-pyridyl)- $\alpha$ -alaninato]-nickel(II) and cobalt(III) complexes.<sup>17,18</sup> The remaining

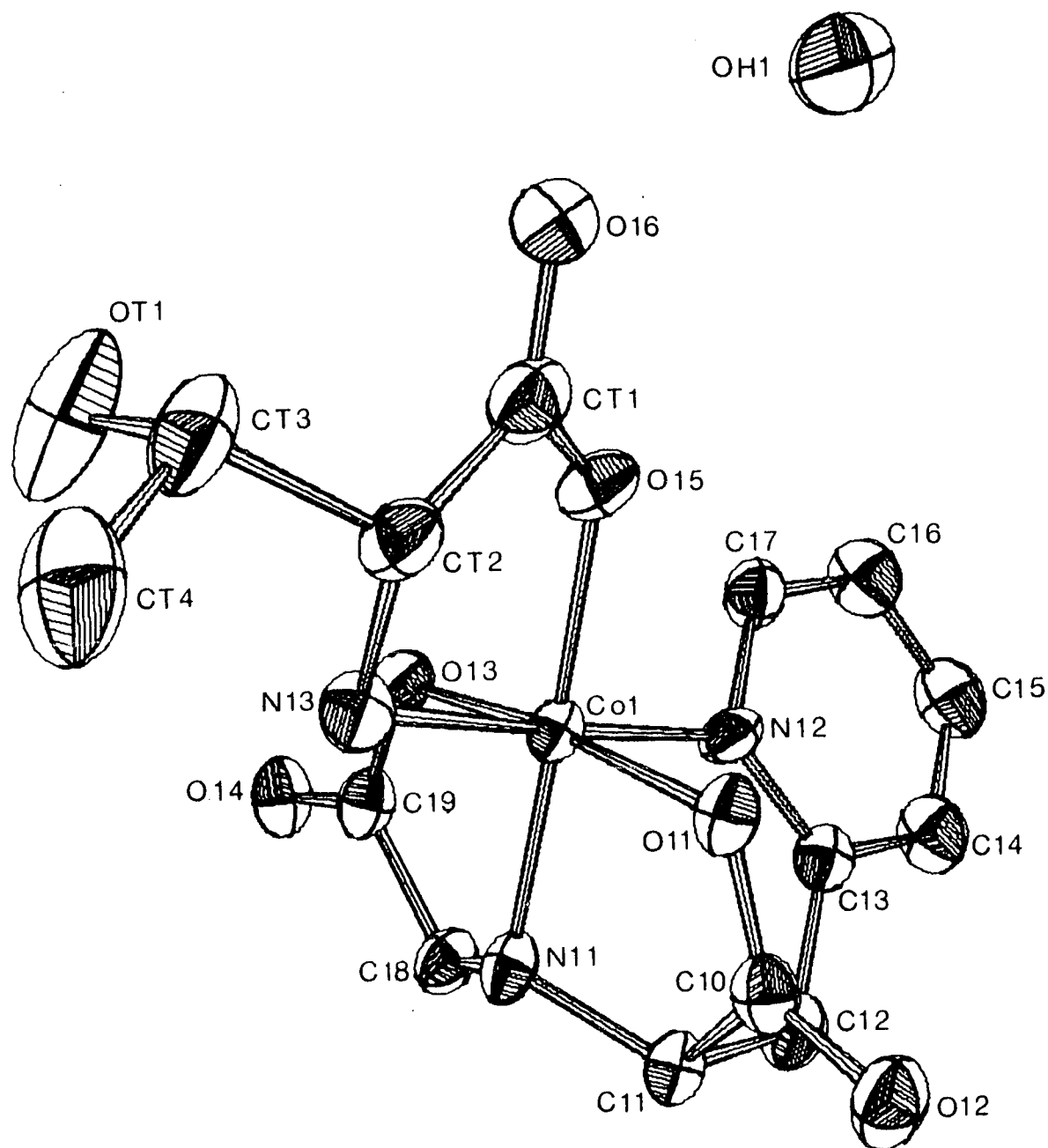


Figure 2. ORTEP drawing of  $[\text{Co}(\text{N-Cm-L-Pyala})(\text{D-Thr})] \cdot 1/2\text{H}_2\text{O}$

N-carboxymethyl oxygen (O13) is coordinated to the cobalt in a position trans to the  $\alpha$ -carboxylate oxygen, O11. The bidentate amino acidate, D-threoninate, occupies the two remaining coordination sites, with its  $\alpha$ -amino nitrogen (N13) coordinated to the cobalt trans to the pyridine nitrogen (N12) of N-Cm-L-Pyala<sup>2-</sup> and its  $\alpha$ -carboxylate oxygen (O15) trans to the  $\alpha$ -amino nitrogen (N11) of N-Cm-L-Pyala<sup>2-</sup>. This structure (Figure 1c) in which the pyridine is coordinated trans to the amino nitrogen of the D-threoninate ligand confirms the structure predicted on the basis of its visible spectrum (see next section). The term meridional isomer used throughout the remainder of this paper will apply to this isomer (Figure 1c).

The bond distances and bond angles observed for the L- $\beta$ -(2-pyridyl)- $\alpha$ -alanine, L-Pyala, fragment of N-Cm-L-Pyala<sup>2-</sup> agree quite well with those reported for the M(D-Pyala)<sub>2</sub> complexes, where M is Ni(II) or Co(III).<sup>17,18</sup> The bond distances and angles found in the N-carboxymethyl group agree with those reported for bis(iminodiacetato)-cobaltate(III).<sup>19</sup> The observed bond distances and angles in the D-threoninate ligand are similar to those reported for L-threonine and bis(L-threoninato)copper(II).<sup>20-22</sup>

The three  $\text{CO}_2^-$  groups each contain one short and one long C-O bond. The C-O distances for the three coordinated oxygens (C10-O11 = 1.29(1) Å, C19-O13 = 1.28(1) Å, CT1-O15 = 1.30(1) Å) and the C-O distances for the shorter uncoordinated "carbonyl-type" oxygens (C10-O12 = 1.24(1) Å, C19-O14 = 1.24(1) Å, CT1-O16 = 1.21(1) Å) correspond well with those found in other amino acidato cobalt(III) complexes.<sup>3, 18, 23-26</sup>

The bond distances Col-N11 (1.911(7) Å), Col-N13 (1.946(7) Å), Col-O11 (1.882(6) Å), Col-O13 (1.900(6) Å) and Col-O15 (1.898(5) Å) are comparable to cobalt(III) secondary amino nitrogen,<sup>3, 26, 27</sup> cobalt(III) primary nitrogen,<sup>18, 26, 28</sup> and cobalt(III) carboxylate oxygen<sup>3, 18, 26, 29</sup> distances found in cobalt(III) complexes of polyamines, amino acids and amino polycarboxylates. The cobalt pyridine nitrogen bond distance (Col-N12 = 1.970(6) Å) is equal (within experimental error) to the Co-N pyridine bond distances reported for  $\text{Co}(\underline{\text{D}}\text{-Pyala})_2^+$ .<sup>18</sup>

The bond angles around the cobalt atom deviate significantly from ideal octahedral geometry with the smallest deviation being 0.4° and the greatest being 6.2°. The three angles, O11-Col-N11 (86.6(3)°), O13-Col-N11 (87.3(3)° and O15-Col-N13 (83.8(3)°) contained in the three



five-membered chelate rings are consistent with other values reported for cobalt(III) complexes containing "glycinate-type" chelate rings.<sup>3,18,23-29</sup> The angle, N11-Co1-N12 (89.1(3)°), contained in the six-membered chelate ring of the N-Cm-L-Pyala<sup>2-</sup> ligand is consistent with values reported for Co(D-Pyala)<sub>2</sub><sup>+18</sup> and other Co(III) complexes containing six-membered rings.<sup>30-31</sup> There is considerable deviation from the ideal value of 180° for the O11-Co1-O13 (173.8(3)°) bond angle. This distortion seems to be due to the formation of two five-membered chelate rings (Co1-O11-C10-C12-N11 and Co1-N11-C18-C19-O13) in the same plane. Chelation of O11, N11 and O13 meridionally pulls O11 and O13 toward N11 and distorts the coordination plane (formed by O11, N11, O13, O15) as shown in Figure 3a. Additional evidence of angular strain caused by the formation of the two five-membered chelate rings (Figure 3b), in the same plane is found in the C11-N11-C18 (120.7(6)°) bond angle which is severely distorted from the ideal tetrahedral value of 109.5°. Similar angular strain and distortions have been reported previously for Co(III) complexes containing EDTA, IMDA and related ligands.<sup>23,26,29</sup>

The cobalt atom does not deviate significantly (greatest deviation is 0.03 Å) from any of the three coordination

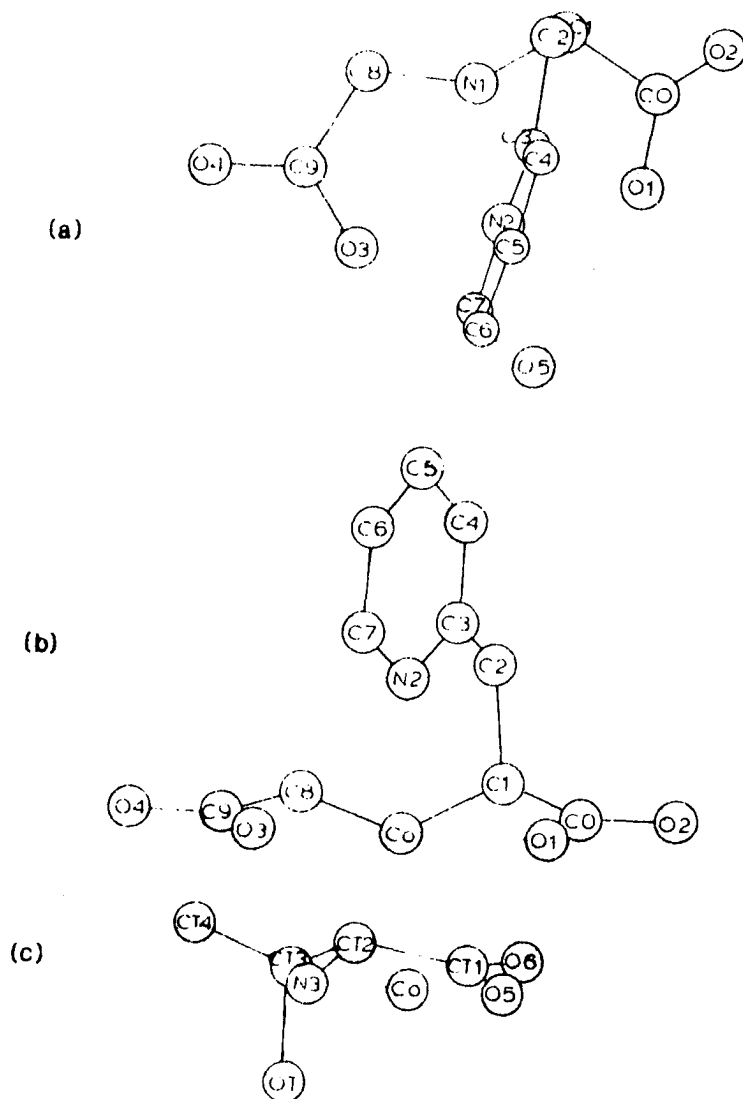


Figure 3. Three projections of various fragments of  $[\text{Co}(\text{N-Cm-L-Pyala})(\text{D-Thr})] \cdot 1/2\text{H}_2\text{O}$ , Molecule 1, as viewed a) down the N2-Co bond, b) down the Co-N1 bond and c) bisecting the N3-Co-O5 bond angle

planes defined by N13-O13-N12-O11, N11-O11-O15-O13 and N11-N12-O15-N13. The distance from the cobalt atom to the plane defined by the pyridine ring is 0.20 Å and is similar to the distances previously reported.<sup>18</sup> The least-squares plane of the pyridine ring (Plane 1, Table IV) is not coincident with either the O11-N12-O13-N13 plane or the O15-N12-N11-N13 plane (Planes 2 and 3, Table IV). The dihedral angles between the pyridine plane and the O11-N12-O13-N13 plane is 60.6° while the angle between the pyridine plane and the O15-N12-N11-N13 plane is 30.1°. This is illustrated in Figure 3a.

The two five-membered chelate rings (Co1-N11-C11-C10-O11 and Co1-N11-C18-C19-O13) of the tetradentate ligand, N-Cm-L-Pyala<sup>2-</sup>, exist in an asymmetric-envelope configuration which has been noted before for other bidentate amino acidato metal complexes (Figure 3b).<sup>32, 33</sup> The carbon atoms C11 and C18 are displaced in the same direction due to constraints placed on the two chelate rings by the facial coordination of the L-Pyala fragment and the configuration around the nitrogen. The facial coordination of the L-Pyala fragment causes C12 to be in an axial position when referenced to the N11-O13-O15-O11 plane (Figure 3a) and C11 to be displaced a greater distance from the

Table IV. Equations of least-squares planes<sup>a</sup>

Atom	D <sup>b</sup>	Atom	D
Plane 1: (pyridine ring) N12-C13-C14-C15-C16-C17			
-0.0886 X - 0.9012 Y + 0.4230 Z - 2.746 = 0			
Co1	0.197	C14	-0.002
N12	-0.009	C15	-0.004
C11	-0.101	C16	-0.008
C12	0.151	C17	0.010
C13	0.005		
Plane 2: O11-N12-O13-N13			
-0.4022 X - 0.0766 Y + 0.9123 Z - 5.240 = 0			
Co1	-0.020	O13	0.079
O11	0.083	N13	-0.082
N12	-0.080		
Plane 3: O15-N12-N11-N13			
0.0109 X + 0.9966 Y + 0.0823 Z - 0.5523 = 0			
Co1	-0.019	N11	-0.019
O15	-0.020	N13	0.019
N12	0.020		

<sup>a</sup>Planes are defined as  $C_1X + C_2Y + C_3Z + C_4 = 0$  where X, Y and Z are Cartesian coordinates.

<sup>b</sup>D is the distance (Å) of the given atom from the fitted plane.

Table IV. (continued)

---

Atom	D	Atom	D
------	---	------	---

---

Plane 4: O11-N11-O13

$0.9371 X - 0.0235 Y + 0.3483 Z - 3.413 = 0$

Co	0.023	C10	0.272
O11	0.000	C11	0.683
O13	0.000	C12	2.210
N11	0.000	C18	0.505
N12	1.992	C19	0.205

Plane 5: N13-Col-O15

$0.0302 X + 0.9956 Y + 0.0885 Z - 0.5979 = 0$

Col	0.000	CT1	0.325
N13	0.000	CT2	0.577
O15	0.000	CT3	0.145
O16	0.437	CT4	0.769
OT1	-1.280		

---

O13-Col-O11 plane than C18. Additional evidence of the axial position of C12 is seen in the O11-C10-C11-C12 torsional angle of  $89.7^\circ$  and a displacement of  $2.21 \text{ \AA}$  for C12 above the O11-N11-O13 plane (Plane 4, Table IV). The torsional angles, O11-C10-C11-N11 ( $28.6^\circ$ ) and O13-C19-C18-N11 ( $20.6^\circ$ ), fall within the  $0-30^\circ$  range observed for other coordinated amino acids.<sup>33</sup>

The D-threoninate chelate ring, Col-N13-CT2-CT1-O15, also exists in an asymmetric-envelope configuration (Figure 3c), which allows the R-group to be in an equatorial position when referenced to the N13-Col-O15 plane. The  $0.15 \text{ \AA}$  displacement of CT3 from the N13-Col-O15 plane, also supports an equatorial position for CT3 (Plane 5, Table IV). The O15-CT1-CT2-N13, torsional angle of  $17.2^\circ$  is within the range noted above.

The meridional coordination of O11, N11 and O13 gives rise to an asymmetric secondary nitrogen which has the S absolute configuration. This configuration is opposite to the R configuration found in the other diastereomer, *fac*-[Co(N-Cm-L-Pyala)(D-Thr)]·H<sub>2</sub>O (Figure 1a).

There appears to be very little stabilization of the crystal structure by hydrogen bonding. The asymmetric units are linked to each other by hydrogen bonds between

O16, OH1 and N23 of a neighboring asymmetric unit (symmetry operation  $x, y, 1 - z$ ) but there are no hydrogen bonds between the molecules in the same asymmetric unit. Other possible hydrogen bonds are OT1-N13 (2.77(1) Å) and OT2-O26 (2.78(1) Å). Figure 4 gives a stereographic view down the  $c$ -axis of the molecular packing in the crystal lattice.

Discussion of spectra The visible spectrum of fac-[Co(N-Cm-L-Pyala)(D-Thr)]·H<sub>2</sub>O (Figure 5) with its two symmetrical peaks at 520 nm ( $\epsilon = 153 \text{ cm}^{-1}\text{M}^{-1}$ ) and 367 nm ( $\epsilon = 113 \text{ cm}^{-1}\text{M}^{-1}$ ) is characteristic of other facial Co(III)N<sub>3</sub>O<sub>3</sub> complexes reported previously.<sup>3-7</sup> Since only one of the four possible isomers of Co(N-Cm-L-Pyala)-(D-Thr) is facial, the structure in Figure 1a is assigned to fac-[Co(N-Cm-L-Pyala)(D-Thr)]·H<sub>2</sub>O. The visible spectrum of mer-[Co(N-Cm-L-Pyala)(D-Thr)]·1/2H<sub>2</sub>O given in Figure 5 (maxima at 542 nm,  $\epsilon = 188 \text{ cm}^{-1}$  and 371 nm,  $\epsilon = 189 \text{ cm}^{-1}\text{M}^{-1}$ ) is typical of previously reported meridional Co(III)N<sub>3</sub>O<sub>3</sub> complexes.<sup>3-7</sup> The position of the shoulder at 470 nm ( $\epsilon = 100 \text{ cm}^{-1}\text{M}^{-1}$ ), which is on the high energy side of the peak at 542 nm, is characteristic of complexes containing pyridine or imidazole coordinated trans to an amino

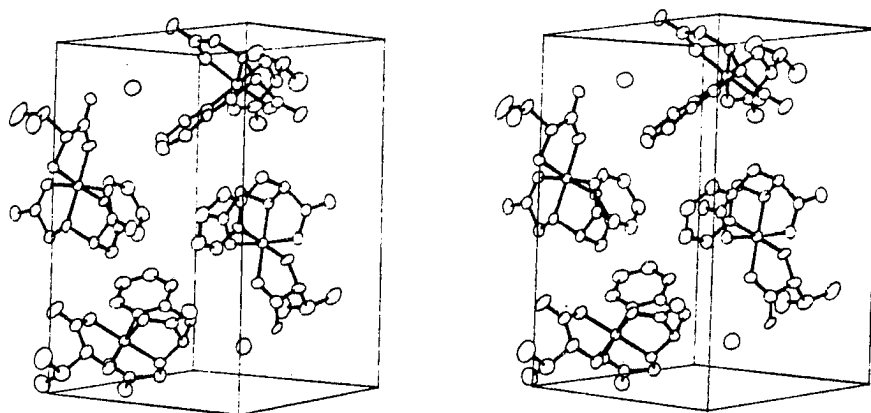


Figure 4. Stereographic view of the  $[\text{Co}(\text{N-Cm-L-Pyala})-(\text{D-Thr})] \cdot 1/2\text{H}_2\text{O}$  unit cell as viewed down the edge (C axis) of the cell



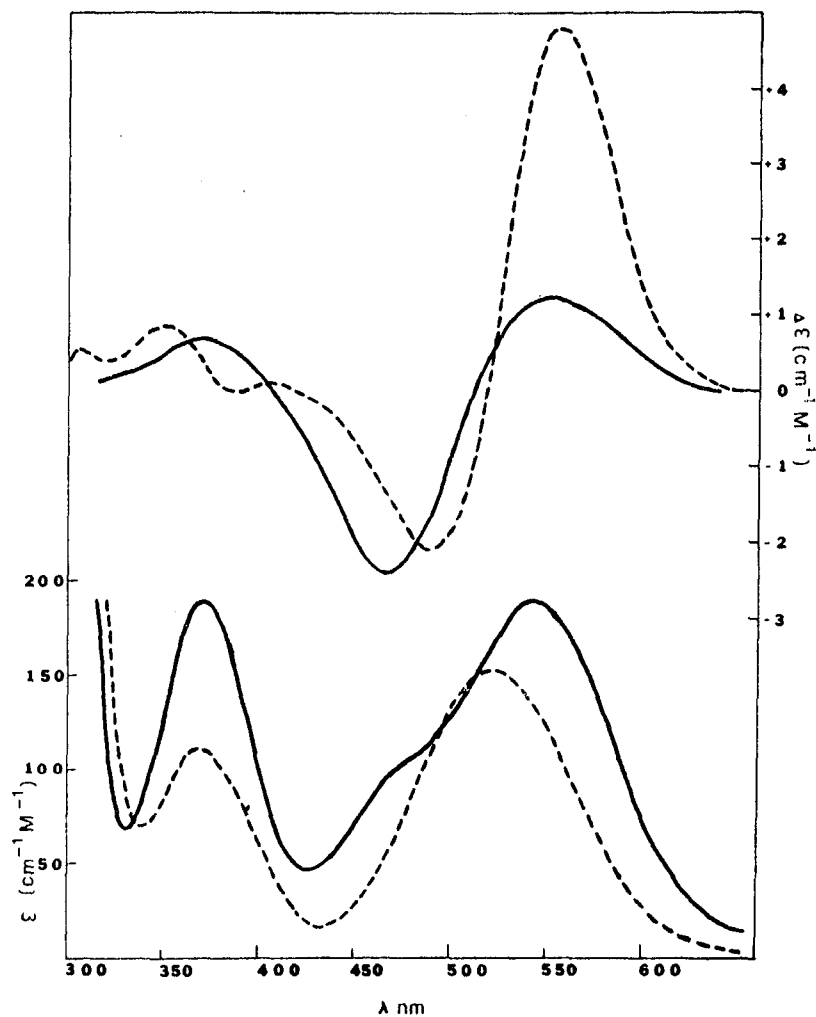


Figure 5. Visible (lower) and circular dichroism (upper) spectra of (—)  $\text{mer-}[\text{Co}(\text{N-Cm-L-Pyala})(\text{D-Thr})] \cdot 1/2\text{H}_2\text{O}$  and (----)  $\text{fac-}[\text{Co}(\text{N-Cm-L-Pyala})(\text{D-Thr})] \cdot \text{H}_2\text{O}$

group.<sup>7,18</sup> Based on the position of the shoulder, the meridional isomer can be assigned the structure in Figure 1c, which is that found in the X-ray analysis.

The CD spectra of fac- and mer-Co(N-Cm-L-Pyala)-(D-Thr) are given in Figure 5. The overall shape of the CD spectrum of fac-[Co(N-Cm-L-Pyala)(D-Thr)]·H<sub>2</sub>O is nearly identical to those of the cis-N, cis-O<sub>5</sub>-Co(N-Cm-L-Asp)(AA) complexes, where the ligands are N-carboxymethyl-L-aspartate (N-Cm-L-Asp<sup>3-</sup>) and D-amino acidates, reported by Bernauer.<sup>34</sup> The major difference is that the N-Cm-L-Pyala<sup>2-</sup> mixed cobalt(III) complexes have a  $\Delta\epsilon$  which is almost twice those of the N-Cm-L-Asp<sup>3-</sup> analogs.<sup>34</sup> Thus, it seems that substitution of a carboxylate group with a pyridine group increases the  $\Delta\epsilon$  of the CD spectrum. A similar increase has been noted before for complexes containing pyridine and imidazole.<sup>35</sup> The CD spectrum of the mer-[Co(N-Cm-L-Pyala)(D-Thr)]·1/2H<sub>2</sub>O complex cannot be compared to its N-Cm-L-Asp<sup>3-</sup> analog because the corresponding isomer of the mixed ligand cobalt(III)(N-Cm-L-Asp)(AA) complex has not been reported.

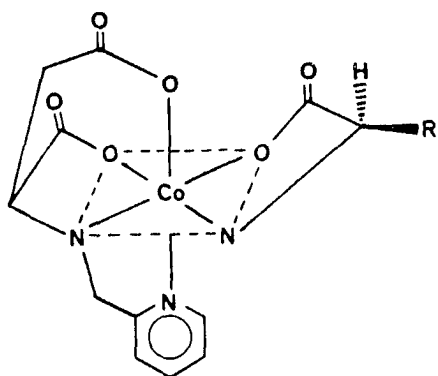
The proton nmr spectrum of the D-threoninate fragment of the facial isomer consists of a doublet at  $\delta$  1.27 for the  $\gamma$ -methyl protons, a multiplet at  $\delta$  4.4 for the  $\beta$ -methine

proton and a doublet at  $\delta$  3.54 for the  $\alpha$ -proton. The N-Cm-L-Pyala<sup>2-</sup> portion of the facial isomer consists of a multiplet at  $\delta$  3.9 for the  $\beta$ -methylene and  $\alpha$ -protons, two doublets at  $\delta$  3.60 and  $\delta$  4.33 with  $J = 18$  Hz for the N-carboxymethylene protons, an overlapping doublet and triplet at  $\delta$  7.46 for the meta pyridyl protons, a triplet at  $\delta$  7.98 for the para pyridyl proton and a doublet at  $\delta$  8.12 for the ortho proton of pyridine.

The proton nmr spectrum of the D-threoninate ligand of the meridional isomer exhibits a doublet at  $\delta$  1.37 for the  $\gamma$ -methyl protons, a multiplet at  $\delta$  4.4 for the  $\beta$ -methine proton and a doublet which overlaps the N-carboxymethyl singlet at  $\delta$  3.62 for the  $\alpha$ -proton. The N-Cm-L-Pyala<sup>2-</sup> fragment consists of a broad singlet at  $\delta$  3.62 for the N-carboxymethylene protons, a multiplet at  $\delta$  4.00 for the  $\beta$ -methine and  $\alpha$ -protons, an overlapping doublet and triplet at  $\delta$  7.61 for the meta pyridyl protons, a triplet at  $\delta$  8.07 for the para pyridyl proton and a doublet at  $\delta$  8.99 for the ortho pyridyl proton.

Comparison of the <sup>1</sup>H nmr spectra for the facial and meridional isomers reveals that the two spectra are very similar, with the major differences being in the splitting of the N-carboxymethyl protons and in the chemical shifts of the ortho pyridyl protons. Since the splitting of the

N-carboxymethyl protons in  $\text{fac-}[\text{Co}(\text{N-Cm-L-Pyala})(\text{D-Thr})]\cdot\text{H}_2\text{O}$  is similar to the two doublets reported previously for the N-pyridylmethyl protons of the  $\text{fac-Co(PLASP)(AA)}$  complexes (see figure below). Comparison of the ortho



$\text{fac-Co(PLASP)(AA)}$

pyridyl proton (doublet at  $\delta$  8.69) of the free ligand,  $\text{N-Cm-L-PyalaH}_2$ , to the ortho pyridyl proton (doublet at  $\delta$  8.12) of the facial isomer and to the ortho pyridyl proton (doublet at  $\delta$  8.99) of the meridional isomer shows the ortho pyridyl proton of the facial isomer to be shifted upfield (shielded) while the proton of the meridional isomer is shifted downfield (deshielded). This shielding and deshielding is presumably due to the magnetic anisotropy of the  $\text{D-threoninate}$  carboxylate group. In the facial isomer, the ortho proton is positioned over the  $\text{D-Thr}^-$  carboxylate plane and is shielded while in the meridional isomer, the ortho proton is nearly in the plane of the  $\text{D-Thr}^-$  carboxylate group and is deshielded. It may be noted that since the  $^- \text{O}_2\text{C-C(R)-N(H)-CH}_2\text{-CO}_2^-$

portion of the N-Cm-L-Pyala<sup>2-</sup> ligand resembles the tridentate ligand IMDA<sup>2-</sup>, <sup>-</sup>O<sub>2</sub>C-CH<sub>2</sub>-N(H)-CH<sub>2</sub>-CO<sub>2</sub><sup>-</sup>, the <sup>1</sup>H nmr spectra reported above for the facial and meridional isomers of Co(N-Cm-L-Pyala)(D-Thr) are also comparable to the cis (facial coordination of IMDA<sup>2-</sup>) and trans (meridional coordination of IMDA<sup>2-</sup>) isomers of [Co(IMDA)(diethylenetriamine)]<sup>+</sup> reported by Legg and Cooke.<sup>36</sup>

## CONCLUSION

Previously we reported that for a series of Co(PLASP)-(AA) complexes the only isomer isolated was the fac-Co(PLASP)(AA) isomer shown above in the discussion of spectra.<sup>3,4</sup> However for the Co(N-Cm-L-Pyala)(AA) complexes reported herein, two isomeric forms, one facial and one meridional were isolated. Since the donor groups in the PLASP<sup>2-</sup> and N-Cm-L-Pyala<sup>2-</sup> ligands are essentially identical, electronic differences between the two ligands are unlikely to account for the different geometries of their cobalt(III) complexes. However, the flexibility of the group attached to the amino nitrogen differs significantly. The N-carboxymethyl chelate ring of N-Cm-L-Pyala<sup>2-</sup> which has only one sp<sup>2</sup> carbon and an sp<sup>3</sup> oxygen (C1-C13-C19 bond angle is 112.7°) coordinated to the cobalt is flexible and capable of coordinating trans to both the pyridyl group and the  $\alpha$ -carboxylate group of the N-Cm-L-Pyala<sup>2-</sup> ligand. This has been reported previously for Co(III) complexes containing ethylenediametetraacetic acid and iminodiacetic acid.<sup>23,26,29</sup> On the other hand, the N-pyridylmethyl chelate ring of PLASP<sup>2-</sup> which has two sp<sup>2</sup> centers, one at carbon and the other at the coordinated

pyridine nitrogen, is less flexible and therefore less capable of coordinating in the more strained position trans to the  $\alpha$ -carboxylate group of the PLASP<sup>2-</sup> ligand. Thus the difference in angular strain in the N-Cm-L-Pyala<sup>2-</sup> and PLASP<sup>2-</sup> ligands accounts for the geometries of their Co(III) complexes. The effects of electronic and steric factors on the overall geometry of the facial and meridional isomers of Co(N-Cm-L-Pyala)(AA) will be discussed in greater detail in a later paper.

## REFERENCES

1. Nakon, R.; Rechani, P. R.; Angelici, R. J. Inorg. Chem. 1973, 12, 2431.
2. Bedell, S. A.; Rechani, P. R.; Angelici, R. J.; Nakon, R. Inorg. Chem. 1977, 16, 972.
3. Meiske, L. A.; Jacobson, R. A.; Angelici, R. J. submitted for publication to Inorg. Chem.
4. Meiske, L. A.; Jacobson, R. A.; Angelici, R. J. Abstract of the 14th Midwest Regional ACS Meeting, Oct., 1978.
5. Douglas, B. E.; Yamada, S. Inorg. Chem. 1965, 4, 1561.
6. Watabe, M.; Onuki, K.; Yoshikawa, S. Bull. Chem. Soc. Japan 1975, 48, 687; 1976, 49, 1845.
7. Watabe, M.; Onuki, K.; Yoshikawa, S. Bull. Chem. Soc. Japan 1978, 51, 1354.
8. Jacobson, R. A. J. Appl. Cryst. 1976, 9, 115.
9. Rohrbaugh, W. J.; Jacobson, R. A. Inorg. Chem. 1974, 13, 2535.
10. Lawton, S. L.; Jacobson, R. A. Inorg. Chem. 1968, 7, 2124.
11. Busing, W. R.; Martin, K. O.; Levy, H. A. "ORFLS, A Fortran Crystallographic Least Squares Program", U. S. Atomic Energy Commission Report ORNL-TM-305. Oak Ridge National Laboratory, Oak Ridge, Tenn., 1962.
12. Hubbard, C. A.; Quicksall, C. O.; Jacobson, R. A. "The Fast Fourier Algorithm and the Programs ALFF, ALFFDP, ALFFPROJ, ALFFT and FRIEDEL", U. S. Atomic Energy Commission Report IS-2625. Iowa State University and Institute for Atomic Research, Ames, Iowa, 1971.
13. Lapp, R. L.; Jacobson, R. A. "ALL A Generalized Crystallographic Least Squares Program", U. S. DOE Report, 1979, in preparation.



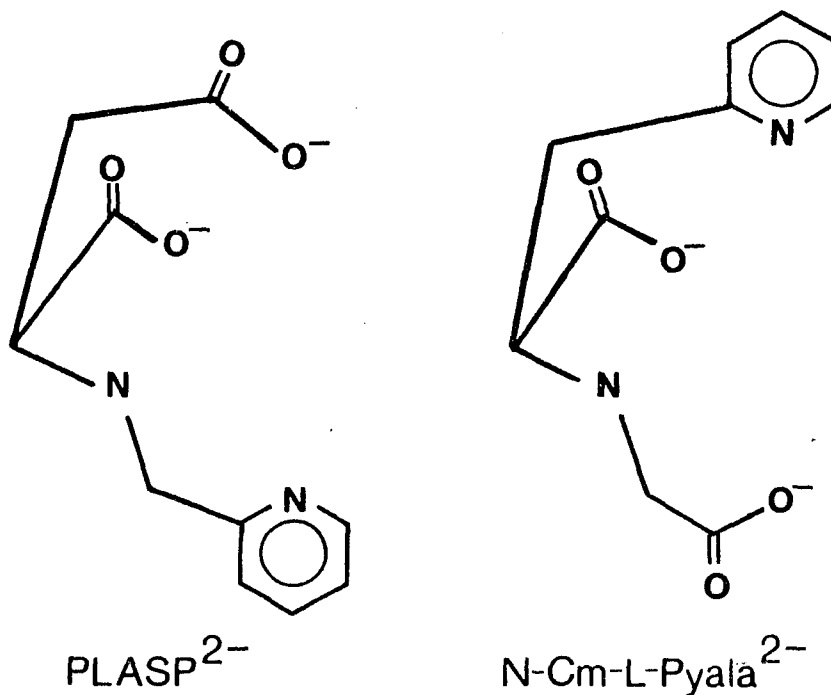
14. Hanson, H. P.; Herman, F.; Lea, J. D.; Skillman, S. Acta Crystallogr. 1960, 17, 1040.
15. Templeton, D. H. "International Tables for X-ray Crystallography", The Kynoch Press: Birmingham, England, 1962; Vol. III, Table 3.3.2C, p. 215-216.
16. Busing, W. R.; Martin, K. O.; Levy, H. A. "ORFFE, A Fortran Crystallographic Function and Error Program", U. S. Atomic Energy Commission Report ORNL-TM-306. Oak Ridge National Laboratory, Oak Ridge, Tenn., 1964.
17. Ebner, S. R.; Helland, B. J.; Jacobson, R. A.; Angelici, R. J. Inorg. Chem. 1980, 19, 175.
18. Ebner, S. R.; Jacobson, R. A.; Angelici, R. J. Inorg. Chem. 1979, 18, 765.
19. Corradi, A. B.; Palmieri, C. G.; Nardelli, M.; Pellinghelli, M. A.; Tani, M. E. V. J. Chem. Soc. Dalton Trans. 1973, 655.
20. Ramanadham, M.; Sikka, S. K.; Chidambaram, R. Pramana 1973, 1, 247.
21. Amirthalingham, V.; Muralidharan, K. V. Pramana 1975, 4, 83.
22. Shoemaker, D. P.; Donohue, J.; Shoemaker, V.; Corey, R. B. J. Am. Chem. Soc. 1950, 72, 2328.
23. Halloran, L. J.; Caputo, R. E.; Willett, R. D.; Legg, J. I. Inorg. Chem. 1975, 14, 1762.
24. Anderson, B. F.; Buckingham, D. A.; Gainsford, G. J.; Robertson, G. B.; Sargeson, A. M. Inorg. Chem. 1975, 14, 1658.
25. Liu, C. F.; Ibers, J. A. Inorg. Chem. 1969, 8, 1911.
26. Voss, K. E.; Angelici, R. J.; Jacobson, R. A. Inorg. Chem. 1978, 17, 1922.
27. Buckingham, D. A.; Cresswell, P. J.; Dellaca, R. J.; Dwyer, M.; Gainsford, G. J.; Marzilli, L. G.; Maxwell, I. E.; Robinson, W. T.; Sargeson, A. M.; Turnbill, K. R. J. Am. Chem. Soc. 1974, 96, 1713.

28. Gillard, R. D.; Payne, N. C.; Robertson, G. B. J. Am. Chem. Soc. A. 1970, 2579.
29. Weakliem, H. A.; Hoard, J. L. J. Am. Chem. Soc. 1959, 81, 549.
30. Oonishi, I.; Shibata, M.; Marumo, F.; Saito, Y. Acta Crystallogr. 1973, 1329, 2448.
31. Oonishi, I.; Sato, S.; Saito, Y. Acta Crystallogr. 1975, B31, 1318.
32. Freeman, H. C. Adv. Protein Chem. 1967, 22, 258.
33. Hawkins, C. J. "Absolute Configuration of Metal Complexes", Wiley-Interscience: New York, N.Y., 1971, p. 94.
34. Colomb, G.; Bernauer, K. Helv. Chim. Acta 1977, 60, 459.
35. Ebner, S. R.; Angelici, R. J. submitted to Inorg. Chem.
36. Legg, J. I.; Cooke, D. W. Inorg. Chem. 1966, 5, 594.

SECTION IV. SYNTHESIS AND SPECTRAL CHARACTERIZATION OF  
THE MIXED LIGAND COMPLEXES, [N-Carboxymethyl-  
L- $\beta$ -(2-pyridyl)- $\alpha$ -alaninato][amino acidato]-  
cobalt(III), Co(N-Cm-L-Pyala)(AA)

## INTRODUCTION

The preparation and characterization of the mixed ligand  $\text{Co(III)N}_3\text{O}_3$  complexes containing the tetradentate  $\text{N-(2-pyridylmethyl)-L-aspartate}$ ,  $\text{PLASP}^{2-}$  (see below),



and a bidentate amino acidate,  $\text{AA}^-$ , have been reported previously.<sup>1,2</sup> The only isomer isolated for the various amino acidates was the facial  $\text{Co(III)N}_3\text{O}_3$  isomer shown in Figure 1a in which the  $\beta\text{-CO}_2^-$  group of  $\text{PLASP}^{2-}$  is coordinated trans to the pyridyl group. The bidentate amino acidate is coordinated with its amino group trans

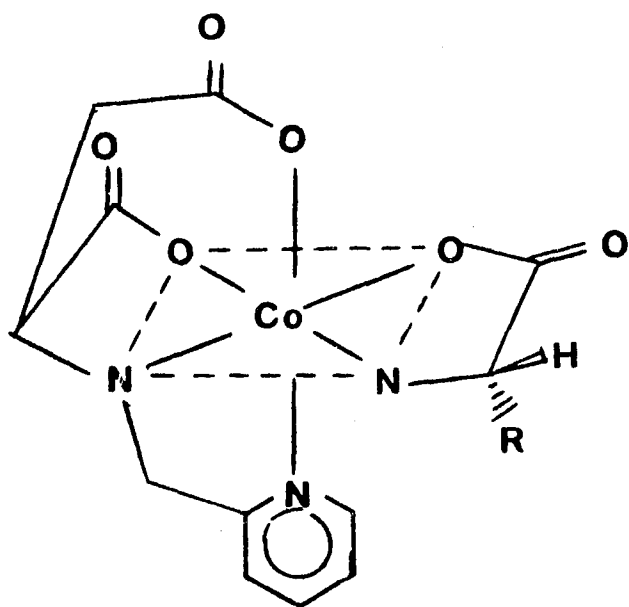
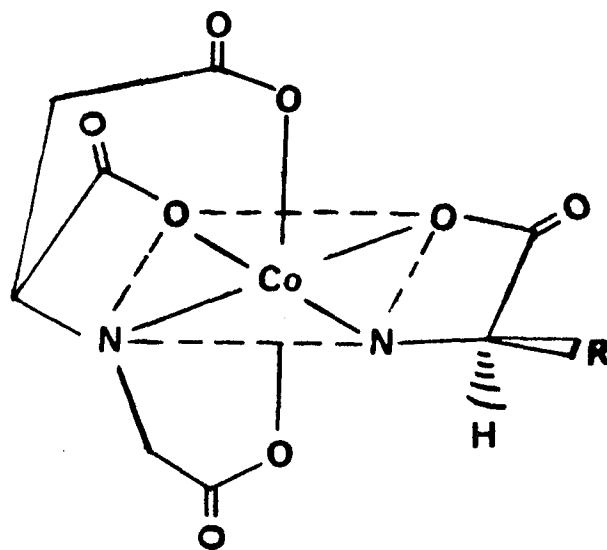
**a****b**

Figure 1. The (a) facial isomer of  $\text{Co(PLASP)(L-AA)}$  and  
 (b)  $\text{cis-N, cis-O}_5$ - isomer of  $\text{Co(N-Cm-L-Asp)(D-AA)}$

to the  $\alpha\text{-CO}_2^-$  of  $\text{PLASP}^{2-}$  and its  $\alpha\text{-CO}_2^-$  group trans to the secondary amino group of  $\text{PLASP}^{2-}$ . We suggested that coordination as in Figure 1a would be electronically favored since the amino nitrogens (and pyridyl nitrogen) are coordinated trans to oxygens (carboxylate groups).<sup>1,2</sup> This is consistent with other results which indicate that amino nitrogens avoid trans positions<sup>3</sup> and that for  $\text{ML}_3\text{L}_3'$  systems the facial isomers should be favored.<sup>4</sup> We also noted that steric factors (interactions of the amino acidate chelate ring and the pyridyl group of  $\text{PLASP}^{2-}$ ) do not appear to play a large role in determining the overall geometry of the  $\text{Co}(\text{PLASP})(\text{AA})$  complexes.<sup>2</sup> Finally, we concluded that coordination as in Figure 1a would give the least strained bond angle around the secondary amino nitrogen of  $\text{PLASP}^{2-}$  and would be favored over the more strained structures in which the pyridyl group is trans to the  $\alpha\text{-CO}_2^-$  of  $\text{PLASP}^{2-}$ .

We have also reported the preparation and characterization of the mixed ligand  $\text{Co}(\text{N-Cm-L-Pyala})(\underline{\text{D}}\text{-Thr})$  complex, where  $\text{N-Cm-L-Pyala}^{2-}$  is N-carboxymethyl-L- $\beta$ -(2-pyridyl)- $\alpha$ -alaninate (see above) and  $\underline{\text{D}}\text{-Thr}^-$  is the bidentate amino acidate,  $\underline{\text{D}}$ -threoninate.<sup>5</sup> We found that the major isomer is the facial isomer shown in Figure 2a.

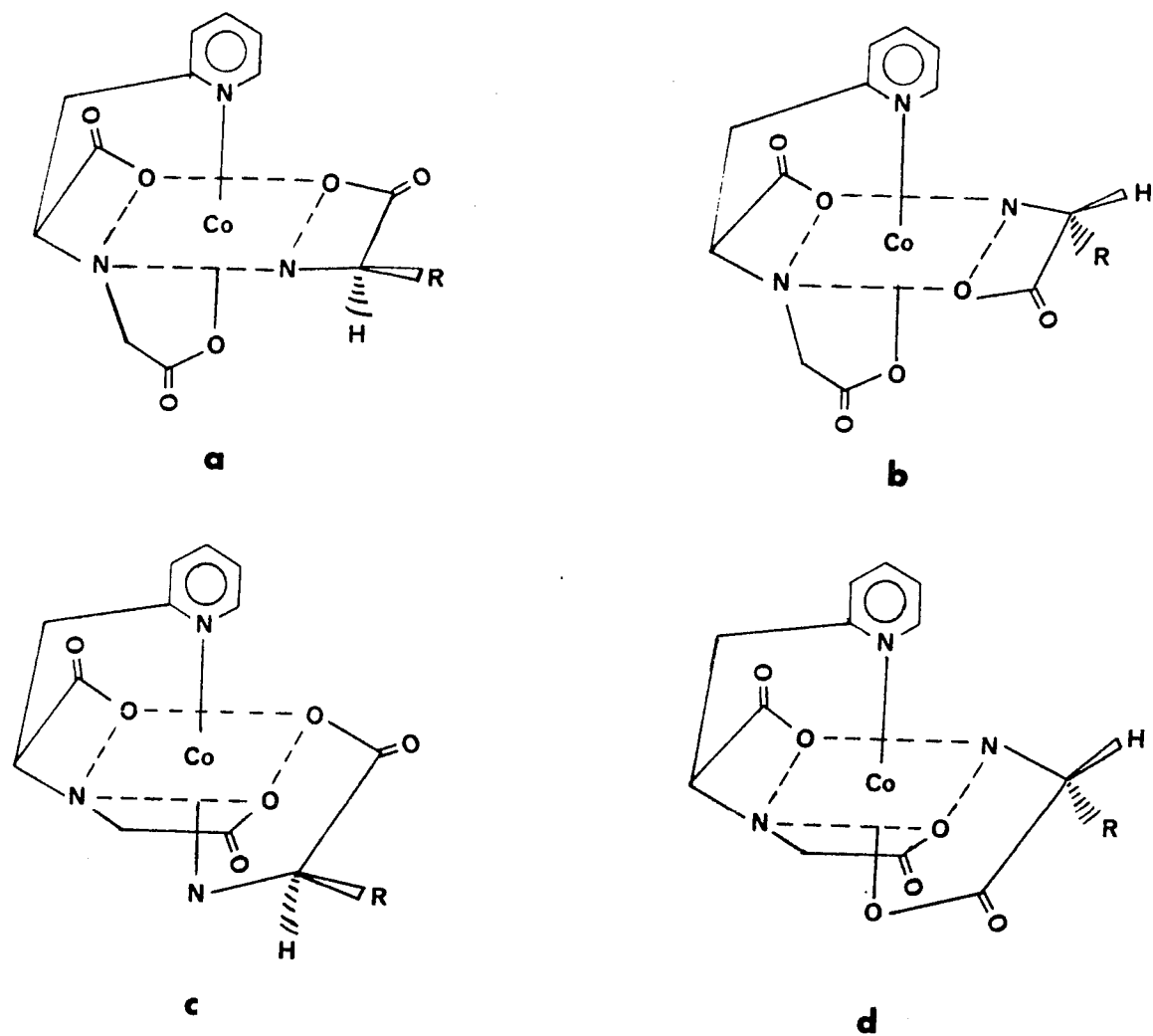


Figure 2. The four possible geometrical isomers of  $[\text{Co}(\text{N-Cm-L-Pyala})(\text{D-AA})]$ : a) *fac*, b) *mer*  $\text{N-Cm-CO}_2^-$ , c) *mer*  $\text{AA}^-$  amino and d) *mer*  $\text{AA}^- \text{CO}_2^-$

A second isomer which has the meridional geometry as shown in Figure 2c was also isolated but in lower yield. We concluded that the formation of the meridional isomer in the N-Cm-L-Pyala<sup>2-</sup> case and not in the PLASP<sup>2-</sup> case is due to the greater flexibility of the N-carboxymethyl chelate ring as compared to the N-pyridylmethyl chelate ring.<sup>3</sup>

In order to study further the effect of electronic and structural factors on the overall geometries of Co(III)N<sub>3</sub>O<sub>3</sub> complexes, a series of complexes of the type Co(N-Cm-L-Pyala)(AA) was prepared where AA<sup>-</sup> is one of the following: glycinate, Gly<sup>-</sup>, α-aminoisobutyrate, α-AIBA<sup>-</sup>, D,L-alaninate, D,L-Ala<sup>-</sup>, D-threoninate, D-Thr<sup>-</sup>, D and L and D,L-valinate, Val<sup>-</sup>, and D-asparaginate, D-AsN<sup>-</sup>. Their structures and trends in their visible, CD and nmr spectra are compared to those reported for the Co(PLASP)-(AA) complexes.



## EXPERIMENTAL SECTION

Materials All amino acids were purchased from Aldrich or Eastman Chemicals and were used without further purification. The ligand, N-Cm-L-PyalaH<sub>2</sub>, was prepared as previously reported.<sup>6</sup>

Preparation of the [N-carboxymethyl-L-β-(2-pyridyl)-α-alaninato][amino acidato]cobalt(III), Co(N-Cm-L-Pyala)-(AA), complexes The method of preparation, yields and elemental analyses of each Co(N-Cm-L-Pyala)(AA) complex are given in Table I.

Method A This procedure which uses excess hydrogen peroxide to oxidize Co(II) to Co(III) in the presence of N-Cm-L-Pyala<sup>2-</sup> and AA<sup>-</sup> has been described previously.<sup>5</sup> All reactions were carried out using 2.5 mmol N-Cm-L-Pyala<sup>2-</sup>, 2.5 mmol AA<sup>-</sup>, 2.5 mmol CoSO<sub>4</sub>·7H<sub>2</sub>O and activated carbon (0.1 g). The less soluble facial isomer of Co(N-Cm-L-Pyala)(AA) precipitated during the reaction and was filtered off with the activated carbon. The reddish pink isomer was separated from the carbon by stirring the carbon and product mixture with 100 ml of water and filtering off the carbon. This was repeated until the filtrate was colorless. All filtrates were

Table I. Syntheses, yields and elemental analyses of  
Co(N-Cm-L-Pyala) (AA) complexes

Complex	Method of Preparation
I, fac-[Co(N-Cm- <u>L</u> -Pyala) (Gly)] · H <sub>2</sub> O	C
II, fac-[Co(N-Cm- <u>L</u> -Pyala) ( <u>D</u> , <u>L</u> -Ala)] · 1/2H <sub>2</sub> O	B
III, fac-[Co(N-Cm- <u>L</u> -Pyala) (α-AIBA)] · 1/2H <sub>2</sub> O	A C
IV, fac-[Co(N-Cm- <u>L</u> -Pyala) ( <u>D</u> -Thr)] · H <sub>2</sub> O	A
V, fac-[Co(N-Cm- <u>L</u> -Pyala) ( <u>D</u> -Val)]	A C
VI, fac-[Co(N-Cm- <u>L</u> -Pyala) ( <u>D</u> -Val)] <sup>a</sup>	A
VII, fac-[Co(N-Cm- <u>L</u> -Pyala) ( <u>D</u> -Asn)] <sup>a</sup>	C
VIII, mer-[Co(N-Cm- <u>L</u> -Pyala) ( <u>D</u> , <u>L</u> -Ala)] · 2H <sub>2</sub> O	B
IX, mer-[Co(N-Cm- <u>L</u> -Pyala) (α-AIBA)] · 1/2H <sub>2</sub> O	A C
X, mer-[Co(N-Cm- <u>L</u> -Pyala) ( <u>D</u> -Thr)] · 1/2H <sub>2</sub> O	A
XI, mer-[Co(N-Cm- <u>L</u> -Pyala) ( <u>D</u> -Val)] · 1/2H <sub>2</sub> O	A
XII, mer-[Co(N-Cm- <u>L</u> -Pyala) ( <u>L</u> -Val)] · H <sub>2</sub> O	A
XIII, mer-[Co(N-Cm- <u>L</u> -Pyala) ( <u>D</u> , <u>L</u> -Val)] · H <sub>2</sub> O	A

<sup>a</sup>Isolated using D,L-AA<sup>-</sup> in the synthesis.

<sup>b</sup>Based on total D and L-AA<sup>-</sup>.

Yield	Formula		%C	%H	%N
56	$C_{12}H_{14}N_3O_6Co \cdot H_2O$	Theory	38.62	4.29	11.26
		Found	38.63	4.50	11.19
31	$C_{13}H_{16}N_3O_6Co \cdot 1/2H_2O$	Theory	41.28	4.50	11.11
		Found	41.50	5.16	11.24
9	$C_{14}H_{18}N_3O_6Co \cdot 1/2H_2O$	Theory	42.87	4.86	10.74
31		Found	43.23	4.63	10.64
15	$C_{14}H_{18}N_3O_7Co \cdot H_2O$	Theory	40.30	4.80	10.07
		Found	40.36	5.14	10.05
30	$C_{15}H_{20}N_3O_6Co$	Theory	45.35	5.42	10.58
40		Found	45.18	5.27	10.52
25 <sup>b</sup>	$C_{15}H_{20}N_3O_6Co$	Theory	45.35	5.04	10.58
		Found	45.07	5.04	10.48
22 <sup>b</sup>	$C_{14}H_{17}N_4O_7Co$	Theory	39.08	4.42	13.03
		Found	38.62	4.85	13.68
5	$C_{13}H_{16}N_3O_6Co \cdot 2H_2O$	Theory	38.78	4.94	10.37
		Found	38.60	5.05	10.32
18	$C_{14}H_{18}N_3O_6Co \cdot 1/2H_2O$	Theory	42.87	4.86	10.74
<1		Found	42.95	4.88	10.70
7	$C_{14}H_{18}N_3O_7Co \cdot 1/2H_2O$	Theory	41.19	4.66	10.30
		Found	41.87	4.79	10.30
1	$C_{15}H_{20}N_3O_6Co \cdot 1/2H_2O$	Theory	42.46	5.42	9.91
		Found	42.39	5.19	9.95
13	$C_{15}H_{20}N_3O_6Co \cdot H_2O$	Theory	43.38	5.30	10.12
		Found	43.62	5.50	10.32
32 <sup>b</sup>	$C_{15}H_{20}N_3O_6Co \cdot H_2O$	Theory	43.38	5.30	10.12
		Found	43.64	5.47	10.15

combined and reduced to near dryness under vacuum to give a reddish pink solid. This solid was filtered, washed with MeOH and then vacuum dried. Identification of the reddish pink solid as the facial isomer was based on its visible spectrum.

The original filtrate from the reaction mixture was reduced to near dryness (5-10 ml) and placed on a Dowex 50W-X8 ion exchange column (2.5 X 65 cm, 200-400 mesh) in the Na<sup>+</sup> form. The column was eluted with water to give, usually, two bands; the first contained the meridional isomer, salts and unreacted materials; the second contained any remaining facial isomer. The solution from band two containing the facial isomer was reduced to near dryness in a rotary evaporator to give a reddish pink solid. The band containing the meridional isomer was reduced to 5 ml and placed on an acidic alumina column. (The size of the column depended upon the yield of the meridional isomer; for amounts of less than 0.1 g a 1.9 X 50 cm column was used, while a column 2.5 X 65 cm was used for amounts greater than 0.1 g as for the Co(N-Cm-L-Pyala)(L-Val) complex.) The meridional complex was eluted with a 75:25 MeOH:H<sub>2</sub>O solvent to give two bands. Band one contained salts and decomposition

products while band two contained the purple meridional isomer. The purple band was collected and reduced under vacuum to near dryness. Next a large volume (100-150 ml) of absolute ethanol was added to cause precipitation. The resulting solid was filtered and washed with acetone. The meridional product, identified by its visible spectrum, can be recrystallized for analysis by dissolving in a minimum volume of water and adding a volume of ethanol equal to 4 to 5 times that of water to force precipitation.

Method B, preparation of [Co(N-Cm-L-Pyala)-(D,L-Ala)] This procedure uses PbO<sub>2</sub> to oxidize Co(II) to Co(III) in the presence of N-Cm-L-Pyala<sup>2-</sup> and D,L-Ala<sup>-</sup> and is similar to the synthesis described for (Co(PLASP)-(D,L-Val)<sup>2-</sup>. The N-Cm-L-PyalaH<sub>2</sub> (.056 g, 2.5 mmol), D,L-AlaH (0.20 g, 2.5 mmole), CoSO<sub>4</sub>·7H<sub>2</sub>O (0.70 g, 2.5 mmol) and 5 ml of 1N NaOH were dissolved in 50 ml of water and PbO<sub>2</sub> (0.35 g, 1.5 mmol) was added. After the solution was heated at 70° C for 45 minutes, 2.5 ml of 1N H<sub>2</sub>SO<sub>4</sub> was added, and the solution was filtered. The filtrate was reduced under vacuum until a reddish pink precipitate formed. This was filtered and found to be the facial isomer by its visible spectrum. The remaining solution was reduced

to 1-2 ml and placed on a Dowex 50W-X8 column in the  $\text{Na}^+$  form. The facial and meridional isomers were chromatographed and isolated as described in Method A.

Method C The ligands, N-Cm-L-PyalaH<sub>2</sub> (.056 g, 2.5 mmol) and AAH (2.5 mmol), and CoSO<sub>4</sub>·7H<sub>2</sub>O (0.70 g, 2.5 mmol) were placed in 10 ml of water. Next 7.5 ml of 1N NaOH was added to give a brown solution of pH 9. After stirring the solution for 5 minutes, activated carbon (0.1 g) was added. This was followed by the addition of a solution of K<sub>2</sub>S<sub>2</sub>O<sub>4</sub> (0.4 g, 1.5 mmol) in 15 ml of water. At this point each reaction was treated somewhat differently. Each product discussed below was identified by its visible spectrum.

In the synthesis of the  $\alpha$ -AIBA<sup>-</sup> complexes, the solution was heated for 1 hour at 60° C and filtered to give a deep reddish purple solution. The solution was reduced to 10-15 ml and placed on a 2.5 X 65 cm Dowex 50W-X8 column in the  $\text{Na}^+$  form. Elution with water gave two bands. The first band contained the meridional isomer which was further purified by chromatography on an acidic alumina column as described in Method A. The second band containing the facial isomer was reduced to near dryness and ~150 ml of ethanol was added to cause precipitation. The precipitate was filtered off and vacuum dried.

The facial  $\underline{D}$ -AsN<sup>-</sup> complex was prepared as described for the  $\alpha$ -AIBA<sup>-</sup> complex above using  $\underline{D,L}$ -AsN<sup>-</sup> in the synthesis. A trace of the meridional isomer was isolated and identified by its <sup>13</sup>C nmr spectrum.

For the synthesis of the  $\underline{D}$ -Val<sup>-</sup> complexes, the reaction solution was stirred for 1 hour at room temperature to give the facial isomer as a reddish pink precipitate mixed with the activated charcoal. The facial isomer and carbon were filtered off. The filtrate was reduced to 5-10 ml to give more of the facial isomer which was filtered and washed with 30 ml of water. Reduction of this second filtrate followed by chromatography on Dowex 50W-X8 in the Na<sup>+</sup> form as for the  $\alpha$ -AIBA<sup>-</sup> complex above failed to yield any of the meridional isomer. The facial isomer and carbon were extracted with water (100 ml) and filtered. This was repeated until the filtrate was clear. The solutions containing the facial isomer were combined and reduced to near dryness. The solid was filtered, washed with MeOH and dried in vacuum.

In the synthesis of the Gly<sup>-</sup> complex the reaction solution was stirred for 1 hour at room temperature and filtered to give a deep purple solution characteristic

of the meridional isomer. This solution was placed on a rotary evaporator, and upon heating a reddish pink precipitate which was identified by its visible spectrum to be the facial isomer formed. The facial isomer was filtered off. The filtrate was reduced to 5-10 ml and chromatographed on Dowex 50W-X8 in the  $\text{Na}^+$ . Upon elution with water two bands formed. The first was purple in color but no solid resembling the meridional isomer was isolated from it. The second band contained more of the facial isomer.

Isomerization of mer-Co(N-Cm-L-Pyala) ( $\alpha$ -AIBA) Upon standing for several weeks at room temperature, an aqueous solution of the meridional  $\alpha$ -AIBA<sup>-</sup> isomer was chromatographed on Dowex 50W-X8 in the  $\text{Na}^+$  form to give two bands. Band one contained the major product and was identified by its visible spectrum as the meridional isomer. The visible spectrum of band two showed it to be fac-Co(N-Cm-L-Pyala) ( $\alpha$ -AIBA).

A sample of the meridional isomer (~0.1 g) was placed in 10 ml of water and heated at ~60° C for 1 hour. The solution was cooled to room temperature and chromatographed on Dowex 50W-X8 in the  $\text{Na}^+$  form to give two bands. The first band off the column was the meridional isomer while



the second band was the facial isomer. Each isomer was identified by its visible spectrum.

Spectra Visible spectra were recorded at room temperature in water on a Cary Model 14 spectrophotometer, while the circular dichroism spectra were measured in water at room temperature using a Jasco ORD/UV/CD-5 spectrophotometer. Proton nmr spectra were recorded at room temperature on a Jeol FX90Q Fourier transform nmr spectrometer in 99.7% deuterium oxide, using t-butyl alcohol ( $\delta$  1.23) as an internal standard. The  $^{13}\text{C}$  nmr spectra were also recorded on the above nmr spectrometer in either 99.7% deuterium oxide or 70%  $\text{H}_3\text{PO}_4$  (aqueous), using 1,4-dioxane (67.0 ppm downfield from TMS) as an internal standard.

## RESULTS AND DISCUSSION

The four possible geometric isomers of the  $\text{Co}(\text{N-Cm-L-Pyala})(\underline{\text{D-AA}})$  complex are shown in Figure 2. The structure in Figure 2a has a facial arrangement of oxygen atoms while the three structures in Figures 2b, 2c and 2d have a meridional arrangement of oxygen atoms. To differentiate the various meridional isomers, the terms  $\text{N-Cm-CO}_2^-$ ,  $\text{AA}^-$  amino and  $\text{AA}^- \text{CO}_2^-$  following the word mer in Figure 2 are used to denote which group is coordinated trans to the pyridyl group of  $\text{N-Cm-L-Pyala}^{2-}$ . It should be noted that the term meridional isomer will be used throughout the rest of this paper to refer to the mer  $\text{AA}^-$  amino isomer in Figure 2c.

Visible spectra of the  $\text{Co}(\text{N-Cm-L-Pyala})(\text{AA})$  complexes  
 Figure 3 shows visible spectra of mer- $[\text{Co}(\text{N-Cm-L-Pyala})(\underline{\text{D-Thr}})] \cdot 1/2\text{H}_2\text{O}$  and fac- $[\text{Co-Cm-L-Pyala})(\underline{\text{D-Thr}})] \cdot \text{H}_2\text{O}$ . These spectra are typical of the other  $\text{Co}(\text{N-Cm-L-Pyala})(\text{AA})$  complexes whose maxima are presented in Table II. The visible spectra of the facial isomers with their two symmetrical peaks at  $520 \pm 1 \text{ nm}$  ( $\epsilon = \sim 160$ ) and  $368 \pm 2 \text{ nm}$  ( $\epsilon = \sim 125$ ) are comparable to those reported for the facial  $\text{Co}(\text{PLASP})(\text{AA})$  mixed ligand complexes which have two symmetrical peaks at  $513 \pm 4 \text{ nm}$  and  $370 \pm 3 \text{ nm}$ .<sup>1,2</sup> Since

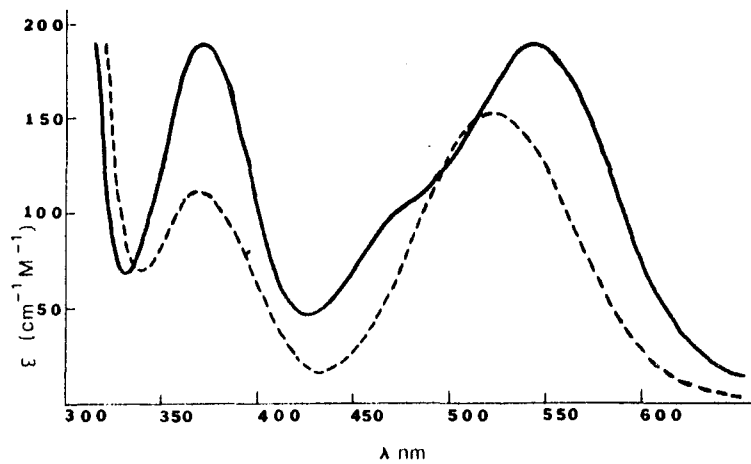


Figure 3. Visible spectra of mer-[Co(N-Cm-L-Pyala)(D-Thr)]·1/2H<sub>2</sub>O (—) and fac-[Co(N-Cm-L-Pyala)(D-Thr)]·H<sub>2</sub>O (----) in water

Table II. Visible absorption maxima for Co(N-Cm-L-Pyala) -  
(AA) complexes in water

Complex	$\lambda_{nm}$	$\epsilon (\text{cm}^{-1}\text{M}^{-1})$	$\lambda_{nm}$	$\epsilon (\text{cm}^{-1}\text{M}^{-1})$	$\lambda_{nm}$	$\epsilon (\text{cm}^{-1}\text{M}^{-1})$
I	522	153			367	120
II	521	155			368	117
III	521	164			369	127
IV	522	159			369	131
V	520	167			368	119
VI <sup>a</sup>	520	169			368	125
VII <sup>a</sup>	520	168			370	127
VIII	546	194	474	105	373	194
IX	543	191	474	104	371	197
X	545	177	472	96	370	184
XI	544	182	472	99	372	186
XII	543	186	474	101	371	189
XIII	544	177	472	97	371	184

<sup>a</sup>Isolated from the reaction using D,L-AA<sup>-</sup>.

the absorption maxima and extinction coefficients for the facial complexes listed in Table II are so similar, they are all assigned the structure of the facial isomer shown in Figure 2a. Visible spectra of the meridional isomers in Table II are comparable to other meridional  $\text{Co(III)N}_3\text{O}_3$  complexes reported previously.<sup>3,5,7</sup> Since the X-ray structure analysis of the mer-[Co(N-Cm-L-Pyala)-(D-Thr)]·1/2H<sub>2</sub>O showed the structure of this complex to be that shown in Figure 2c and the spectra of all the meridional isomers in Table II are so similar, they are all assigned this structure.<sup>5</sup> The shoulder (~474 nm) on the high energy side of the peak at ~544 nm is typical of other reported complexes having imidazole or pyridine coordinated trans to an amino group.<sup>3,7</sup>

Circular dichroism spectra of the Co(N-Cm-L-Pyala) (AA) complexes Circular dichroism spectra in water of various fac-Co(N-Cm-L-Pyala) (AA) complexes are shown in Figure 4 and are typical of the spectra of the other facial isomers isolated; their minima and maxima are listed in Table III. Since the CD spectrum of the facial complex isolated from the reaction using D,L-Val<sup>-</sup> is identical (within experimental error) to that of the fac-Co(N-Cm-L-Pyala) (D-Val) complex isolated using optically pure D-Val<sup>-</sup>, the complex is

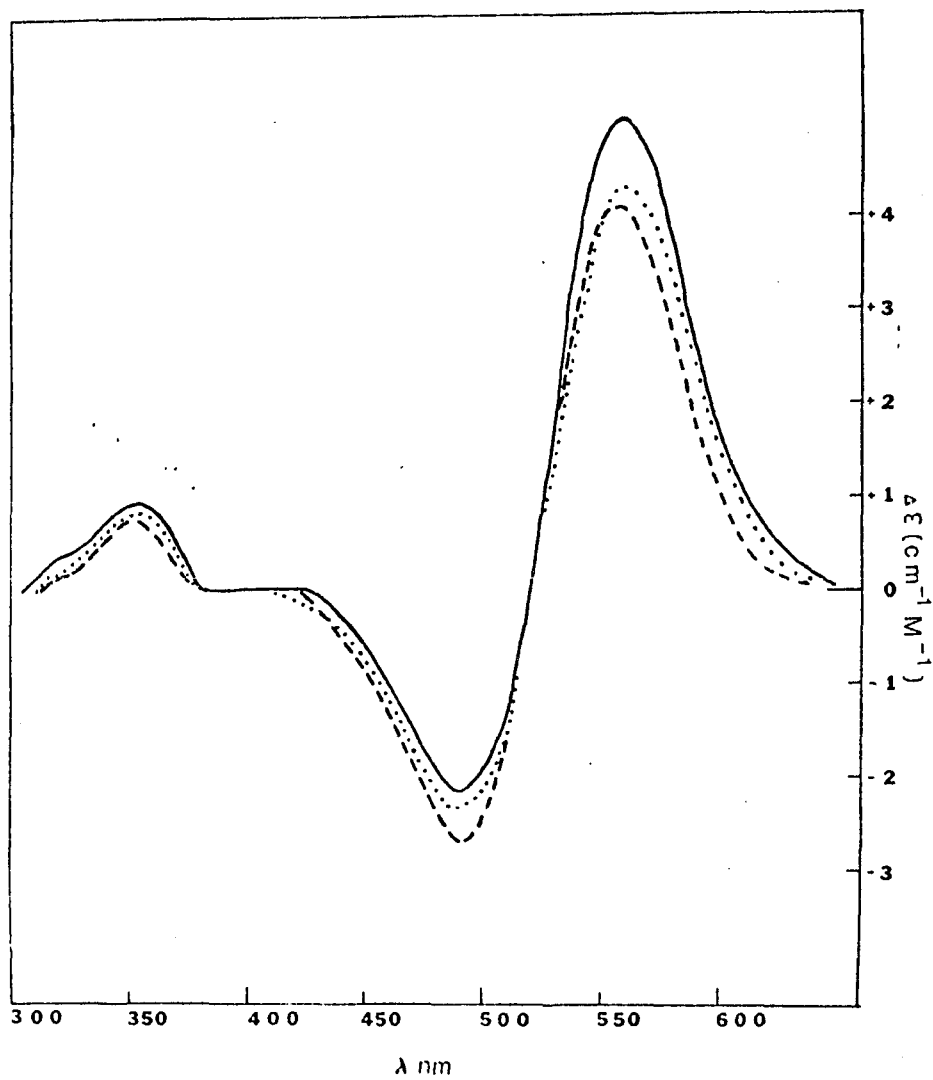


Figure 4. Circular dichroism spectra of various facial  $\text{Co}(\text{N-Cm-L-Pyala})(\text{AA})$  complexes in water:  
 $\text{D-Val}^-$  (—),  $\alpha\text{-AIBA}^-$  (····) and  $\text{Gly}^-$  (----)

Table III. Circular dichroism maxima and minima for the  
Co(N-Cm-L-Pyala)(AA) complexes in water

Complex	BAND I				BAND II	
	$\lambda$ nm	$\Delta\epsilon^a$	$\lambda$ nm	$\Delta\epsilon$	$\lambda$ nm	$\Delta\epsilon$
I	554	+4.19	488	-2.60	350	+0.77
II	555	+4.10	490	-2.67	352	+0.78
III	557	+4.30	488	-2.27	353	+0.82
IV	555	+4.82	488	-2.17	353	+0.87
V	557	+4.99	488	-2.02	352	+0.89
VI <sup>b</sup>	557	+5.05	488	-2.12	352	+0.94
VII <sup>b</sup>	557	+3.63	488	-1.82	353	+0.76
VIII	555	-.13	465	-1.50	380	+0.34
IX	554	+.06	468	-1.80	375	+0.36
X	553	+1.22	465	-2.37	370	+0.68
XI	554	+0.83	464	-1.86	372	+0.50
XII	545	-0.83	460	-1.57	376	+0.11
XIII	545	-.14	465	-1.65	375	+0.36

<sup>a</sup>Units for  $\Delta\epsilon$  are ( $\text{cm}^{-1}\text{M}^{-1}$ ) and an estimate of experimental error in  $\Delta\epsilon \pm .05$  ( $\text{cm}^{-1}\text{M}^{-1}$ ) for band I of the facial isomer. All others are approximately  $\pm .1$  ( $\text{cm}^{-1}\text{M}^{-1}$ ).

<sup>b</sup>Isolated from the procedure using  $\underline{\text{D}}, \underline{\text{L}}\text{-AA}^-$  in the synthesis.

formulated as fac-Co(N-Cm-L-Pyala)(D-Val). This assignment is consistent with the proton nmr spectra of the two complexes (see below). Thus, the formation of fac-Co(N-Cm-L-Pyala)(D-Val) appears to be stereoselective since it is the only facial isomer isolated when D,L-Val<sup>-</sup> is used in the synthesis.

The spectra of the facial isomers can be divided into two major bands (Table III) with band I in the 450 to 600 nm region and band II in the 320 to 400 nm region. The positive peak at ~555 nm and negative peak at 488 nm of band I are very similar in shape to the positive and negative peaks of band I of the cis-N, cis-O<sub>5</sub> Co(N-Cm-L-Asp)-(AA) complexes (Figure 1b), where N-Cm-L-Asp<sup>3-</sup> is the tetradentate N-carboxymethyl-L-aspartate ligand.<sup>8</sup> Comparison of these two complexes shows that they are structurally identical in terms of the sizes and positions of their chelate rings, and each contains one six-membered ring and three five-membered rings. Thus, the similarity in the overall shape of their CD spectra may be related to their structural similarities. It should be noted that the intensities of band I differ considerably for these two complexes with Co(N-Cm-L-Pyala)(AA) having Δε values of ~+5.00 (554 nm) and ~-2.50 (488 nm) and Co(N-Cm-L-Asp)(AA)



having  $\Delta\epsilon$  values of  $\sim+2.00$  (580 nm) and  $\sim-0.80$  (490 nm). Since these two complexes differ only in the group (either a pyridyl or carboxylate) coordinated trans to the N-carboxymethyl carboxylate group, the difference in CD intensities is attributed to the substitution of a pyridyl group for the  $\beta$ -carboxylate group of the aspartate fragment of N-Cm-L-Asp<sup>3-</sup>. A similar increase in  $\Delta\epsilon$  has been noted before when pyridine is substituted for imidazole in the Co(Pyala)<sub>2</sub><sup>+</sup> and Co(Hist)<sub>2</sub><sup>+</sup> complexes, where Pyala<sup>-</sup> is  $\beta$ -(2-pyridyl- $\alpha$ -alaninate) and Hist<sup>-</sup> is histidinate.<sup>3</sup>

A comparison of the fac-Co(N-Cm-L-Pyala)( $\alpha$ -AIBA) circular dichroism spectrum to that of fac-Co(PLASP)( $\alpha$ -AIBA)<sup>2-</sup> (Figure 1a) shows that both have a positive peak at  $\sim 550$  nm, but the PLASP<sup>2-</sup> complex has a positive peak at 495 nm while the N-Cm-L-Pyala<sup>2-</sup> complex has a negative peak at 488 nm. Similar differences are observed in comparisons of the other fac-Co(N-Cm-L-Pyala)(AA) CD spectra to the corresponding fac-Co(PLASP)(AA) circular dichroism spectra. These differences may be attributed to a change of symmetry when the pyridyl group and carboxylate group are interchanged in PLASP<sup>2-</sup> and N-Cm-L-Pyala<sup>2-</sup>.

Band II consists of one positive peak at  $\sim 352$  nm. This peak remains fairly constant for all the facial complexes in Table II.

In Figure 5 are shown circular dichroism spectra in water of the various meridional  $\text{Co}(\text{N-Cm-L-Pyala})(\text{AA})$  complexes; their minima and maxima are given in Table III. As in the case of the facial isomers, the CD spectra of the meridional isomers can be divided into two bands, with band I in the 600 to 400 nm region and band II in the 400 to 320 nm region.

For the CD spectra (Figure 5) of the meridional complexes containing  $\underline{\text{D}}, \underline{\text{L}}\text{-Val}^-$ ,  $\alpha\text{-AIBA}^-$  and  $\underline{\text{D}}, \underline{\text{L}}\text{-Ala}^-$ , (where the terms  $\underline{\text{D}}, \underline{\text{L}}\text{-AA}$  refers to complexes containing equal amounts of the two diastereomers,  $\text{Co}(\text{N-Cm-L-Pyala})(\underline{\text{L}}\text{-AA})$  and  $\text{Co}(\text{N-Cm-L-Pyala})(\underline{\text{D}}\text{-AA})$ ) band I consists of a large negative peak at  $\sim 460$  nm. The small negative or positive peak at  $\sim 550$  nm is of the same magnitude as experimental error ( $\pm .1$ ) and will not be discussed. Band I of the meridional complexes containing  $\underline{\text{D}}\text{-Val}^-$  and  $\underline{\text{D}}\text{-Thr}^-$  consists of two peaks, one positive at  $\sim 554$  nm and one negative at  $\sim 465$  nm, while for the  $\underline{\text{L}}\text{-Val}^-$  complex band I has a negative peak at 465 nm but it also has a negative peak at 545 nm instead of a positive peak as for the  $\underline{\text{D}}$ -amino acidates. Band II of the meridional isomers consists of a broad peak at  $\sim 370$  nm. The intensity of this peak remains constant for the  $\alpha\text{-AIBA}^-$ ,  $\underline{\text{D}}, \underline{\text{L}}\text{-Val}^-$  and  $\underline{\text{D}}, \underline{\text{L}}\text{-Ala}^-$  complexes but varies for the  $\underline{\text{L}}\text{-Val}^-$ ,  $\underline{\text{D}}\text{-Val}^-$  and  $\underline{\text{D}}\text{-Thr}^-$  complexes.

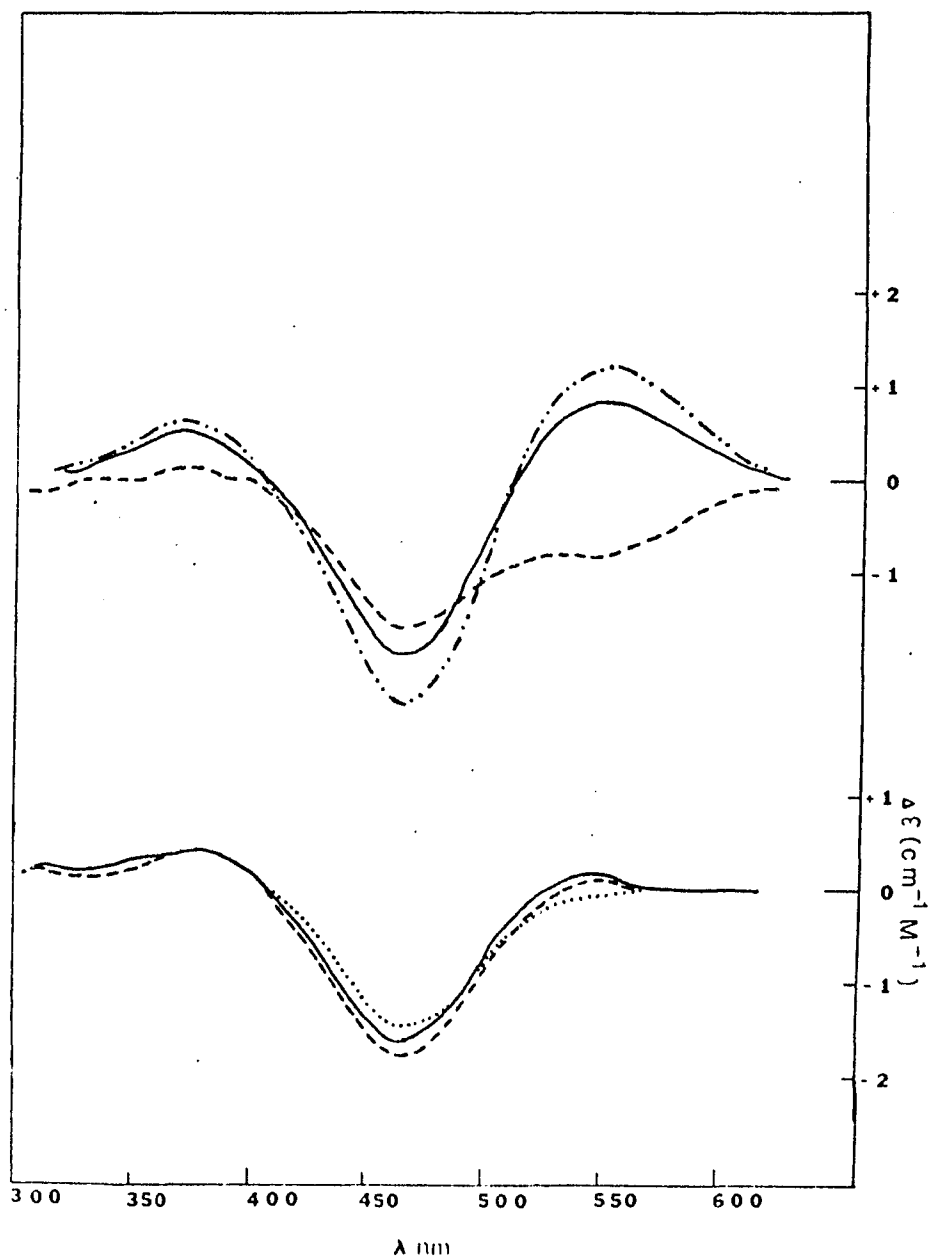


Figure 5. Circular dichroism spectra of various meridional  $\text{Co}(\text{N-Cm-L-Pyala})(\text{AA})$  complexes in water: lower,  $\alpha\text{-AIBA}^-$  (----),  $\text{D,L-Val}^-$  (—),  $\text{D,L-Ala}^-$  (····); upper,  $\text{D-Val}^-$  (—),  $\text{D-Thr}^-$  (-·-·-),  $\text{L-Val}^-$  (----)

As noted previously, differences in the CD spectra of the Co(PLASP)(AA) complexes were attributed to changes at the  $\alpha$ -carbon of the amino acidate. Their CD spectra were resolved into two contributions, one associated with the optically active portion of the amino acidate chelate ring (Y), and the other with the rest of the molecule (X). Similarly, the differences in the overall shapes and intensities of the CD spectra for the meridional isomers of Co(N-Cm-L-Pyala)(AA) must be related to changes at the  $\alpha$ -carbon of the amino acidates. Therefore the CD spectra of the meridional isomers can also be resolved into X and Y terms. Using the same argument as presented for the Co(PLASP)(AA) CD spectra, the value of  $\Delta\epsilon$  at a given wavelength in the CD spectrum of a mer-Co(N-Cm-L-Pyala)(AA) complex can be expressed as follows:

$$X + Y_{\underline{D} \text{ or } \underline{L}} = CD[\text{Co(N-Cm-}\underline{L}\text{-Pyala)}(\underline{D} \text{ or } \underline{L}\text{-AA)}] \quad (1)$$

If it is assumed that  $Y_{\underline{D}} = -Y_{\underline{L}}$ , then

$$X = \frac{CD[\text{Co(N-Cm-}\underline{L}\text{-Pyala)}(\underline{L}\text{-AA)}] + CD[\text{Co(N-Cm-}\underline{L}\text{-Pyala)}(\underline{D}\text{-AA)}]}{2} \quad (2)$$

The X value calculated using CD data for the pair, mer-Co(N-Cm-L-Pyala)(D-Val) and mer-Co(N-Cm-L-Pyala)(L-Val) is given in Figure 6 and is identical (within experimental error) to that observed for the mer-D,L-Val<sup>-</sup> complex.

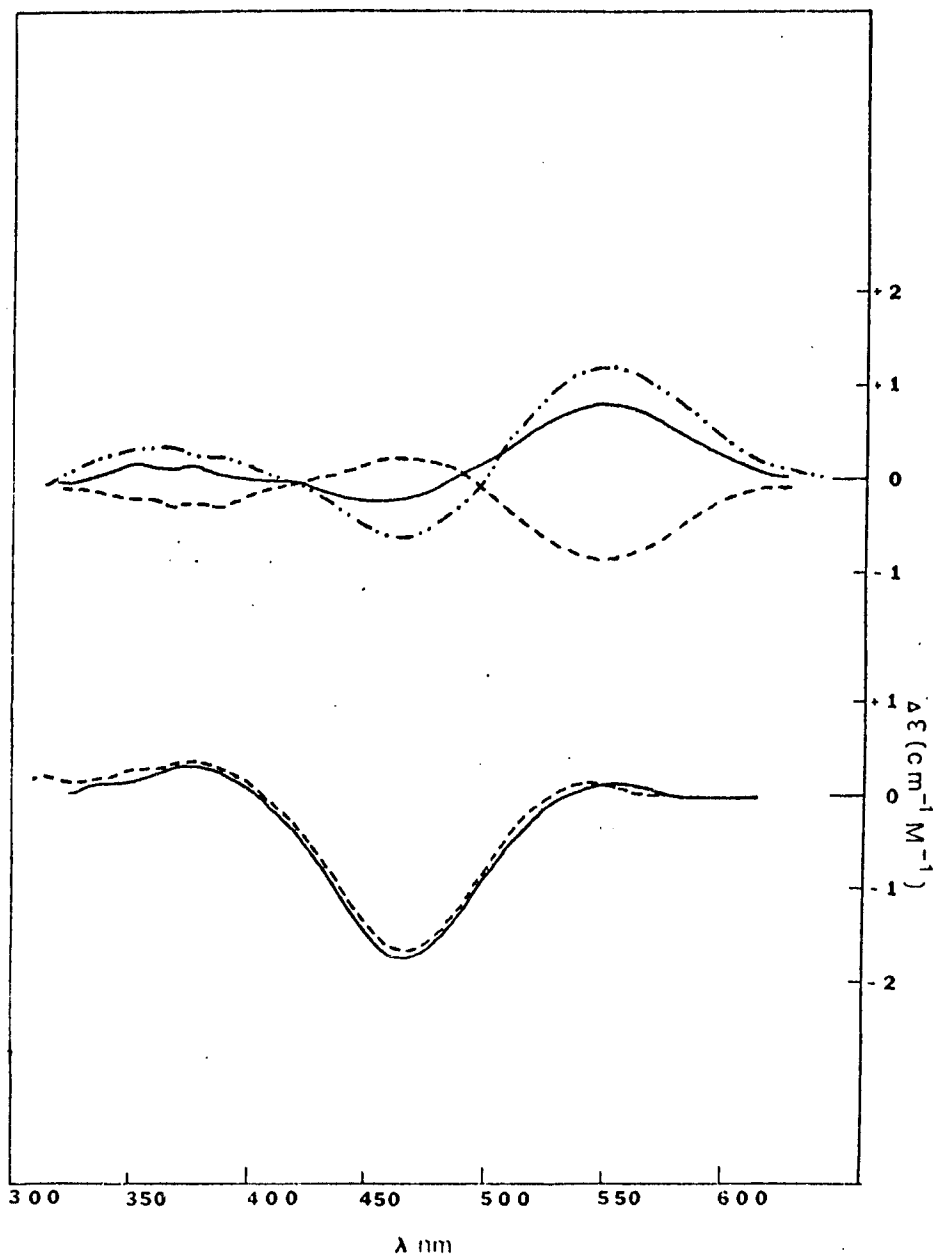


Figure 6. Circular dichroism (lower) X term from  $\{mer-[Co(N-Cm-\underline{L}-Pyala)(\underline{D}-Val)] + mer-[Co(N-Cm-\underline{L}-Pyala)-(\underline{L}-Val)]\}/2$  (—) and the CD spectrum for  $mer-[Co(N-Cm-\underline{L}-Pyala)(\underline{D},\underline{L}-Val)] \cdot H_2O$  (----) and (upper) Y terms calculated from  $mer-[Co(N-Cm-\underline{L}-Pyala)-(AA)] - mer-[Co(N-Cm-\underline{L}-Pyala)(\alpha-AIBA)] \cdot 1/2H_2O$  for  $\underline{D}-Val^-$  (—),  $\underline{D}-Thr^-$  (-·-·-) and  $\underline{L}-Val^-$  (----)

It should be noted the CD spectra of  $\underline{D}, \underline{L}\text{-Val}^-$ ,  $\underline{D}, \underline{L}\text{-Ala}^-$  and  $\alpha\text{-AIBA}^-$  (Figure 5) are nearly identical (within experimental error) to that of the calculated X term. Thus, as in the case of the facial  $\text{Co(PLASP)(AA)}$  complex, the assumption that X is essentially equal to the observed spectrum of  $\text{mer-Co(N-Cm-}\underline{L}\text{-Pyala)}(\alpha\text{-AIBA})$  can also be made. A comparison of the X terms for  $\text{fac-Co(PLASP)(AA)}$  and  $\text{mer-Co(N-Cm-}\underline{L}\text{-Pyala)}(\text{AA})$  shows no similarity between the two since the X term for the  $\text{PLASP}^{2-}$  complexes<sup>2</sup> has two positive peaks at 545 and 495 nm while that of the  $\text{mer-N-Cm-}\underline{L}\text{-Pyala}^{2-}$  complexes has only a negative peak at  $\sim 470$  nm.

Calculated Y terms for the  $\underline{D}\text{-Val}^-$ ,  $\underline{L}\text{-Val}^-$  and  $\underline{D}\text{-Thr}^-$  meridional complexes using eq. 1 and assuming X is equal to the observed CD spectrum of  $\text{mer-Co(N-Cm-}\underline{L}\text{-Pyala)}(\alpha\text{-AIBA})$  are given in Figure 6. An examination of the Y curves for  $\underline{D}\text{-Val}^-$  and  $\underline{L}\text{-Val}^-$  shows that to a first approximation the assumption of  $Y_D = -Y_L$  in formulating eq. 2 is valid. The Y term for the  $\underline{D}$ -amino acidates has a positive peak at  $\sim 550$  nm while the  $\underline{L}$ -amino acidate has a negative peak at  $\sim 550$  nm. This trend has been observed before for the Y terms of the  $\text{fac-Co(PLASP)(AA)}$  complexes where the Y term of a  $\underline{D}\text{-AA}^-$  has a positive peak in the 520 nm region and an  $\underline{L}\text{-AA}^-$  has a negative peak at  $\sim 520$  nm.

Attempts to calculate X and Y terms from the CD spectra of the facial  $\text{Co}(\text{N-Cm-L-Pyala})(\text{AA})$  complexes is complicated by the sharp changes in the spectra in the 480-540 nm region. It should be noted that the Y term at  $\sim 550$  for the  $\underline{\text{D-Val}}^-$  and  $\underline{\text{D-Thr}}^-$  complexes would be positive since these two  $\underline{\text{D-AA}}^-$  complexes have a higher  $\Delta\epsilon$  at 550 nm than the corresponding facial  $\alpha\text{-AIBA}^-$  complex.

$^1\text{H}$  nmr spectra of the  $\text{Co}(\text{N-Cm-L-Pyala})(\text{AA})$  complexes  
Proton nmr spectra of the various  $\text{Co}(\text{N-Cm-L-Pyala})(\text{AA})$  complexes and  $\text{N-Cm-L-PyalaH}_2$  in 99.7% deuterium oxide are given in Table IV. The chemical shifts of the  $\text{N-Cm-L-Pyala}^{2-}$  portion for both the facial and meridional isomers are explained in detail in a previous paper.<sup>5</sup> The major difference between the  $\text{N-Cm-L-Pyala}^{2-}$  chemical shifts in the meridional and facial isomers is in the ortho pyridyl protons and the N-carboxymethyl protons. In the facial isomers the ortho proton ( $\sim\delta$  8.0) is positioned over the amino acidate carboxylate plane and is shielded relative to the meridional ortho proton ( $\sim\delta$  9.0) which is nearly in the plane of the amino acidate carboxylate group and is deshielded. An examination of the chemical shifts of the ortho pyridyl proton for the facial isomer shows that they do not remain constant from one amino

Table IV. The  $^1\text{H}$  chemical shifts of various  $\text{Co}(\text{N-Cm-L-Pyala})(\text{AA})$  complexes in 99.7%  $\text{D}_2\text{O}^{\text{a}}$

Isomer	AA <sup>-</sup>	N-Cm-L-Pyala <sup>2-</sup>						AA <sup>-</sup>		
		$\delta$ $\alpha\text{-H}^{\text{b}}$	$\delta$ $\beta\text{-H}^{\text{b}}$	$\delta$ N-Cm-H <sup>c</sup>	$\delta$ <u>o</u> -py	$\delta$ <u>m</u> -py <sup>d</sup>	$\delta$ <u>p</u> -py	$\delta$ $\alpha\text{-H}$	$\delta$ $\beta\text{-H}$	$\delta$ $\gamma\text{-H}$
fac	Gly <sup>-</sup>	3.9m	3.9m	3.60d 4.34d	8.13d	7.55m	8.03t	3.54s		
fac	<u>D,L</u> -Ala <sup>-</sup>	3.9m	3.9m	3.59d	8.0m	7.47m	8.0m	4.24t	1.48d	
fac	$\alpha$ -AIBA <sup>-</sup>	3.9m	3.9m	3.56d 4.37d	8.0m	7.50m	8.0m	1.47s		1.50s
fac	<u>D</u> -Thr <sup>-</sup>	3.9m	3.9m	3.60d 4.33d	8.12d	7.46m	7.98t	3.54d	4.4m	1.27d
fac	<u>D</u> -Val <sup>-</sup>	3.9m	3.9m	3.57d 4.40d	8.0m	7.50m	8.0m	3.58d	2.33m	0.97d <sup>e</sup> 1.05d
fac	<u>D</u> -Val	3.9m	3.9m	3.57d 4.40d	8.0m	7.55m	8.0m	3.58d	2.33m	0.97d <sup>e</sup> 1.05d
fac	<u>D</u> -AsN <sup>-</sup>	3.9m	3.9m	3.59d 4.37d	8.41d	7.50m	7.99t	3.78m	2.91m	
mer	<u>D,L</u> -Ala <sup>-</sup>	4.1m	4.1m	3.65s	8.97d <sup>f</sup> 8.92d	7.58m	8.04t	1.51d		1.54d
mer	$\alpha$ -AIBA <sup>-</sup>	4.0m	4.0m	3.62s	9.03d	7.63m	8.09t	1.52s		
mer	<u>D</u> -Thr <sup>-</sup>	4.0m	4.0m	3.62s	8.99d	7.61m	8.07t	3.62d	4.4m	1.37d
mer	<u>D</u> -Val <sup>-</sup>	4.0m	4.0m	3.61s	9.01d	7.60m	8.07t	3.73d	2.36m	0.94d <sup>e</sup> 1.15d



mer	<u>L</u> -Val <sup>-</sup>	4.0m	4.0m	3.63s	8.97d	7.61m	8.08t	3.76d	2.44m	0.90d <sup>e</sup> 1.16d
mer	<u>D,L</u> -Val <sup>-</sup>	4.0m	4.0m	3.63s	8.96d 9.02d	7.64m	8.08t	3.72d 3.76d	2.5- 2.2	0.90d <sup>e</sup> 0.94d 1.16d
mer	<u>L</u> -Pro <sup>-</sup>	4.0m	4.0m	3.61s	8.96d	7.62m	8.08t	4.22m	1.8- 3.3m <sup>g</sup>	
	N-Cm-L- PyaLaH <sub>2</sub>	4.15q	3.66m	3.78s	8.69d	7.92m	8.49t			

<sup>a</sup>The center of each peak (or peaks) is given and the multiplicity is given by s = singlet, d = doublet, t = triplet, q = quartet and m = multiplet.

<sup>b</sup>The resonances for the  $\alpha$  and  $\beta$  hydrogens overlap and the value given represents the center of the multiplet.

<sup>c</sup>The coupling constant for the doublets given in this column is 18 Hz.

<sup>d</sup>This multiplet consists of an overlapping doublet and triplet.

<sup>e</sup> $J = 7$  Hz for each doublet.

<sup>f</sup> $J = 5$  Hz for each doublet.

<sup>g</sup>This region includes the  $\beta$ ,  $\gamma$  and  $\delta$  protons of the proline ligand.

acidate to another. In the  $\text{Gly}^-$ ,  $\underline{\text{D}}\text{-Thr}^-$  and  $\underline{\text{D}}\text{-AsN}^-$  complexes, the doublet of the ortho proton is shifted downfield relative to that of the other complexes in which the doublet overlaps with the triplet of the para proton. In the facial isomer the ortho pyridyl proton is situated over the  $\pi$  cloud of the amino acidate  $\text{CO}_2^-$  group. In the case of a  $\underline{\text{D}}$ -amino acidate the  $\text{CO}_2^-$  is bent away from the ortho hydrogen, while in that of an  $\underline{\text{L}}$ -amino acidate it is bent toward the ortho hydrogen. Thus any changes in the bending of the amino acidate chelate ring will cause a change in the chemical shifts of the ortho proton. This has also been noted for the ortho pyridyl proton in the  $\text{Co(PLASP)(AA)}$  complexes.<sup>2</sup>

The deshielding of the ortho proton ( $\delta$  8.41) of the facial  $\underline{\text{D}}\text{-AsN}^-$  complex relative to the other facial isomers is presumably due to the presence of a polar amide group near the ortho proton. This deshielding by the  $\text{AsN}^-$  R-group is similar to that found in the  $\text{Co(PLASP)(\underline{\text{L}}\text{-AsN})}$  complexes where the polar amide group is near the ortho pyridyl proton of  $\text{PLASP}^{2-}$ .<sup>2</sup> Thus, the assignment of the complex isolated from the reaction of  $\underline{\text{D}}, \underline{\text{L}}\text{-AsN}^-$  as  $\text{fac-Co(N-Cm-}\underline{\text{L}}\text{-Pyala)(}\underline{\text{D}}\text{-AsN)}$  is consistent with the proton nmr data. Further evidence for this assignment is given in the discussion of the  $^{13}\text{C}$  nmr spectrum of the  $\underline{\text{D}}\text{-AsN}^-$  complex, to be presented below.

The splitting of the N-carboxymethyl protons of the facial isomers is similar to the splitting observed for the N-pyridylmethyl protons of the fac-Co(PLASP)(AA) complexes previously reported.<sup>2</sup> It should be noted that no splitting is observed for the meridional N-carboxymethyl protons which occur as a broad singlet. The difference in the N-carboxymethyl protons in the meridional and facial isomers may be due to the magnetic anisotropy of the C-N bonds of the secondary amino nitrogen of the N-Cm-L-Pyala<sup>2-</sup> and/or the difference in position of the C-N bonds in the two isomers. This has been noted before in other Co(III) complexes containing polyaminocarboxylates ligands.<sup>9,10</sup>

The amino acidate  $\alpha$ -H chemical shifts of the facial Co(N-Cm-L-Pyala)(D-AA) isomers are comparable to those of the corresponding Co(PLASP)(L-AA) complexes. This seems reasonable since the  $\alpha$ -H proton of the amino acidate in fac-Co(N-Cm-L-Pyala)(D-AA) and that in Co(PLASP)(L-AA) are in similar environments. In the PLASP<sup>2-</sup> complex the  $\alpha$ -H is in the vicinity of the  $\beta$ -CO<sub>2</sub><sup>-</sup> and in the N-Cm-L-Pyala<sup>2-</sup> complex it is in the vicinity of the N-carboxymethyl carboxylate.

$^{13}\text{C}$  nmr spectra of the  $\text{Co}(\text{N-Cm-L-Pyala})(\text{AA})$  complexes

The  $^{13}\text{C}$  nmr spectra of the free ligand  $\text{N-Cm-L-PyalaH}_2$  and the various  $\text{Co}(\text{N-Cm-L-Pyala})(\text{AA})$  complexes in  $\text{D}_2\text{O}$  and 70%  $\text{H}_3\text{PO}_4$  (aqueous) are assigned in Table V. The chemical shifts of the  $\text{N-Cm-L-Pyala}^{2-}$  ligand in the facial complexes remain constant and do not seem to be affected by the amino acidate. This is also true for the  $\text{N-Cm-L-Pyala}^{2-}$  fragment of the meridional complexes. The chemical shifts of the  $\text{fac-Co}(\text{N-Cm-L-Pyala})(\text{AA})$  complexes are comparable to those reported for the facial  $\text{Co}(\text{PLASP})(\text{AA})$  complexes.<sup>2</sup>

The chemical shifts of the facial  $\alpha$ -,  $\beta$ - and N-carboxymethyl carbons of the  $\text{N-Cm-L-Pyala}^{2-}$  ligand are approximately 5-8 ppm upfield from those of the meridional isomer. This difference may be due to a change in chelate ring positions between the two isomers and/or a change in the magnetic anisotropy around the cobalt caused by a changing from meridional to facial coordination.

It may be noted that all the various carbon resonances for the  $\text{fac-Co}(\text{N-Cm-L-Pyala})(\text{D-AsN})$  complex occur as distinct singlets (protons are broad band decoupled) and no evidence for the presence of the other diastereomer was found. This is consistent with the proton nmr and CD spectral assignment of the complex as  $\text{fac-Co}(\text{N-Cm-L-Pyala})(\text{D-AsN})$ .

Table V.  $^{13}\text{C}$  nmr of the  $\text{Co}(\text{N-Cm-L-Pyala})(\text{AA})$  complexes in  $\text{D}_2\text{O}$ <sup>a</sup>

Complex	$\text{N-Cm-L-Pyala}^{2-}$				
	$\alpha\text{-CO}_2^-$	$\text{N-Cm-CO}_2^-$	$\alpha\text{-C}$	$\beta\text{-C}$	$\text{N-Cm-CO}_2^-$
I	184.9	183.5	66.6	35.4	57.5
II	183.8	183.0	66.5	35.4 35.5	56.8 57.1
III	183.8	182.9	66.5	35.5	57.1
IV <sup>b</sup>	185.3	183.9		35.5	
V <sup>b</sup>	185.3	183.9	66.6	35.4	
VII <sup>c</sup>	183.7	183.2	66.7	35.5	56.9
$\text{N-Cm-L-PyalaH}_2$	171.4	171.2	60.7	33.8	48.5
VIII	183.1	182.8	59.2	30.8 30.9	49.1 49.4
IX	183.1	182.8	59.1	30.9	49.3
X	183.2	182.8	59.1	30.1	49.7
XI <sup>d</sup>	183.2	182.8	59.1	30.9	49.6
XII	183.2	182.9	59.3	30.8	49.3
XIII	183.2	182.8 182.9	59.1 59.3	30.8 30.9	49.3 49.6
XIV <sup>e</sup>	183.0	182.8	58.9	30.8	49.3
XV <sup>f</sup>	183.6	183.4	59.7	30.7	50.0

<sup>a</sup>The chemical shifts are given downfield from TMS with dioxane used as an internal reference at 67.0 ppm.

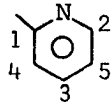
<sup>b</sup>In 70%  $\text{H}_3\text{PO}_4$  (aqueous).

<sup>c</sup>Isolated using  $\text{D,L-AsN}^-$  in the synthesis.

<sup>d</sup>Chemical shifts are from the  $^{13}\text{C}$  nmr spectrum of the  $\text{mer-D,L-Val}^-$  complex minus those of the  $\text{L-Val}^-$  complex.

<sup>e</sup> $\text{mer-Co}(\text{N-Cm-L-Pyala})(\text{L-Pro})$ .

<sup>f</sup> $\text{mer-Co}(\text{N-Cm-L-Pyala})(\text{AsN})$ .

N-Cm-L-Pyala <sup>2-</sup>					AA <sup>-</sup>			
					$\alpha$ -CO <sub>2</sub>	$\alpha$ -C	$\beta$ -C	$\gamma$ -C
1	2	3	4	5				
157.3	150.9	142.0	129.4	126.3	186.6	47.6		
158.0	151.0	141.2	128.8	125.2	188.2	54.5 54.8	18.1 18.4	
157.9	150.6	141.2	128.9	125.2	189.8	62.1	27.3 28.7	
157.0	151.0	142.2	129.5	126.5	185.5		64.8	18.7
157.4	150.0	142.2	129.8	126.2	186.9	64.8	30.3	16.5, 18.5
157.6	152.5	141.1	128.5	124.8	184.3	55.2	35.6	175.3
151.7	146.6	142.4	128.3	126.1				
156.4	153.1 153.4	140.9	127.9	125.0		54.9 55.4	18.3 18.6	
156.4	153.3	140.9	127.9	125.0	187.9	62.2	27.0 27.7	
156.4	153.5	140.9	127.9	125.0	184.0	66.6	64.3	19.2
156.4	153.5	140.9	127.9	125.0	185.9	64.5	30.4	15.8, 18.5
156.4	153.3	140.9	127.8	125.0	185.7	64.1	30.2	15.5, 18.6
156.4	153.3 153.5	140.9	127.9	125.0	185.9	64.1 64.5	30.2 30.4	15.5, 15.8 18.5, 18.6
156.5	153.2	140.9	127.8	125.1	186.9	66.3	47.8	25.0, 29.2
156.6	153.0	140.8	127.8	124.9	184.9	56.9	35.8	176.8

Discussion of isomer distribution The isolation of the facial isomers of  $\underline{D}$ -Val<sup>-</sup>,  $\underline{D}$ -Thr<sup>-</sup>,  $\underline{D},\underline{L}$ -Ala<sup>-</sup>,  $\underline{D}$ -AsN<sup>-</sup> and Gly<sup>-</sup> in higher yields than the meridional isomers suggests that these facial isomers are preferred over the corresponding meridional isomers. It should be noted, however, that the lower solubilities of the facial isomers may be responsible for the higher yields of the facial isomers. These facial complexes also appear to be sterically favored. In the cases of  $\underline{D}$ -Val<sup>-</sup>,  $\underline{D}$ -Thr<sup>-</sup>,  $\underline{D}$ -AsN<sup>-</sup> and possibly the Gly<sup>-</sup> complexes, the chelate ring is bent down and away from the pyridine ring. This bending would be caused by the bulky R groups of the  $\underline{D}$ -amino acidates favoring the equatorial rather than the axial position.

Although the facial isomer appears to be preferred, the meridional isomer (Figure 2c) cannot be ignored since it was isolated for all the amino acidates except Gly<sup>-</sup>. In the case of the Co(N-Cm- $\underline{L}$ -Pyala)( $\underline{L}$ -Val) complex the meridional isomer is the only one isolated. There was no evidence for the facial isomer. In fac-Co(N-Cm- $\underline{L}$ -Pyala)-( $\underline{L}$ -Val) the chelate ring would be bent upward toward the pyridine; an examination of models indicates that there would be considerable steric interaction between the  $\alpha$ -CO<sub>2</sub><sup>-</sup> of  $\underline{L}$ -Val<sup>-</sup> and the ortho hydrogen of the pyridyl ring.

Thus it appears the meridional isomer of  $\text{Co}(\text{N-Cm-}\underline{\underline{\text{L}}}\text{-Pyala})\text{-}(\underline{\underline{\text{L}}}\text{-Val})$  is sterically favored over the facial. It should be noted that, since  $\text{fac-Co}(\text{N-Cm-}\underline{\underline{\text{L}}}\text{-Pyala})(\underline{\underline{\text{D}}}\text{-Val})$  was the only facial isomer isolated from the reaction using  $\underline{\underline{\text{D}}}\text{,}\underline{\underline{\text{L}}}\text{-Val}^-$ , the formation of this complex appears to be stereospecific.

The arguments presented above are for the two extremes; one ( $\underline{\underline{\text{D}}}\text{-AA}$ ) involves little steric interaction, while the other ( $\underline{\underline{\text{L}}}\text{-AA}$ ) involves considerable interaction in the facial isomer. An examination of molecular models of the facial  $\alpha\text{-AIBA}^-$  isomer shows some interaction between the pyridine ring and a methyl group of  $\alpha\text{-AIBA}^-$  is possible. Isomerization studies of  $\text{mer-Co}(\text{N-Cm-}\underline{\underline{\text{L}}}\text{-Pyala})(\alpha\text{-AIBA})$  seem to show that the meridional and facial isomers are both present in substantial amounts at equilibrium. It should be noted that both the mer- and fac- $\alpha\text{-AIBA}^-$  isomers are quite soluble, and their solubilities would not affect their equilibrium distribution. The comparable stabilities of these isomers suggest that steric interaction in the facial  $\alpha\text{-AIBA}^-$  isomer is somewhere between the two extremes for the  $\text{fac-}\underline{\underline{\text{D}}}\text{-Val}^-$  and  $\text{fac-}\underline{\underline{\text{L}}}\text{-Val}^-$  complexes.

The above discussion suggests some general trends for these complexes. First, the facial isomers appear to



be preferred if steric interaction between the amino acidate chelate ring and the pyridyl group is small. This is consistent with the stabilities of the facial Co(PLASP)(AA) complexes and a theoretical account of  $d^6$  low-spin  $ML_3L_3'$  complexes reported previously.<sup>1,2,4</sup> Second, the meridional isomer seems to be favored if there is significant steric interaction between the amino acidate chelate ring and the pyridyl group in the facial isomer, as in the case of Co(N-Cm-L-Pyala)(L-Val).

## CONCLUSION

Previously we reported that the facial structure (Figure 1a) of the Co(PLASP)(AA) complexes was favored by electronic and structural factors.<sup>1,2</sup> The facial coordination was suggested to be electronically favored since the amino groups avoid coordinating trans to each other and structurally favored since coordination of the pyridyl group of PLASP<sup>2-</sup> trans to the  $\beta$ -CO<sub>2</sub><sup>-</sup> of PLASP<sup>2-</sup> gives the least strained bond angle around the secondary amino nitrogen of PLASP<sup>2-</sup>. Finally we concluded that steric factors did not play an important role in determining the overall geometry of the complex.

In the case of the Co(N-Cm-L-Pyala)(AA) complexes, the stability of the isomer isolated may be attributed to a combination of electronic, structural and steric factors. As in the Co(PLASP)(AA) case, the fac- and mer-Co(N-Cm-L-Pyala)(AA) complexes in Figures 2a and 2c appear to be electronically favored over the other possible structures (2b and 2d) since the amino groups avoid coordinating trans to each other. However, it is not clear whether 2a or 2c is electronically the more stable structure.

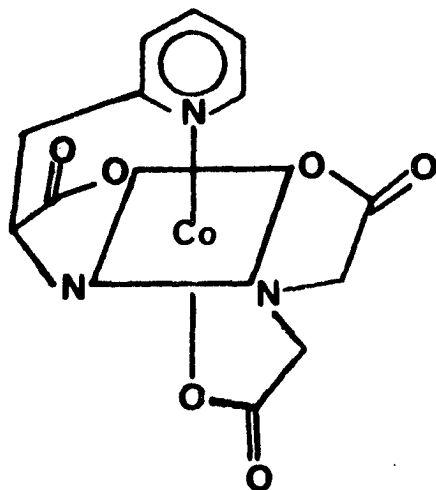
However, strain in the tetradentate ligand would be expected to be different in these two structures. The coordination of the N-carboxymethyl  $\text{CO}_2^-$  group trans to the pyridyl group in the facial isomer should produce little strain in the C-N-C bond angle. This has been noted above for the  $\text{Co}(\text{PLASP})(\text{AA})$  complexes and is consistent with the coordination of polydentate ligands such as  $^- \text{O}_2\text{C}-\text{CH}_2-\text{NH}-\text{CH}_2-\text{CO}_2^-$ ,  $\text{IMDA}^{2-}$  reported previously.<sup>1,11-13</sup> In the facial mode of coordination the glycinate chelate rings of  $\text{IMDA}^{2-}$  are  $90^\circ$  to each other, and there is very little strain in the C-N-C angle. However, in the meridional  $\text{Co}(\text{N-Cm-}\underline{\text{L}}\text{-Pyala})(\text{AA})$  complexes the coordination of the N-carboxymethyl  $\text{CO}_2^-$  trans to the  $\alpha\text{-CO}_2^-$  of  $\text{N-Cm-}\underline{\text{L}}\text{-Pyala}^{2-}$  produces considerable strain in the C-N-C angle. The X-ray structure analysis of  $\text{mer-}[\text{Co}(\text{N-Cm-}\underline{\text{L}}\text{-Pyala})(\underline{\text{D}}\text{-Thr})] \cdot 1/2\text{H}_2\text{O}$  has shown that the  $120^\circ$  C-N-C bond angle is severely distorted from the ideal tetrahedral value. Similar C-N-C angular strain has been found in the meridional coordination of the glycinate chelate ring of other polydentate ligands in the same plane.<sup>11-13</sup> Thus, the facial isomer of  $\text{Co}(\text{N-Cm-}\underline{\text{L}}\text{-Pyala})(\underline{\text{D}}\text{-AA})$  appears to be structurally favored over the meridional isomer. It should be noted that although the structural strain in the N-carboxymethyl chelate ring (or C-N-C angle)

of the meridional isomer is greater than that of the facial isomer, the flexibility of the N-carboxymethyl chelate ring may tend to reduce this difference. The flexibility of the N-carboxymethyl ring has been discussed previously.<sup>5</sup> Thus steric factors as discussed below, may play an even larger role in determining the isomer distribution than electronic and/or structural factors.

As noted above in the discussion of isomer distribution, the facial isomer appears to be the most stable isomer if steric interaction between the amino acidate chelate ring and the pyridyl group is not significant. Sterically the facial isomer is favored for the D-amino acidates since the amino acidate chelate ring conformation is such that its  $\alpha$ -CO<sub>2</sub><sup>-</sup> and  $\alpha$ -carbon are pointing downward, away from the pyridine ring. This conformation allows the R-group of the D-AA<sup>-</sup> to be equatorial instead of axial. Thus, for the Co(N-Cm-L-Pyala)-(D-AA) complexes the facial isomer appears to be favored both sterically and structurally. This is consistent with the stereospecific formation of the fac-Co(N-Cm-L-Pyala)(D-Val) isomer as the only facial isomer when D,L-Val<sup>-</sup> was used in the synthesis.

The facial isomer, however, does not seem to be favored sterically, when the amino acidate has both a large

R group and an L-configuration. This is consistent with the isolation of only the mer-Co(N-Cm-L-Pyala)(L-Val) isomer and the failure to isolate any fac-Co(N-Cm-L-Pyala)(L-Val). In the fac-Co(N-Cm-L-Pyala)(L-AA)<sup>-</sup> isomer, the L-AA<sup>-</sup> chelate ring such as that in L-Val would adopt a conformation in which the  $\alpha$ -carbon and  $\alpha$ -CO<sub>2</sub><sup>-</sup> groups are pointing upward toward the pyridine ortho hydrogen. Although this conformation allows the bulky R-group to be in the favored equatorial position, there appears, from examination of molecular models to be considerable interaction between the pyridyl ortho hydrogen and the  $\alpha$ -carboxylate of the amino acidate. Thus the statement, the meridional isomer (Figure 2c) is favored if there is significant steric interaction between the amino acidate chelate ring and the pyridyl group in the facial isomer, appears to be valid for L-amino acidates such as L-valinate. A similar argument may be used to explain the failure to isolate the facial isomer of Co(L-Pyala)(IMDA) (see structure below)



Co(L-Pyala)(IMDA)

where  $\text{IMDA}^{2-}$  is iminodiacetate.<sup>3</sup> In the facial coordination of the  $\text{IMDA}^{2-}$  ligand, the "glycinate type" chelate ring which is trans to the five-membered  $\text{Pyala}^-$  chelate ring would be pointing upward toward the pyridyl ortho hydrogen (just as an  $\text{L-AA}^-$  chelate ring would) causing considerable steric interaction. Thus, the meridional isomer with the pyridine coordinated trans to the  $\text{IMDA}^{2-}$  amino group (which is the one isolated) would be favored not only electronically as noted before<sup>3</sup> but sterically as well.

## REFERENCES

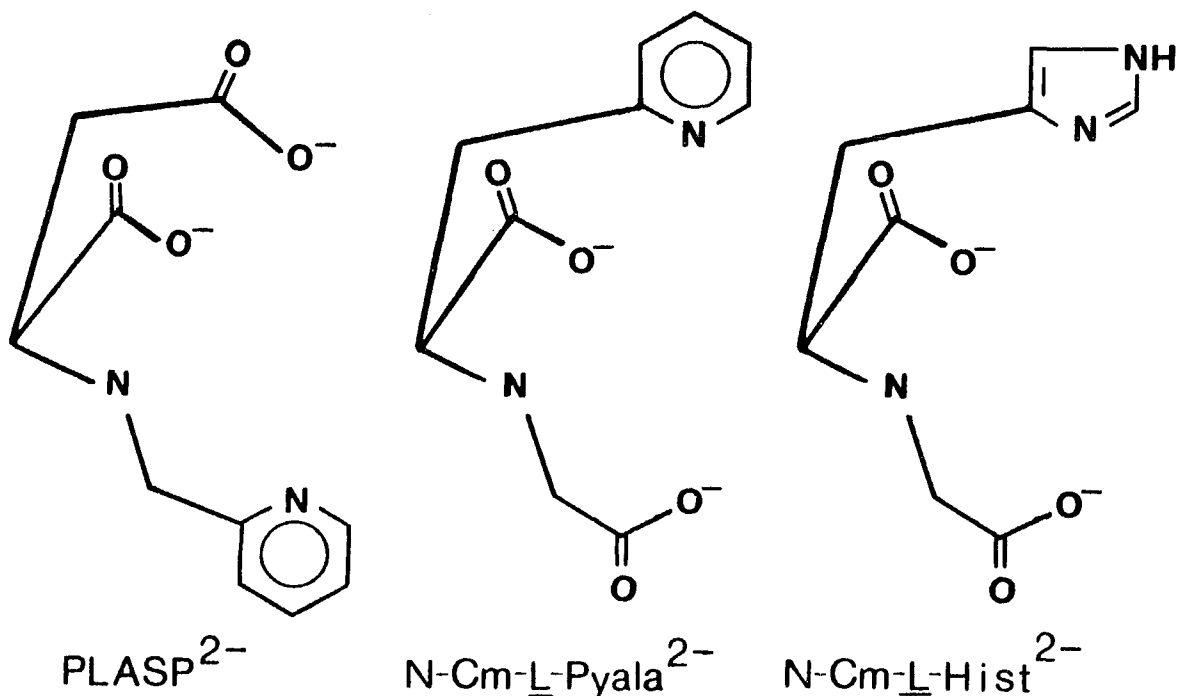
1. Meiske, L. A.; Jacobson, R. A.; Angelici, R. J. submitted for publication to Inorg. Chem.
2. Meiske, L. A.; Angelici, R. J. submitted for publication to Inorg. Chem.
3. Ebner, S. R.; Angelici, R. J. accepted for publication to Inorg. Chem.
4. Burdett, J. K. Adv. Inorg. Radiochem. 1978, 21, 113.
5. Meiske, L. A.; Jacobson, R. A.; Angelici, R. J. submitted for publication to Inorg. Chem.
6. Bedell, S. A.; Rechani, P. R.; Angelici, R. J.; Nakon, R. Inorg. Chem. 1977, 16, 972.
7. Watabe, M.; Zama, M.; Yoshikawa, S. Bull. Chem. Soc. Japan 1978, 51, 1354.
8. Colomb, G.; Bernauer, K. Helv. Chim. Acta 1977, 60, 459.
9. Legg, J. I.; Cooke, D. W. Inorg. Chem. 1965, 4, 1576.
10. Legg, J. I.; Cooke, D. W. Inorg. Chem. 1966, 5, 595.
11. Halloran, L. J.; Caputo, R. E.; Willett, R. D.; Legg, J. I. Inorg. Chem. 1975, 14, 1762.
12. Weakliem, H. A.; Hoard, J. L. J. Am. Chem. Soc. 1959, 81, 549.
13. Corradi, A. B.; Palmieri, C. G.; Nardelli, M.; Pellinghelli, M. A.; Tani, M. E. V. J. Chem. Soc., Dalton Trans. 1973, 655.

SECTION V. SYNTHESIS AND SPECTRAL CHARACTERIZATION OF  
THE MIXED LIGAND COMPLEXES, [N-Carboxymethyl-  
L-histidinato][amino acidato]cobalt(III),  
Co(N-Cm-L-Hist)(AA)



## INTRODUCTION

Previous work in our laboratory has shown that the overall structures of the  $\text{Co(III)[Y][AA]}$  complexes, where Y is either N-carboxymethyl-L- $\beta$ -(2-pyridyl)- $\alpha$ -alaninate, N-Cm-L-Pyala<sup>2-</sup>, or N-(2-pyridylmethyl)-L-aspartate, PLASP<sup>2-</sup>, (see below) and AA<sup>-</sup> is a bidentate amino acidate,



are determined by a combination of electronic, structural and steric factors.<sup>1-3</sup> For the  $\text{Co(N-Cm-L-Pyala)(AA)}$  and the  $\text{Co(PLASP)(AA)}$  complexes in which no steric interaction between the amino acidate chelate ring and the pyridyl ring is evident, the facial isomers having

nitrogen coordinated trans to oxygen (Figures 1a and 1b) appear to be electronically favored.<sup>1-3</sup> Also coordination of the PLASP<sup>2-</sup> as shown in Figure 1a gives the least strained bond angle around the secondary amino nitrogen and is presumably favored structurally over the more strained structure in which the pyridyl group is trans to the  $\alpha$ -CO<sub>2</sub><sup>-</sup> of PLASP<sup>2-</sup>.<sup>1,2</sup> On the other hand, the meridional isomer of Co(N-Cm-L-Pyala)(AA) in which the pyridyl group is coordinated trans to the amino nitrogen of the amino acidate (Figure 1c) appears to be the favored isomer when steric interaction between the amino acidate chelate ring and the pyridyl ring is present in the facial isomer as in the Co(N-Cm-L-Pyala)(L-Val) complex.<sup>3</sup> In order to compare the effects of substituting an imidazole group for a pyridyl group in the above complexes, the structurally similar ligand, N-carboxymethyl-L-histidinate, N-Cm-L-Hist<sup>2-</sup>, (see above) and its Co(III) mixed amino acidate, Co(N-Cm-L-Hist)(AA), complexes where the amino acidate is either  $\alpha$ -aminoisobutyrate ( $\alpha$ -AIBA<sup>-</sup>), D-threoninate (D-Thr<sup>-</sup>), D-asparaginate (D-AsN<sup>-</sup>) or D or L-valinate (Val<sup>-</sup>), were prepared. It is also of interest to compare the spectra of the Co(N-Cm-L-Hist)(AA) complexes to those of the corresponding Co(N-Cm-L-Pyala)(AA) and Co(PLASP)(AA) complexes.

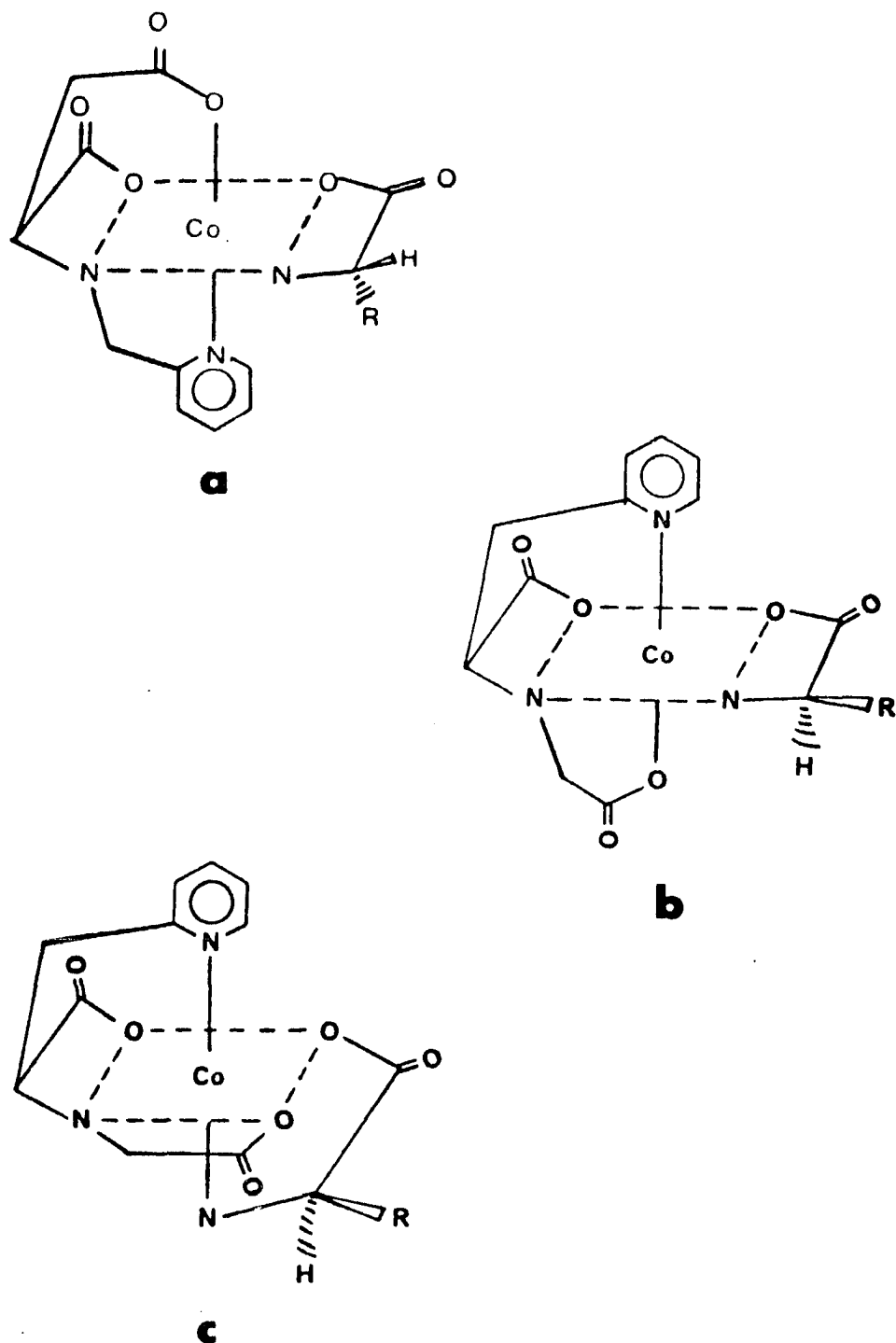


Figure 1. Structures of (a) fac-Co(PLASP)(AA),  
 (b) fac-Co(N-Cm-L-Pyala)(AA) and (c) mer-Co(N-Cm-L-Pyala)(AA) complexes

## EXPERIMENTAL SECTION

Preparation of N-carboxymethyl-L-histidine, N-Cm-L-HistH<sub>2</sub> To a solution of L-histidine (12.0 g, 77 mmol) in 50 ml of water, enough base (~6N NaOH) was added to bring the histidine solution to pH 9.8-10.0. The solution was then placed in an ice bath. Next a solution of glyoxylic acid hydrate (13.0 g, 170 mmol) in 35 ml of water was added dropwise to the histidinate solution over a period of 45 minutes. In order to maintain pH 9.8-10.0, 6N NaOH was added simultaneously with the glyoxylic acid solution. Upon addition of the glyoxylic acid solution, the reaction solution acquired a light yellow color. The solution was stirred for 1 hour and a solution of NaBH<sub>4</sub> (1.50 g, 40 mmol) in 20 ml of water was added dropwise. The addition of the NaBH<sub>4</sub> resulted in the partial disappearance of the yellow color. To maintain a pH 9.8-10.0, ~2N HCl was added periodically during the borohydride addition. The solution was stirred for 30 minutes, and NaBH<sub>4</sub> (1.50 g, 40 mmol) in 20 ml of water was again added; the solution was stirred for an additional 3 hours. Next, the solution was brought to pH 3.5 with 6N HCl and removed from the ice bath. The acidified solution was reduced to

half its volume in a rotary evaporator and placed on a Dowex 50W-X8 ion exchange column (2.6 X 85 cm, 400 ml of resin, 100-200 mesh) in the  $H^+$  form. After washing with one liter of water (eluant pH 5-6), the product was eluted off with 0.25N aqueous  $NH_3$ . Fractions (25 ml) were collected and those of pH 3.5 were combined and reduced to near dryness. The resulting slurry was treated with 250 ml of absolute ethanol, chilled to  $-10^\circ C$  in a freezer and then filtered. Additional fractions of product were obtained by reducing the ethanol solution to near dryness and adding more absolute ethanol. The total yield was 14.2 g (86%). Anal. calcd. for N-Cm-L-HistH<sub>2</sub>,  $C_8H_{11}N_3O_4$ : C, 45.07; H, 5.16; N, 19.72. Found: C, 45.11; H, 5.27; N, 19.64.

Preparation of [N-carboxymethyl-L-histidinato]-  
[amino acidato]cobalt(III) complexes, Co(N-Cm-L-Hist)(AA)  
To a solution containing N-Cm-L-HistH<sub>2</sub> (0.54 g, 2.5 mmol), amino acid (AAH) (2.5 mmol),  $CoSO_4 \cdot 7H_2O$  (0.70 g, 2.5 mmol) in 15 ml of water, 7.5 ml of 1N NaOH was added. The initial pH was between 9-10. Next 0.1 g of activated charcoal was added to the reaction mixture. This was followed by the addition over a 30 minute period of a solution containing  $K_2S_2O_8$  (0.40 g, 1.5 mmol) in 15 ml

of water. The solution began to turn reddish purple in color, and the pH began dropping. The solution was heated at 50-60° C for 1 hour to give a final pH 5.0-6.0 and a deep reddish purple solution. The individual complexes were isolated and purified as described below.

Isolation of [Co(N-Cm-L-Hist)(D-Val)]·1/2H<sub>2</sub>O using D-Val<sup>-</sup>  
 The complex [Co(N-Cm-L-Hist)(D-Val)]·1/2H<sub>2</sub>O precipitated out of the reaction mixture and was filtered off with the activated carbon. The product was isolated by extraction with hot water and filtering off the carbon. The extraction was repeated with hot water until the filtrate was colorless. The filtrates were combined and reduced to dryness. Reduction and filtration of the reaction mixture yielded additional fractions of product. The yield of [Co(N-Cm-L-Hist)(D-Val)]·1/2H<sub>2</sub>O was 293 mg (30%). Anal. calcd. for [Co(N-Cm-L-Hist)(D-Val)]·1/2H<sub>2</sub>O, C<sub>13</sub>H<sub>19</sub>N<sub>4</sub>O<sub>6</sub>Co·1/2H<sub>2</sub>O: C, 39.50; H, 5.06; N, 14.18.  
 Found: C, 39.60; H, 5.00; N, 14.26.

Isolation of [Co(N-Cm-L-Hist)(L-Val)]·4H<sub>2</sub>O using L-Val<sup>-</sup>  
 The activated carbon was filtered off, and the reaction mixture was reduced to 5-10 ml in vacuum. The reduced solution was placed on a Dowex 50W-X8 ion exchange column (2.4 X 60 cm, 200-400 mesh) in the Na<sup>+</sup> form and eluted

with water to give an initial band containing various anionic and decomposition products. The second and major band, containing the product was collected and reduced to a few ml under vacuum. To force precipitation, a large volume (100-150 ml) of absolute ethanol was added. The resulting slurry was chilled at  $-10^{\circ}$  C overnight and filtered. The yield of  $[\text{Co}(\text{N-Cm-L-Hist})(\text{L-Val})] \cdot 4\text{H}_2\text{O}$  was 470 mg (41%). Anal. calcd. for  $[\text{Co}(\text{N-Cm-L-Hist})(\text{L-Val})] \cdot 4\text{H}_2\text{O}$ ,  $\text{C}_{13}\text{H}_{19}\text{N}_4\text{O}_6\text{Co} \cdot 4\text{H}_2\text{O}$ : C, 34.07; H, 5.90; N, 12.23. Found: C, 34.37; H, 6.03; N, 12.37.

Isolation of  $[\text{Co}(\text{N-Cm-L-Hist})(\text{D-Val})] \cdot \text{H}_2\text{O}$  using  $\text{D,L-Val}^-$

The  $\text{Co}(\text{N-Cm-L-Hist})(\text{D-Val})$  which precipitated out of the reaction mixture was filtered off with the activated carbon and extracted as described above in the isolation of the  $\text{D-Val}^-$  complex. The filtered reaction solution was reduced in volume to give additional fractions of the  $\text{D-Val}^-$  complex. Chromatography of the remaining reaction solution as described in the section on the isolation of  $\text{Co}(\text{N-Cm-L-Hist})(\text{L-Val})$  (see above) yielded a red band containing only the  $\text{D-Val}^-$  complex. The yield of  $[\text{Co}(\text{N-Cm-L-Hist})(\text{D-Val})] \cdot \text{H}_2\text{O}$  was 362 mg (36% based on total  $\text{D}$  and  $\text{L-Val}^-$ ). Anal. calcd. for  $[\text{Co}(\text{N-Cm-L-Hist})(\text{D-Val})] \cdot \text{H}_2\text{O}$ ,  $\text{C}_{13}\text{H}_{19}\text{N}_4\text{O}_6\text{Co}$ : C, 38.62; H, 5.20; N, 13.86. Found: C, 38.21; H, 5.19; N, 13.89.

Isolation of Co(N-Cm-L-Hist)( $\alpha$ -AIBA) The complex Co(N-Cm-L-Hist)( $\alpha$ -AIBA) was isolated and chromatographed in a manner identical to that described for the [Co(N-Cm-L-Hist)(L-Val)] $\cdot$ 4H<sub>2</sub>O complex above. The yield was 247 mg (27%). Anal. calcd. for Co(N-Cm-L-Hist)( $\alpha$ -AIBA), C<sub>12</sub>H<sub>18</sub>N<sub>4</sub>O<sub>6</sub>Co: C, 38.72; H, 4.84; N, 15.06. Found: C, 38.29; H, 4.70; N, 15.10.

Isolation of [Co(N-Cm-L-Hist)(D-Thr)] $\cdot$ H<sub>2</sub>O using D,L-Thr<sup>-</sup> and [Co(N-Cm-L-Hist)(AsN<sup>-</sup>)] $\cdot$ 2H<sub>2</sub>O using D,L-AsN<sup>-</sup>  
 These two complexes were isolated and purified in the same manner as that described for the isolation of [Co(N-Cm-L-Hist)(D-Val)] $\cdot$ H<sub>2</sub>O using D,L-Val<sup>-</sup>. The yields of [Co(N-Cm-L-Hist)(D-Thr)] $\cdot$ H<sub>2</sub>O and [Co(N-Cm-L-Hist)(D-AsN<sup>-</sup>)] $\cdot$ 2H<sub>2</sub>O were 332 mg (34% based on total D and L-Thr<sup>-</sup>) and 410 mg (45% based on total D and L-AsN<sup>-</sup>), respectively. Anal. calcd. for [Co(N-Cm-L-Hist)(D-Thr)] $\cdot$ H<sub>2</sub>O, C<sub>12</sub>H<sub>17</sub>N<sub>4</sub>O<sub>7</sub>Co $\cdot$ H<sub>2</sub>O: C, 35.48; H, 4.68; N, 13.80. Found: C, 35.52; H, 4.79; N, 13.83. Anal. calcd. for [Co(N-Cm-L-Hist)(D-AsN<sup>-</sup>)] $\cdot$ 2H<sub>2</sub>O, C<sub>12</sub>H<sub>16</sub>N<sub>5</sub>O<sub>7</sub>Co $\cdot$ 2H<sub>2</sub>O: C, 32.96; H, 4.58; N, 16.02. Found: C, 33.03; H, 4.51; N, 16.31.

Spectra Visible spectra were measured in water at room temperature with a Cary Model 14 spectrophotometer. Circular dichroism spectra were measured in water at



room temperature with a Jasco ORD/UV/CD-5 spectrophotometer. The  $^{13}\text{C}$  and  $^1\text{H}$  nmr spectra were recorded on a Jeol FX90Q Fourier transform nmr spectrometer at room temperature. The  $^{13}\text{C}$  nmr spectra of the more soluble complexes and all the  $^1\text{H}$  nmr were recorded in 99.7%  $\text{D}_2\text{O}$ , while the  $^{13}\text{C}$  nmr spectra of the less soluble complexes were recorded in 70%  $\text{H}_3\text{PO}_4$  (aqueous). The proton chemical shifts are reported in ppm downfield from TMS using t-butyl alcohol ( $\delta$  1.23) as an internal standard. The  $^{13}\text{C}$  chemical shifts are also given in ppm downfield from TMS using 1,4-dioxane ( $\delta$  67.0) as the internal standard.

## RESULTS AND DISCUSSION

Figure 2 shows the four possible geometric isomers of the  $\text{Co}(\text{N-Cm-L-Hist})(\text{D-AA})$  complexes. The structure in Figure 2a has a facial arrangement of oxygen atoms. The three meridional isomers in Figures 2b, 2c and 2d are denoted  $\text{mer N-Cm-CO}_2^-$ ,  $\text{mer AA}^- \text{amino}$  and  $\text{mer AA}^- \text{CO}_2^-$ , with the terms  $\text{N-Cm-CO}_2^-$ ,  $\text{AA}^- \text{amino}$  and  $\text{AA}^- \text{CO}_2^-$  being used to denote which group is coordinated trans to the imidazole group.

Visible spectra of the  $\text{Co}(\text{N-Cm-L-Hist})(\text{AA})$  complexes  
 The visible spectrum of  $\text{Co}(\text{N-Cm-L-Hist})(\alpha\text{-AIBA})$  in water is shown in Figure 3 and is typical of the other  $\text{Co}(\text{N-Cm-L-Hist})(\text{AA})$  visible spectra, whose maxima are presented in Table I. The visible spectra of these  $\text{Co}(\text{N-Cm-L-Hist})(\text{AA})$  complexes, which have a symmetrical peak at  $511 \pm 1$  nm and a somewhat lower intensity peak at  $353 \pm 3$  nm, are comparable to those reported for the facial isomers of the  $\text{Co}(\text{N-Cm-L-Pyala})(\text{AA})$  and  $\text{Co}(\text{PLASP})(\text{AA})$  mixed ligand complexes.<sup>1, 3</sup> The major differences in the visible spectra of the facial  $\text{Co}(\text{N-Cm-L-Pyala})(\text{AA})$  (with symmetrical peaks at 522 nm,  $\epsilon = 165$  and 370 nm,  $\epsilon = 132$ ) and the facial  $\text{Co}(\text{N-Cm-L-Hist})(\text{AA})$  complexes are a decrease in  $\epsilon$  and a shift to higher

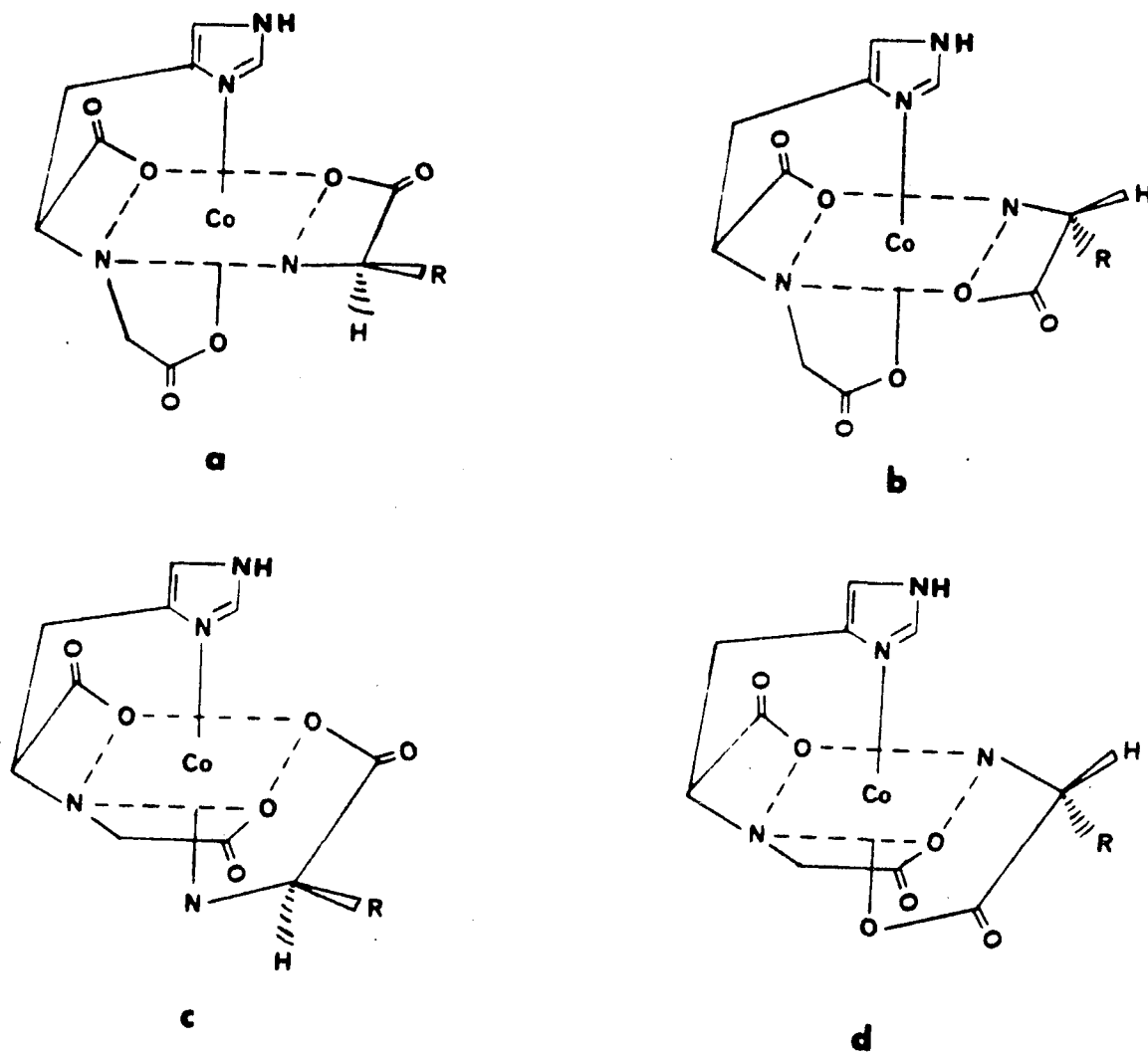


Figure 2. The four possible geometrical isomers of  $[\text{Co}(\text{N-Cm-L-Hist})(\text{D-AA})]$ : (a) fac, (b) mer N-Cm-CO<sub>2</sub><sup>-</sup>, (c) mer AA<sup>-</sup> amino and (d) mer AA<sup>-</sup>CO<sub>2</sub><sup>-</sup>

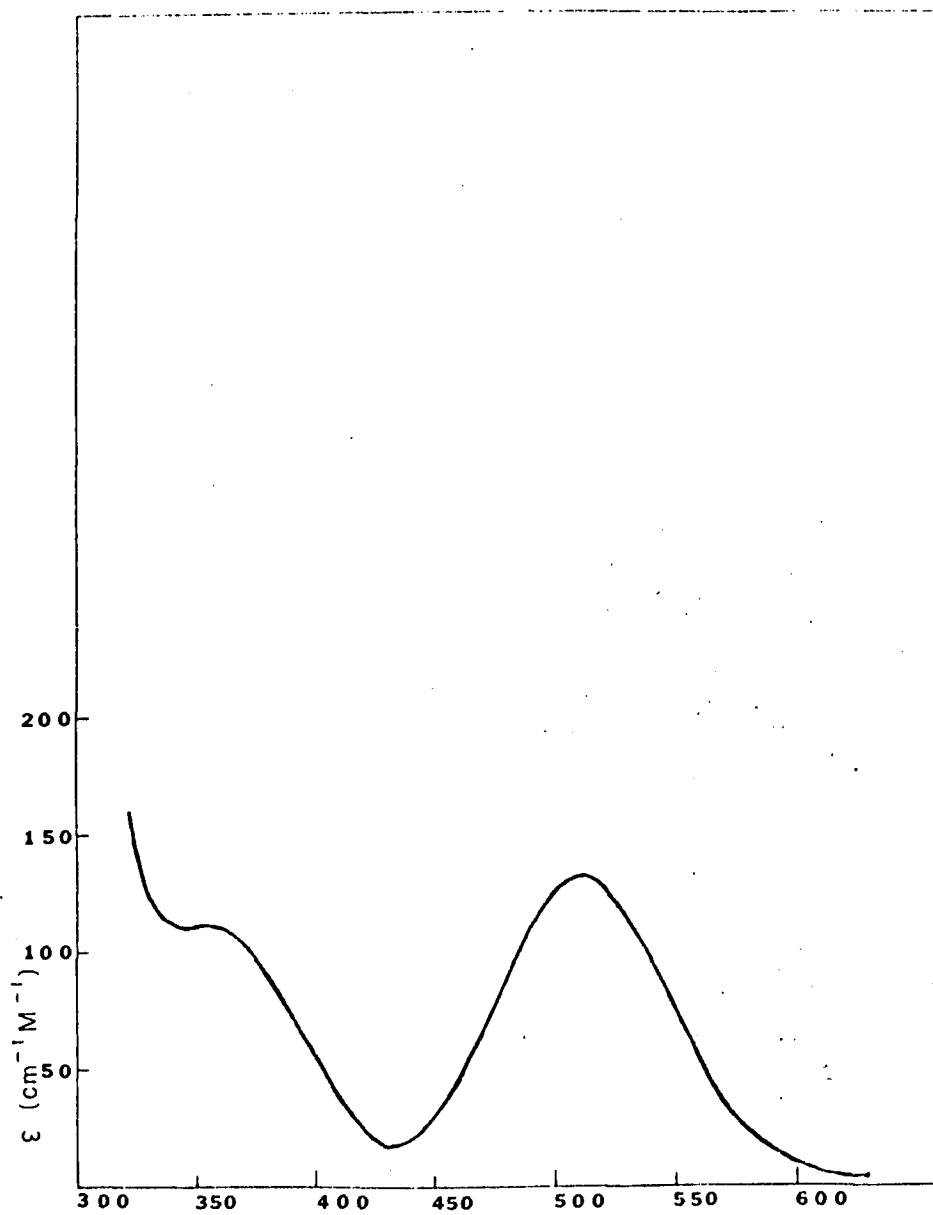


Figure 3. Visible spectrum of  $\text{Co}(\text{N-Cm-L-Hist})(\alpha\text{-AIBA})$  in water

Table I. Visible spectra of the Co(N-Cm-L-Hist) (AA) complexes in H<sub>2</sub>O

Complex	$\lambda$ nm	$\epsilon^a$	$\lambda$ nm	$\epsilon$
[Co(N-Cm- <u>L</u> -Hist) ( $\alpha$ -AIBA) ]	510	138	355	121
[Co(N-Cm- <u>L</u> -Hist) ( <u>L</u> -Val) ] · 4H <sub>2</sub> O	512	139	353	130
[Co(N-Cm- <u>L</u> -Hist) ( <u>D</u> -Val) ] · 1/2H <sub>2</sub> O	511	138	353	117
[Co(N-Cm- <u>L</u> -Hist) ( <u>D</u> -Val) ] · 1/2H <sub>2</sub> O <sup>b</sup>	510	142	353	115
[Co(N-Cm- <u>L</u> -Hist) ( <u>D</u> -Thr) ] · H <sub>2</sub> O <sup>b</sup>	511	138	352	121
[Co(N-Cm- <u>L</u> -Hist) ( <u>D</u> -AsN) ] · 2H <sub>2</sub> O <sup>b</sup>	510	136	350	114

<sup>a</sup>Units for  $\epsilon$  are cm<sup>-1</sup>M<sup>-1</sup>.

<sup>b</sup>Obtained from preparations using D,L-AA<sup>-</sup>.

energy (a 10 nm shift for the lower energy band and 20 nm shift for the higher energy band) when imidazole is substituted for pyridine in the coordination sphere. A similar decrease in extinction coefficients but smaller shifts (10 nm) in the higher energy band have been noted before for some  $\text{Co(III)N}_4\text{O}_2$  complexes containing imidazole and pyridine.<sup>4</sup> The similarity of the absorption maxima and extinction coefficients for the complexes listed in Table I suggests that the coordination sphere around the  $\text{Co(III)}$  is identical for all of the complexes. Since there is only one facial isomer (Figure 2a) possible for the  $\text{Co(N-Cm-L-Hist)(AA)}$  complex, the complexes listed in Table I are assigned that structure. Further evidence for this assignment may be obtained from their CD,  $^1\text{H}$  nmr and  $^{13}\text{C}$  nmr spectra which are discussed below.

Circular dichroism spectra of the  $\text{Co(N-Cm-L-Hist)(AA)}$  complexes The circular dichroism spectra (visible region only) of the  $\text{Co(N-Cm-L-Hist)(AA)}$  complexes in water are shown in Figures 4 and 5, and numerical values for their minima and maxima are listed in Table II. These spectra are all similar in shape, varying only in intensity. They can be divided into two major bands (Table II), with band I in the region from 480 to 555 nm and band II in the region from 340 to 400 nm.

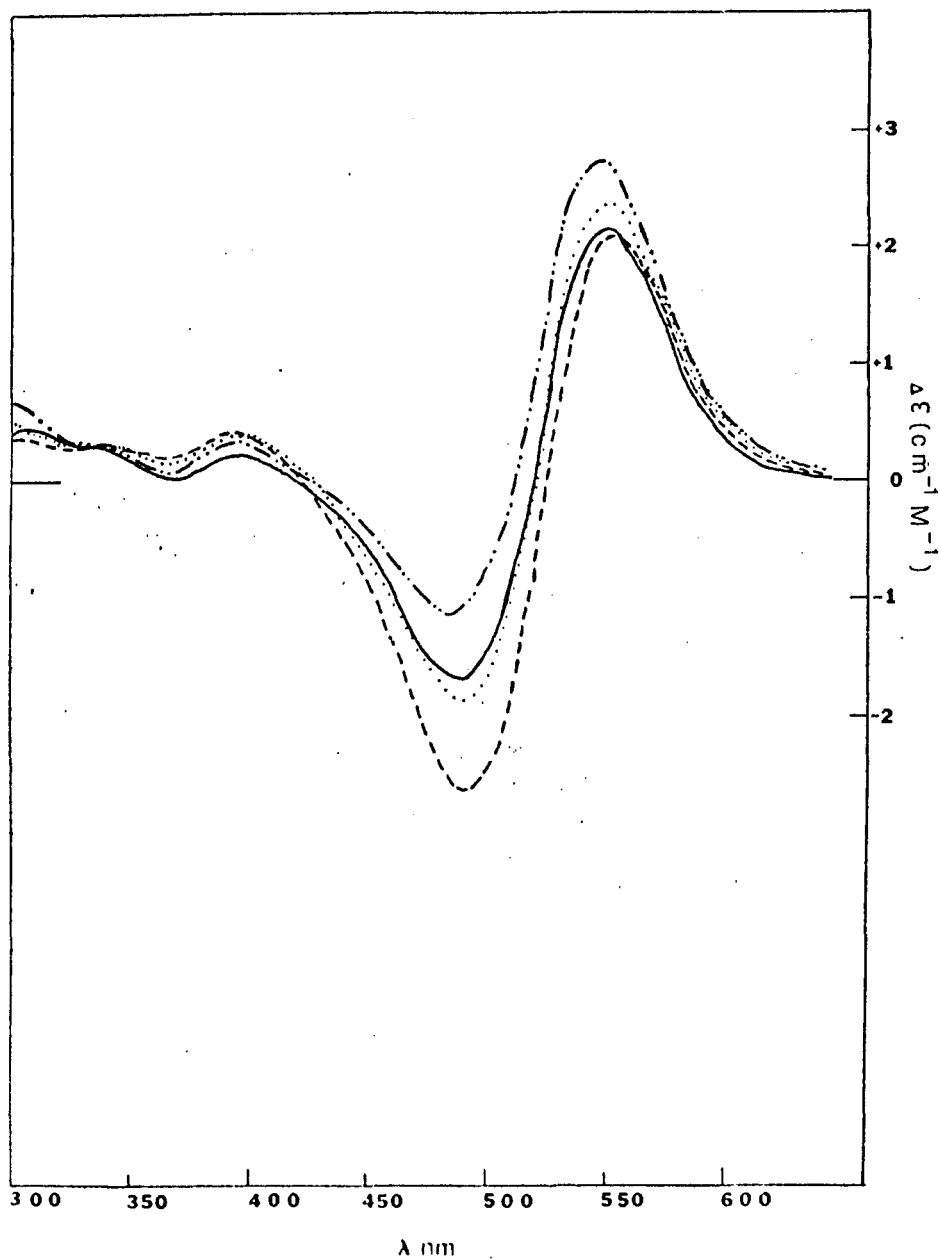


Figure 4. CD spectra of  $\text{Co}(\text{N-Cm-L-Hist})(\text{AA})$  complexes:  
 $\alpha\text{-AIBA}^-$  (—),  $\text{L-Val}^-$  (----),  $\text{D-Val}^-$  (-·-·-) and  $(\text{D} + \text{L})/2\text{-Val}^-$  (.....)

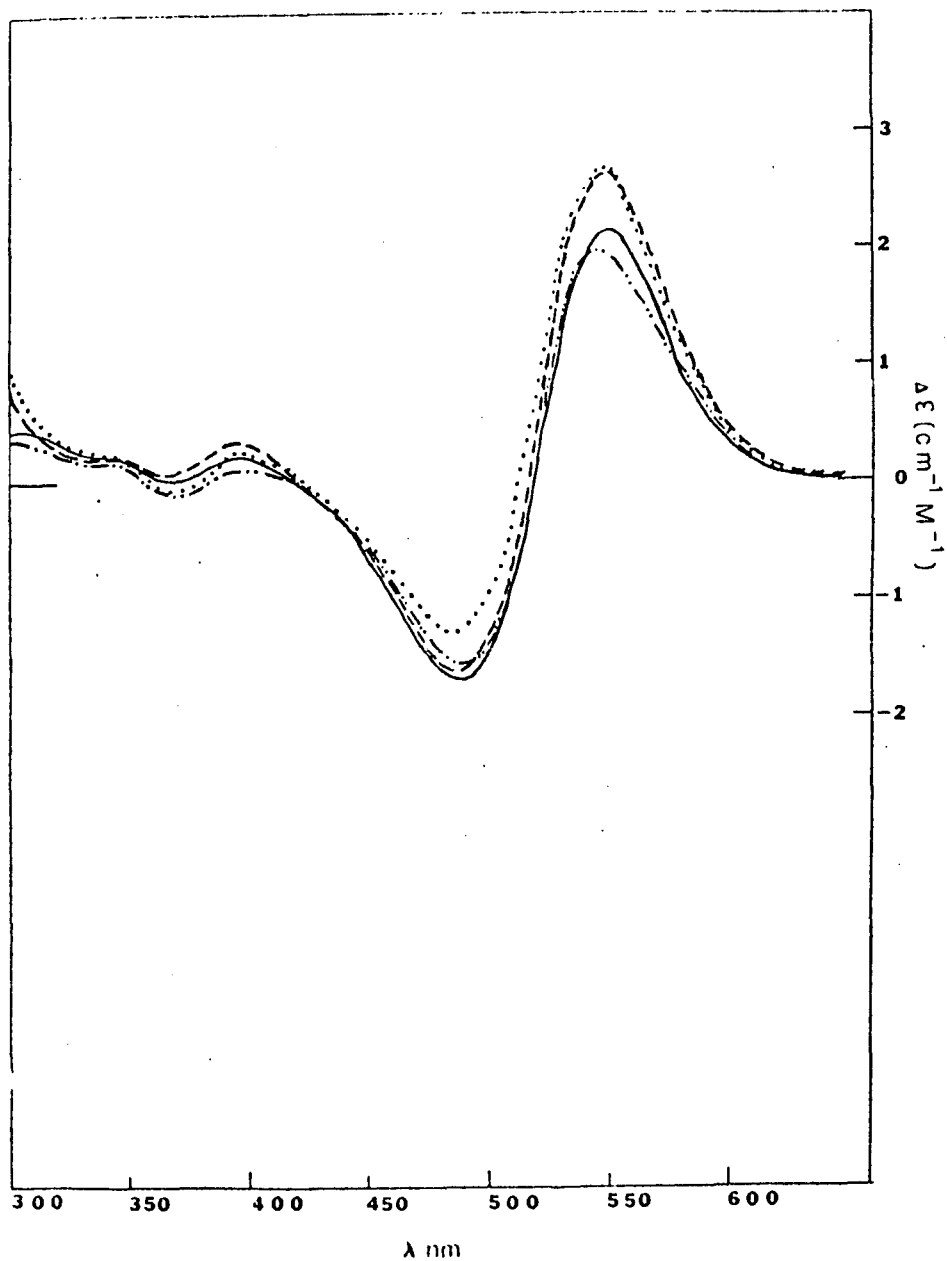


Figure 5. CD spectrum of  $\text{Co}(\text{N-Cm-L-Hist})(\alpha\text{-AIBA})$  (—) and CD spectra of  $\text{Co}(\text{N-Cm-L-Hist})(\text{AA})$  complexes isolated from reactions using  $\text{D,L-AA}^-$  as starting material,  $\text{D-Val}^-$  (.....),  $\text{D-Thr}^-$  (----) and  $\text{D-Asn}^-$  (-.-.-)



Table II. CD spectra of the Co(N-Cm-L-Hist)(AA) complexes  
in H<sub>2</sub>O

AA <sup>-</sup>	Band I				Band II			
	λnm	Δε <sup>a</sup>	λnm	Δε	λnm	Δε	λnm	Δε
α-AIBA <sup>-</sup>	545	+2.14	484	-1.68	394	+0.23	340	+0.29
<u>L</u> -Val <sup>-</sup>	553	+2.38	490	-2.66	393	+0.41	340	+0.31
<u>D</u> -Val <sup>-</sup>	546	+2.73	485	-1.13	395	+0.32	340	+0.33
<u>D</u> -Val <sup>-b</sup>	547	+2.68	485	-1.25	396	+0.29	340	+0.25
<u>D</u> -Thr <sup>-b</sup>	547	+2.64	485	-1.60	393	+0.37	340	+0.25
<u>D</u> -AsN <sup>-b</sup>	547	+1.94	485	-1.54	396	+0.12	340	+0.25

<sup>a</sup>Units for Δε are cm<sup>-1</sup>M<sup>-1</sup>.

<sup>b</sup>Obtained from preparations using D,L-AA<sup>-</sup>.

Band I of fac-Co(N-Cm-L-Hist) ( $\alpha$ -AIBA) with a positive peak at 545 nm and a negative peak at 468 nm is very similar in its overall shape to band I of fac-Co(N-Cm-L-Pyala)- ( $\alpha$ -AIBA) with a positive peak at 557 nm and a negative peak at 488 nm. Band I of the other fac-Co(N-Cm-L-Hist) (AA) complexes in Table II are also similar in shape to band I of the fac-Co(N-Cm-L-Pyala) (AA)<sup>3</sup> and cis-N, cis-O<sub>5</sub>-Co(N-Cm-L-Asp) (AA) complexes (Figure 6a) where N-Cm-L-Asp<sup>3-</sup> is the tetradentate N-carboxymethyl-L-aspartate ligand.<sup>5</sup> This similarity seems reasonable since these three complexes, fac-Co(N-Cm-L-Hist) (AA), fac-Co(N-Cm-L-Pyala) (AA) and Co(N-Cm-L-Asp) (AA) are structurally identical in terms of the size and position of their chelate rings, each containing one six-membered ring and three five-membered rings. They differ only in the type of donor group (either imidazole, pyridyl or carboxylate, respectively) coordinated trans to the N-carboxymethyl carboxylate group. As noted above for their visible spectra, the circular dichroism spectral intensities ( $\Delta\epsilon$ ) of the Co(N-Cm-L-Hist) (AA) complexes are lower than the  $\Delta\epsilon$  values for the corresponding facial Co(N-Cm-L-Pyala) (AA) complexes. Thus substitution of imidazole for pyridine also causes a decrease in  $\Delta\epsilon$

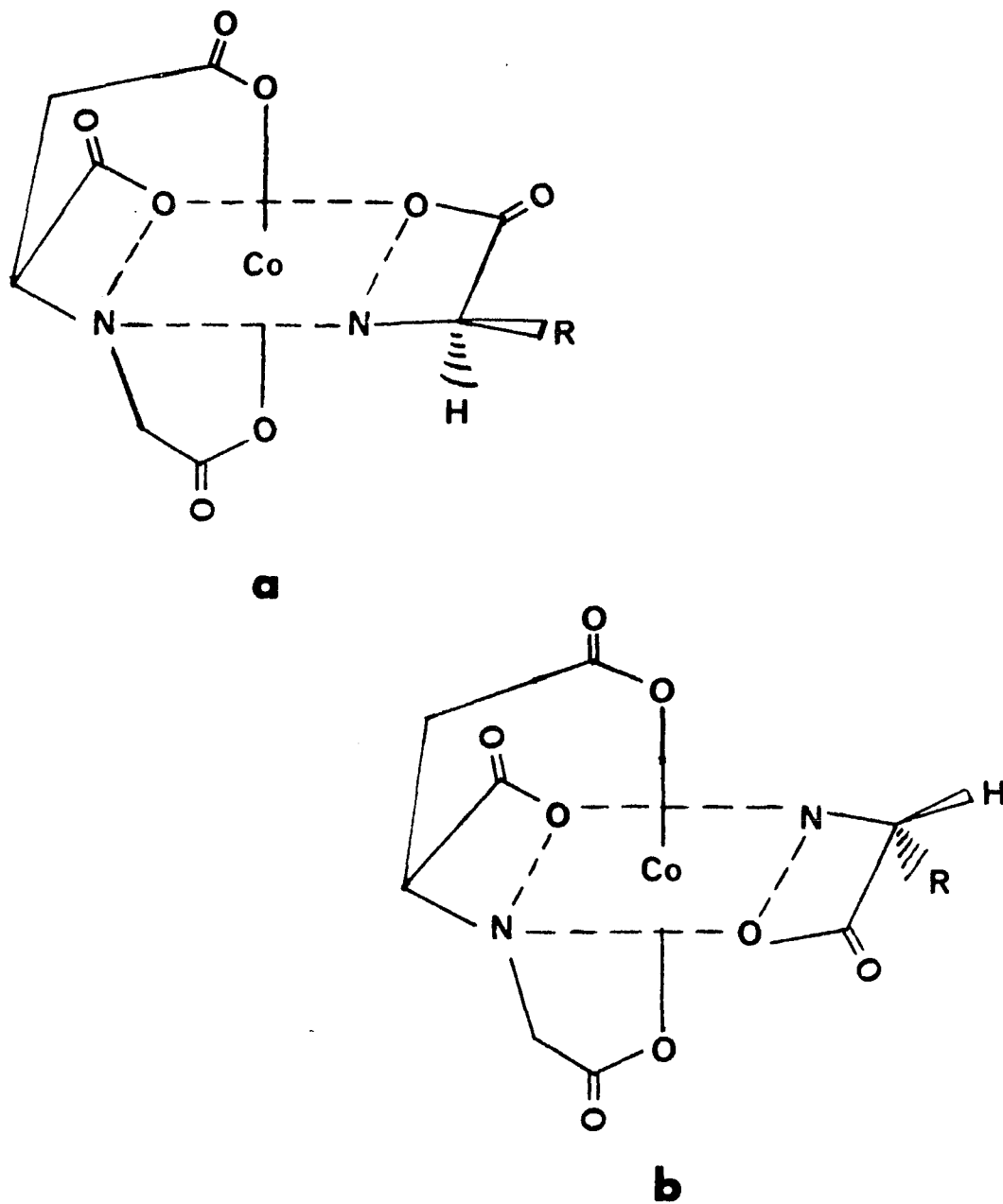


Figure 6. Two  $\text{Co(III)N}_2\text{O}_4$  isomers of a)  $\text{cis-N, cis-O}_5\text{-}$   
 and b)  $\text{trans-N, cis-O}_5\text{- Co(N-Cm-L-Asp)(D-AA)}$

values. This trend has also been reported for the  $\text{Co(Pyala)}_2^+$  and  $\text{Co(Hist)}_2^+$  complexes, where  $\text{Pyala}^-$  is  $\beta$ -(2-pyridyl)- $\alpha$ -alaninate and  $\text{Hist}^-$  is histidinate.<sup>4</sup>

Band II consists of two low intensity positive peaks. The position and intensity of these higher energy peaks do not vary significantly from one amino acidate to another.

A comparison of the CD curves in Figures 4 and 5 reveals that the intensity of the CD curve of the  $\underline{\text{L}}\text{-Val}^-$  complex is lower than that of the  $\alpha\text{-AIBA}^-$  complex and that the intensities of the  $\underline{\text{D}}$ -amino acidate complex curves are higher than that of the  $\alpha\text{-AIBA}^-$  complex. Since the  $\text{Co(N-Cm-}\underline{\text{L}}\text{-Hist)}(\text{AA})$  complexes all have the same basic structure, the differences in their CD spectra must be related to the differences at the  $\alpha$ -carbon of their amino acidates. This has been noted before in the CD spectra of the facial  $\text{Co(PLASP)}(\text{AA})$  and meridional  $\text{Co(N-Cm-}\underline{\text{L}}\text{-Pyala)}(\text{AA})$  complexes. In those cases, their CD spectra were resolved into a Y term representing the contribution of amino acidate chelate ring bending and an X term representing the contribution of the rest of the complex. Using a similar approach, the value of  $\Delta\varepsilon$  at a given wavelength in the CD spectrum of a  $\text{Co(N-Cm-}\underline{\text{L}}\text{-Hist)}(\text{AA})$  complex can be expressed as follows:

$$X + Y_{\underline{D} \text{ or } \underline{L}} = \text{CD}[\text{Co}(\text{N-Cm-}\underline{\text{L}}\text{-Hist})(\underline{\text{D}} \text{ or } \underline{\text{L-AA}})]. \quad (1)$$

If it is assumed that  $Y_{\underline{D}} = -Y_{\underline{L}}$ , then

$$X = \frac{\text{CD}[\text{Co}(\text{N-Cm-}\underline{\text{L}}\text{-Hist})(\underline{\text{L-AA}})] + \text{CD}[\text{Co}(\text{N-Cm-}\underline{\text{L}}\text{-Hist})(\underline{\text{D-AA}})]}{2}. \quad (2)$$

The X value has been calculated using the CD spectra of the  $\text{Co}(\text{N-Cm-}\underline{\text{L}}\text{-Hist})(\underline{\text{D-Val}})$  and  $\text{Co}(\text{N-Cm-}\underline{\text{L}}\text{-Hist})(\underline{\text{L-Val}})$  complexes and is given in Figure 4. It should be noted that the CD spectrum of  $\text{Co}(\text{N-Cm-}\underline{\text{L}}\text{-Hist})(\alpha\text{-AIBA})$  is essentially the same as that of the calculated X term (Figure 4). Thus, as in the cases of facial  $\text{Co}(\text{PLASP})(\alpha\text{-AIBA})$  and mer- $\text{Co}(\text{N-Cm-}\underline{\text{L}}\text{-Pyala})(\alpha\text{-AIBA})$ , the assumption that X is essentially equal to the observed spectrum of  $\text{Co}(\text{N-Cm-}\underline{\text{L}}\text{-Hist})(\alpha\text{-AIBA})$  can be made. The X term for the  $\text{N-Cm-}\underline{\text{L}}\text{-Hist}^{2-}$  complexes consists of a positive peak at  $\sim 550$  nm and a negative peak at 470 nm. This is different than the two positive peaks at 545 nm and 495 nm for the  $\text{Co}(\text{PLASP})(\text{AA})$  X term and the single negative peak at 488 nm for the mer- $\text{Co}(\text{N-Cm-}\underline{\text{L}}\text{-Pyala})(\text{AA})$  X term.

Calculations of the various Y terms, assuming that X is equal to the CD spectrum of  $\text{Co}(\text{N-Cm-}\underline{\text{L}}\text{-Hist})(\alpha\text{-AIBA})$  were made using equation 1; these values are given in Figure 7 for  $\underline{\text{D-Val}}^-$ ,  $\underline{\text{L-Val}}^-$  and  $\underline{\text{D-Thr}}^-$ . A comparison

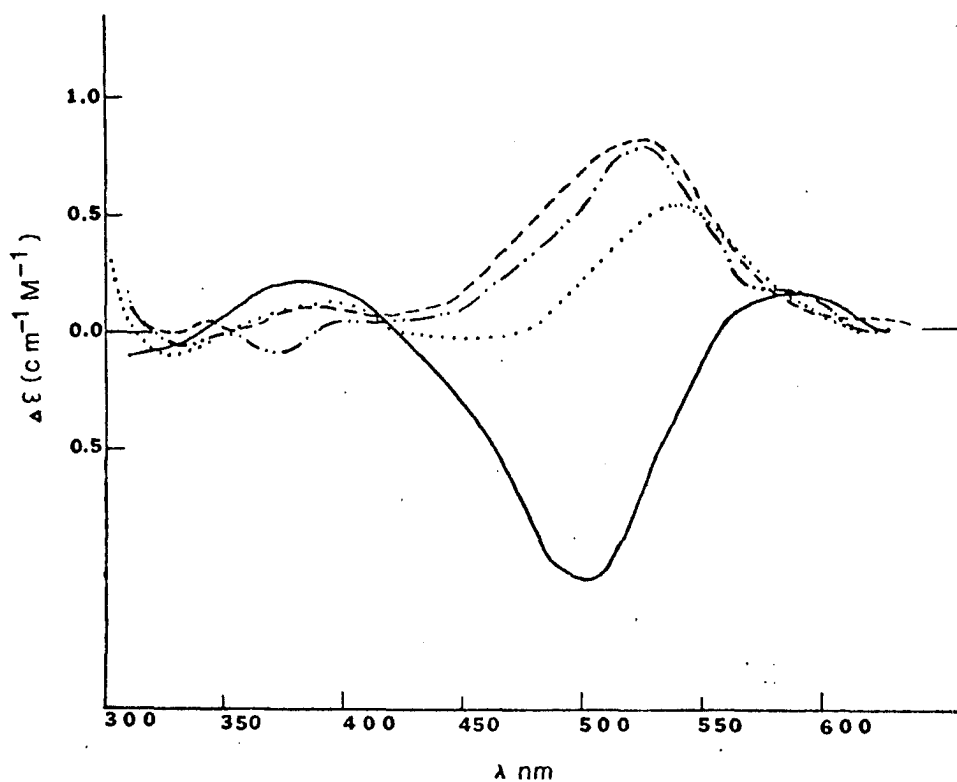


Figure 7. Y contribution to the  $\text{Co}(\text{N-Cm-L-Hist})(\text{AA})$  CD spectra of  $\underline{\text{D}}\text{-Val}^-$  (----),  $\underline{\text{L}}\text{-Val}^-$  (—),  $\underline{\text{D}}\text{-Val}^-$  (-·-·-) isolated from reaction using  $\underline{\text{D}},\underline{\text{L}}\text{-Val}^-$  in the synthesis and  $\underline{\text{D}}\text{-Thr}^-$  (····) isolated from reaction using  $\underline{\text{D}},\underline{\text{L}}\text{-Thr}^-$  in the synthesis

of the Y terms for  $\underline{L}$ -Val<sup>-</sup> and  $\underline{D}$ -Val<sup>-</sup> shows that to a first approximation the assumption of  $Y_{\underline{D}} = -Y_{\underline{L}}$  in formulating eq. 2 for the present system is valid. Since the CD spectrum of Co(N-Cm- $\underline{L}$ -Hist)( $\underline{D}$ -AsN) is very similar to that of the  $\alpha$ -AIBA complex, no attempt was made to calculate a Y term for  $\underline{D}$ -AsN<sup>-</sup>. The assignment of this complex as the  $\underline{D}$ -AsN<sup>-</sup> isomer is discussed in the <sup>1</sup>H nmr section below.

The Y term for  $\underline{D}$ -Val<sup>-</sup> in Co(N-Cm- $\underline{L}$ -Hist)( $\underline{D}$ -Val) with its positive peak at  $\sim 510$  nm is comparable to the positive low energy peak of the Y terms calculated for other  $\underline{D}$ -amino acidates in the Co(PLASP)( $\underline{D}$ -AA) and Co(N-Cm- $\underline{L}$ -Pyala)( $\underline{D}$ -AA) complexes. Similarly the negative peak at  $\sim 510$  nm in the Y term of  $\underline{L}$ -Val<sup>-</sup> in fac-Co(N-Cm- $\underline{L}$ -Hist)( $\underline{L}$ -Val) is comparable to the negative low energy peak in the Y terms of the fac-Co(PLASP)( $\underline{L}$ -AA) and mer-Co(N-Cm- $\underline{L}$ -Pyala)( $\underline{L}$ -AA) complexes. Since the general shapes and intensities of the Y terms in the various complexes listed above vary considerably, only the signs of the low energy peaks are compared. It should be noted that the Val<sup>-</sup> complex prepared using  $\underline{D}, \underline{L}$ -Val<sup>-</sup> has a Y term which is essentially the same as that for the Co(N-Cm- $\underline{L}$ -Hist)( $\underline{D}$ -Val) complex; similarly the Y term for the Thr<sup>-</sup> complex prepared using  $\underline{D}, \underline{L}$ -Thr<sup>-</sup> is characteristic

of a  $\underline{D}$ -AA<sup>-</sup>. Thus, the only complexes isolated using  $\underline{D}, \underline{L}$ -AA<sup>-</sup> in the synthesis are the Co(N-Cm- $\underline{L}$ -Hist) ( $\underline{D}$ -AA) complexes. Further evidence for this assignment may be seen in their <sup>1</sup>H and <sup>13</sup>C nmr spectra to be discussed below.

A comparison of the CD curves and minimum and maximum values reported previously for the cis-N, cis-O<sub>5</sub>- and trans-N, cis-O<sub>5</sub>-Co(N-Cm- $\underline{L}$ -Asp) ( $\underline{D}$ - and  $\underline{L}$ -AA) complexes (Figures 6a and 6b) shows that their overall shapes and intensities are also related to changes at the  $\alpha$ -carbon of the amino acidates.<sup>5</sup> (The amino acidate of the trans-N, cis-O<sub>5</sub> isomer (Figure 6b) has its  $\alpha$ -CO<sub>2</sub><sup>-</sup> coordinated trans to the  $\alpha$ -CO<sub>2</sub><sup>-</sup> of N-Cm- $\underline{L}$ -Asp<sup>3-</sup> and its amino group trans to the N-Cm- $\underline{L}$ -Asp<sup>3-</sup> amino group.) Thus, their CD spectra can also be divided into X and Y terms. From an examination of the CD curves and values of their minima and maxima, the sign of the low energy peak of the Y term for both, cis-N, cis-O<sub>5</sub> and trans-N, cis-O<sub>5</sub>, is found to be positive for  $\underline{D}$ -amino acidates and negative for  $\underline{L}$ -amino acidates.

Thus, there appears to be a general trend in the sign of the low energy peak of the Y terms for the fac-Co(PLASP)-(AA), fac- and mer-Co(N-Cm- $\underline{L}$ -Pyala) (AA), fac-Co(N-Cm- $\underline{L}$ -Hist)-(AA) and Co(N-Cm- $\underline{L}$ -Asp) (AA) complexes. For  $\underline{D}$ -amino acidates



the sign of the low energy peak of the Y term is positive and for L-amino acidates it is negative. As discussed for the Co(PLASP)(AA) complexes, Y may represent the contribution of the amino acidate chelate ring bending to the overall CD spectrum.<sup>1</sup>

<sup>1</sup>H nmr spectra of the Co(N-Cm-L-Hist)(AA) complexes  
 The <sup>1</sup>H nmr spectra of the Co(N-Cm-L-Hist)(AA) complexes and the free ligand N-Cm-L-HistH<sub>2</sub> in 99.7% deuterium oxide are given in Table III. Chemical shifts of protons in the coordinated N-Cm-L-Hist<sup>2-</sup> ligand are assigned as follows: a triplet centered at  $\delta \sim 3.92$  for the  $\alpha$ -proton, a doublet centered at  $\delta \sim 3.45$  for the  $\beta$ -protons, two doublets ( $J = 18\text{Hz}$ ) centered at  $\delta \sim 3.50$  and  $\delta 4.35$  for the N-carboxymethyl protons, a singlet at  $\delta \sim 7.17$  for the proton on the imidazole 4-carbon and a singlet varying from  $\delta 7.43-7.80$  for the proton on the imidazole 2-carbon. The  $\alpha$ -proton and N-carboxymethyl protons of the N-Cm-L-Hist<sup>2-</sup> ligand are comparable to those of the N-Cm-L-Pyala<sup>2-</sup> cobalt analogs, where the  $\alpha$ -proton occurs at  $\delta 3.9$  and the N-carboxymethyl protons occur as two doublets at  $\delta 3.56$  and  $4.37$  with  $J = 18\text{Hz}$ .<sup>3</sup>

The slight shift upfield for the  $\alpha$ -proton ( $\delta 3.89$ ) and  $\beta$ -protons ( $\delta 3.34$ ) of the Co(N-Cm-L-Hist)(L-Val) compared

Table III. Proton nmr spectra of the Co(N-Cm-L-Hist)(AA) complexes in D<sub>2</sub>O<sup>a</sup>

Compound	N-Cm-L-Hist <sup>2-</sup>				AA <sup>-</sup>		
	α-H	β-H	N-Cm-H	Imidazole	α-H	β-H	γ-H
N-Cm-L-HistH <sub>2</sub>	3.99t	3.38d	3.65m	7.38s <sup>b</sup> 8.61s <sup>c</sup>			
Co(N-Cm-L-Hist)(α-AIBA)	3.92t	3.42d	3.51d 4.31d	7.18s 7.50s <sup>c</sup>		1.43s 1.46s	
Co(N-Cm-L-Hist)(L-Val)	3.89t	3.34d	3.44d 4.35d	7.14s 7.43s <sup>c</sup>	3.69d	2.27m	0.86d <sup>d</sup> 0.96d
Co(N-Cm-L-Hist)(D-Val)	3.93t	3.45d	3.50d 4.34d	7.19s 7.46s <sup>c</sup>	3.54d	2.2m	0.89d <sup>d</sup> 1.03d
Co(N-Cm-L-Hist)(D-Val) <sup>e</sup>	3.93t	3.44d	3.51d 4.34d	7.19s 7.47s <sup>c</sup>	3.55d	2.26m	0.89d <sup>d</sup> 1.04d
Co(N-Cm-L-Hist)(D-Thr) <sup>e</sup>	3.92t	3.45d	3.54d 4.35d	7.17s 7.54s <sup>c</sup>	3.50d	4.4m	1.26d
Co(N-Cm-L-Hist)(D-AsN) <sup>e</sup>	3.91t	3.42d	3.54d 4.32d	7.16s 7.80s <sup>c</sup>	3.74t	2.87m	

<sup>a</sup>The chemical shifts (δ) are referenced to t-BuOH (δ = 1.23 ppm) and t = triplet, d = doublet, s = singlet and m = multiplet.

<sup>b</sup>The imidazole protons are given as singlets although they are doublets with a coupling constant of ~1 Hz.

<sup>c</sup>This chemical shift is assigned to the proton on the 2-carbon of the imidazole.

<sup>d</sup> $J = 7$  Hz.

<sup>e</sup>Complex prepared using D,L-AA<sup>-</sup>.

to those of the  $\underline{D}$ -Val<sup>-</sup> analog may be due to a distortion of the imidazole chelate ring caused by an interaction between the  $\underline{L}$ -Val<sup>-</sup> chelate ring and the imidazole ring. This seems reasonable since the  $\underline{L}$ -Val<sup>-</sup> chelate ring would be bent toward the imidazole ring. This direction of bending allows the bulky  $-\text{CH}_2(\text{CH}_3)_2$  R group to be equatorial.

The large shift downfield for the proton on the imidazole 2-carbon in  $\text{Co}(\text{N-Cm-}\underline{L}\text{-Hist})(\underline{D}\text{-AsN})$  compared to those of the other complexes in Table III is probably due to the deshielding of this proton by the polar amide group of  $\text{AsN}^-$  which is on the same side of the complex as the imidazole ring. Similar deshielding has been found for the ortho pyridyl proton in the  $\text{fac-Co}(\text{PLASP})-(\underline{L}\text{-AsN})$  and  $\text{fac-Co}(\text{N-Cm-}\underline{L}\text{-Pyala})(\underline{D}\text{-AsN})$  complexes in which the amide group is also on the same side as the pyridine ring. Thus, the assignment of the complex as  $\text{fac-Co}(\text{N-Cm-}\underline{L}\text{-Hist})(\underline{D}\text{-AsN})$  is consistent with the proton and  $^{13}\text{C}$  nmr spectra (see below).

The assignments of the various protons in the coordinated amino acidates are also given in Table III. A comparison of the  $\alpha$ -protons for the  $\underline{L}$ -Val<sup>-</sup> and  $\underline{D}$ -Val<sup>-</sup>

complexes reveals that the  $\alpha$ -proton of  $\underline{\underline{L}}\text{-Val}^-$  is deshielded relative to the  $\alpha$ -proton of  $\underline{\underline{D}}\text{-Val}^-$ . Since the  $\alpha$ -proton of  $\underline{\underline{L}}\text{-Val}^-$  is positioned nearly in the plane of the imidazole ring which is pointing between the  $\alpha$ -carbon and the  $\alpha$ -carboxylate (this has been found for the pyridine ring of  $\text{Co}(\text{N-Cm-}\underline{\underline{L}}\text{-Pyala})(\underline{\underline{D}}\text{-Thr})^6$ ), it is deshielded relative to the  $\alpha$ -proton of  $\underline{\underline{D}}\text{-Val}^-$  which is on the opposite side of the chelate ring.

A similar argument can be used to explain why the  $\gamma$ -methyl groups of  $\underline{\underline{D}}\text{-Val}^-$  are deshielded relative to those of the  $\underline{\underline{L}}\text{-Val}^-$  complex. In the  $\underline{\underline{D}}\text{-Val}^-$  complex, the  $\gamma$ -methyls are positioned in the plane of the imidazole ring (as is the  $\alpha$ -H of the  $\underline{\underline{L}}\text{-Val}^-$  analogs) and are deshielded relative to the  $\gamma$ -methyls of the  $\underline{\underline{L}}\text{-Val}^-$  complex which are on the opposite side of the chelate ring. It should be noted that the assignment of the  $\text{Val}^-$  complex prepared using  $\underline{\underline{D}},\underline{\underline{L}}\text{-Val}^-$  as the  $\text{Co}(\text{N-Cm-}\underline{\underline{L}}\text{-Hist})(\underline{\underline{D}}\text{-Val})$  diastereomer is based upon the fact that its proton nmr is identical to the complex using  $\underline{\underline{D}}\text{-Val}^-$  in the synthesis (Table III). This conclusion is consistent with that noted in the CD discussion.

The proton nmr spectrum of the complex isolated using  $\underline{\underline{D}},\underline{\underline{L}}\text{-Thr}^-$  in the synthesis gives a doublet at  $\delta$  1.26

for the  $\gamma$ -methyl protons and a doublet at  $\delta$  3.50 for the  $\alpha$ -proton. Since no other doublets were observed, the complex prepared using  $\underline{D},\underline{L}$ -Thr<sup>-</sup> is either Co(N-Cm-L-Hist) (D-Thr) or Co(N-Cm-L-Hist) (L-Thr) instead of the  $\underline{D},\underline{L}$ -Thr complex. Since the calculated Y contribution to the CD spectrum of the complex is characteristic of D-amino acidates, the complex is formulated as Co(N-Cm-L-Hist) (D-Thr).

<sup>13</sup>C nmr spectra of the Co(N-Cm-L-Hist)(AA) complexes

The <sup>13</sup>C nmr spectra of the free ligand N-Cm-L-HistH<sub>2</sub> and the Co(N-Cm-L-Hist)(AA) complexes in D<sub>2</sub>O and 70% H<sub>3</sub>PO<sub>4</sub> are given in Table IV. The assignment of the resonances for the histidinate portion of the free ligand is consistent with that reported for histidine.<sup>7</sup> The chemical shifts of the N-Cm-L-Hist<sup>2-</sup> ligand in the complexes remain constant and do not seem to be affected by the amino acidate. This is consistent with assigning the same structure (Figure 2a) to all the Co(N-Cm-L-Pyala)(AA) complexes listed in Table IV. The spectra obtained in 70% H<sub>3</sub>PO<sub>4</sub> are nearly identical to those obtained in D<sub>2</sub>O, with only the carboxylate carbons being shifted up to 1.5 ppm downfield. This could be due to some protonation

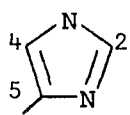
Table IV.  $^{13}\text{C}$  nmr spectra of the  $\text{Co}(\text{N-Cm-L-Hist})(\text{AA})$  complexes in  $\text{D}_2\text{O}^{\text{a}}$

	$\text{N-Cm-L-Hist}^{2-}$				
	$\alpha\text{-CO}_2^-$	$\text{N-Cm-CO}_2^-$	$\alpha\text{-C}$	$\beta\text{-C}$	$\text{N-Cm-C}$
$\text{Co}(\text{N-Cm-L-Hist})(\alpha\text{-AIBA})$	184.1	183.5	67.7	26.9	57.3
$\text{Co}(\text{N-Cm-L-Hist})(\text{D-Val})^{\text{b}}$	185.5	184.2	67.9	27.0	57.7
$\text{Co}(\text{N-Cm-L-Hist})(\text{D-Val})^{\text{b,c}}$	185.5	184.2	68.0	26.9	57.7
$\text{Co}(\text{N-Cm-L-Hist})(\text{L-Val})$	184.0	183.4	67.6	26.6	57.6
$\text{Co}(\text{N-Cm-L-Hist})(\text{D-Thr})^{\text{b,c}}$	185.4	184.4	67.9	26.9	58.1
$\text{Co}(\text{N-Cm-L-Hist})(\text{D-AsN})^{\text{c}}$	184.0	183.6	67.8	26.8	57.0
$\text{Co}(\text{N-Cm-L-Hist})(\text{D-AsN})^{\text{b,c}}$	185.4	184.4	68.1	27.0	57.7
$\text{N-Cm-L-HistH}_2$	171.9	171.3	61.3	25.4	48.8

<sup>a</sup>Chemical shifts are given relative to 1,4-dioxane ( $\delta$  67.0 ppm downfield from TMS) as an internal reference.

<sup>b</sup>Solvent is 70%  $\text{H}_3\text{PO}_4$  (aqueous).

<sup>c</sup>Complex prepared using  $\text{D,L-AA}^-$  in the synthesis.

N-Cm-L-Hist <sup>2-</sup>				AA <sup>-</sup>			
							
5-C	4-C	2-C	$\alpha$ -CO <sub>2</sub> <sup>-</sup>	$\alpha$ -C	$\beta$ -C	$\gamma$ -C	
132.3	117.8	136.7	189.8	61.5	28.3 26.8		
132.0	118.7	136.4	186.7	64.3	30.1	16.1 18.3	
131.8	118.8	136.3	186.6	64.5	30.3	16.1 18.2	
132.2	117.6	136.7	186.7	63.4	30.2	16.0 18.1	
131.6	118.4	137.2	185.4	67.7	64.3	18.6	
132.0	117.3	138.3	184.4	55.0	35.4	175.2	
131.5	118.2	138.0	185.1	55.7	35.2	175.9	
127.8	118.1	134.4					



of these carboxylates by the  $H_3PO_4$  solvent. The chemical shifts of the amino acidates correspond well with those reported for the various fac-Co(PLASP)(AA) and fac-Co(N-Cm-L-Pyala)(AA) complexes.<sup>1,3</sup>

It may be noted that all the carbon resonances occur as distinct singlets (protons were broad band decoupled), and no evidence for the presence of other isomers were found. This is consistent with the CD and proton nmr spectra which indicated that only the Co(N-Cm-L-Hist)-(D-AA) complexes were isolated from reactions using D,L-AA<sup>-</sup>.

## CONCLUSION

Previously we concluded that for several  $\text{Co(III)N}_3\text{O}_3$  complexes, the stability of the isomer isolated may be attributed to a combination of electronic, structural and steric factors. We stated that the facial isomer of the  $\text{Co(PLASP)(AA)}$  complexes (Figure 1a) was electronically favored over other possible geometrical isomers since the amino groups avoid coordinating trans to each other.<sup>1,2</sup> This preferred facial mode of coordination is consistent with an earlier theoretical account of bonding in transition metal complexes which stated that the most stable isomer for low spin- $d^6$   $\text{ML}_3\text{L}_3'$  complexes should be facial if there is no steric interaction present.<sup>8</sup> Also, as noted for the  $\text{Co(III)N}_4\text{O}_2$ ,  $\text{Co(Pyala)}_2^+$ , and  $\text{Co(III)N}_3\text{O}_3$ , fac- and mer- $\text{Co}(\underline{\text{L}}\text{-Pyala})(\text{X})$ , complexes where X is either aspartate or iminodiacetate, amino groups avoid coordinating trans to each other.<sup>4,9</sup> We also reported that fac- and mer- $\text{Co}(\text{N-Cm-}\underline{\text{L}}\text{-Pyala})(\text{AA})$  (Figure 1b and 1c) are electronically favored over other possible isomers in which amino groups are trans to each other.<sup>3</sup> Similar coordination trends have been reported for other  $\text{Co(III)}$  mixed ligand complexes.<sup>10</sup> This criterion would suggest in the present

system that the isomers in Figures 2a and 2c would be more stable than those in Figures 2b and 2d; however it does not indicate whether Figure 2a or 2c is the more stable.

Observations of isomer stability in the Co(PLASP)(AA) system helps to distinguish between those two possibilities. It was concluded that the fac-Co(PLASP)(AA) isomer (Figure 1a) is favored structurally over one in which the pyridyl group is coordinated trans to the  $\alpha$ -CO<sub>2</sub><sup>-</sup> of PLASP<sup>2-</sup>.<sup>2</sup> The coordination of the pyridyl trans to the  $\beta$ -CO<sub>2</sub><sup>-</sup> group of PLASP<sup>2-</sup> gives the least strained bond angle around the secondary amino nitrogen of PLASP<sup>2-</sup>. Similarly it was concluded that fac-Co(N-Cm-L-Pyala)(D-AA) (Figure 1b) was structurally favored over the meridional isomer (Figure 1c) since coordination of the N-carboxymethyl CO<sub>2</sub><sup>-</sup> group trans to the pyridyl should produce little strain in the C-N-C bond angle. As observed in the X-ray structure analysis of mer-Co(N-Cm-L-Pyala)(D-Thr), meridional coordination of the N-carboxymethyl CO<sub>2</sub><sup>-</sup> trans to the  $\alpha$ -CO<sub>2</sub><sup>-</sup> of N-Cm-L-Pyala<sup>2-</sup> as in Figure 1c produces considerable strain in the C-N-C angle.<sup>6</sup> Similar angular strain trends have been observed previously in the facial

and meridional coordination of polydentate ligands such as  $^-O_2C-CH_2-NH-CH_2-CO_2^-$ ,  $IMDA^{2-}$ .<sup>11-13</sup> Facial coordination of the glycinate chelate rings of  $IMDA^{2-}$  produces little strain in the C-N-C bond angle, while meridional coordination of the chelate rings in the same plane produces considerable strain in the C-N-C angle. This criterion suggests that in the present system Figure 2a should be more stable than 2c.

The isolation of only the fac-Co(N-Cm-L-Hist) (AA) isomer can be rationalized by the above two criteria: 1) amino groups avoid coordinating trans to each other and 2) the N-carboxymethyl carboxylate group produces less strain when coordinated trans to the imidazole group. However it is possible that another factor destabilizes the mer isomer (Figure 2c). This is the possible tendency of amino and imidazole groups to avoid coordinating trans to each other.

Although these two criteria rationalize the isolation of only fac-Co(N-Cm-L-Hist) (AA), steric considerations could also affect the structure of the isolated complexes as was observed in the closely related Co(N-Cm-L-Pyala) (AA) system. In this case, the degree of steric interaction

between the amino acidate chelate ring and the pyridyl group of  $N\text{-Cm-}\underline{L}\text{-Pyala}^{2-}$  seems to play a major role in determining which isomer, facial or meridional, is isolated.<sup>3</sup> For the  $\text{Co}(N\text{-Cm-}\underline{L}\text{-Pyala})(\text{AA})$  complexes, the facial isomer is favored over the meridional if steric interaction between the amino acidate chelate ring and the pyridyl group in the facial isomer is not significant. Sterically the facial isomer is favored for  $\underline{D}$ -amino acidates since the amino acidate chelate ring conformation is such that its  $\alpha\text{-CO}_2^-$  and  $\alpha$ -carbon are pointing downward, away from the pyridine ring as in Figure 8a. This conformation allows the R-group of the  $\underline{D}\text{-AA}^-$  to be equatorial instead of axial. This is consistent with the stereospecific formation of the  $\text{fac-Co}(N\text{-Cm-}\underline{L}\text{-Pyala})(\underline{D}\text{-Val})$  isomer as the only facial isomer when  $\underline{D},\underline{L}\text{-Val}^-$  was used in the complex synthesis. On the other hand, the meridional isomer is favored if there is considerable steric interaction between the amino acidate chelate ring and the pyridyl group in the facial isomer. In the  $\text{fac-Co}(N\text{-Cm-}\underline{L}\text{-Pyala})(\underline{L}\text{-AA})$  isomer, the  $\underline{L}\text{-AA}^-$  chelate ring conformation would be one in which its  $\alpha\text{-CO}_2^-$  and  $\alpha$ -carbon are pointing upward toward the

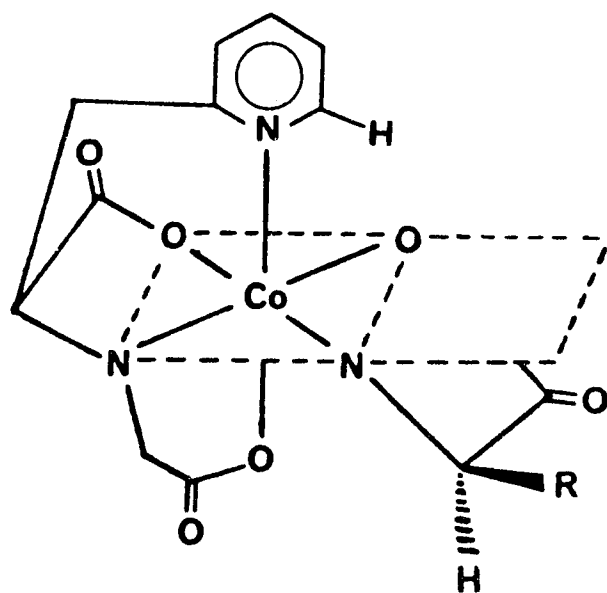
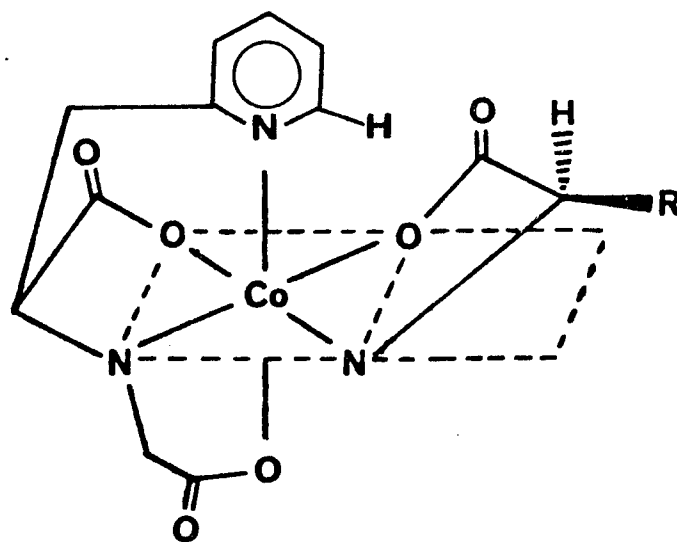
**a****b**

Figure 8. Amino acidate chelate ring conformation for  
 (a)  $\text{fac-Co}(\text{N-Cm-}\underline{\text{L}}\text{-Pyala})(\underline{\text{D}}\text{-AA})$  and (b)  $\text{fac-Co}(\text{N-Cm-}\underline{\text{L}}\text{-Pyala})(\underline{\text{L}}\text{-AA})$

pyridyl ring as in Figure 8b. This conformation allows the R-group to be in the favored equatorial position, but from an examination of molecular models there appears to be considerable interaction between the pyridyl ortho hydrogen and the  $\alpha$ -CO<sub>2</sub><sup>-</sup> of the L-amino acidate. This is consistent with the isolation of only the mer-Co(N-Cm-L-Pyala)(L-Val) isomer and the failure to isolate any fac-Co(N-Cm-L-Pyala)(L-Val).

Since the amino acidate chelate ring conformations in fac-Co(N-Cm-L-Hist)(D-AA) and fac-Co(N-Cm-L-Hist)(L-AA) are the same as those described above for fac-Co(N-Cm-L-Pyala)(D-AA) and fac-Co(N-Cm-L-Pyala)(L-AA), respectively, the fac-Co(N-Cm-L-Hist)(D-AA) complexes should be favored sterically over the fac-Co(N-Cm-L-Hist)(L-AA) complexes. This appears to be the case since only the Co(N-Cm-L-Hist)-(D-AA) complexes were isolated when D,L-AA<sup>-</sup> was used in the synthesis. Thus the fac-Co(N-Cm-L-Hist)(D-AA) complexes appear to be electronically, structurally and sterically favored over the other isomers in Figure 2.

It should be noted that since the imidazole group is not as bulky as the pyridyl, steric interaction between the amino acidate chelate ring and the imidazole group

may not play as large a role in determining the overall structure as it did in the N-Cm-L-Pyala<sup>2-</sup> analogs. The smaller size of the imidazole group relative to pyridine could cause a lower degree of interaction between the imidazole and the L-AA<sup>-</sup> chelate ring compared to that found in fac-Co(N-Cm-L-Pyala)(L-Val). This would account for the isolation of the fac-Co(N-Cm-L-Hist)(L-Val) isomer using L-Val<sup>-</sup> in the complex synthesis.



## REFERENCES

1. Meiske, L. A.; Angelici, R. J. submitted to Inorg. Chem.
2. Meiske, L. A.; Jacobson, R. A.; Angelici, R. J. submitted to Inorg. Chem.
3. Meiske, L. A.; Angelici, R. J. to be submitted to Inorg. Chem.
4. Ebner, S. R.; Angelici, R. J. accepted for publication to Inorg. Chem.
5. Colomb, G.; Bernauer, K. Helv. Chim. Acta 1977, 60, 459.
6. Meiske, L. A.; Jacobson, R. A.; Angelici, R. J. submitted to Inorg. Chem.
7. Horsley, W.; Sternlicht, H.; Cohen, J. S. J. Am. Chem. Soc. 1970, 92, 680.
8. Burdett, J. K. Adv. Inorg. Radiochem. 1978, 21, 113.
9. Ebner, S. R.; Angelici, R. J. submitted for publication to Inorg. Chem.
10. Watabe, M.; Kawaai, S.; Yoshikawa, S. Bull. Chem. Soc. Japan 1976, 49, 1845.
11. Halloran, L. J.; Caputo, R. E.; Willett, R. D.; Legg, J. I. Inorg. Chem. 1975, 14, 1762.
12. Weakliem, H. A.; Hoard, J. L. J. Am. Chem. Soc. 1959, 81, 549.
13. Corradi, A. B.; Palmieri, C. G.; Nardelli, M.; Pellinghelli, M. A.; Tani, M. E. V. J. Chem. Soc. Dalton Trans. 1973, 655.

## SUMMARY

In the present study, the  $\text{Co(PLASP)(AA)}$ ,  $\text{Co(N-Cm-L-Pyala)(AA)}$  and  $\text{Co(N-Cm-L-Hist)(AA)}$  complexes shown in Figure 1 were prepared and trends in their structures were established. The structural assignment of the  $\text{Co(PLASP)(AA)}$  complexes as in Figure 1a was based on their visible, nmr and circular dichroism spectra and the X-ray structure analysis of  $\text{fac-[Co(PLASP)(L-Phe)]}\cdot 3\text{H}_2\text{O}$ ; that of the  $\text{fac-Co(N-Cm-L-Pyala)(AA)}$  and  $\text{fac-Co(N-Cm-L-Hist)(AA)}$  complexes as in Figure 1b and 1c, respectively, was based on their visible, nmr and circular dichroism spectra; that of the  $\text{mer-Co(N-Cm-L-Pyala)(AA)}$  complexes as in Figure 1d was based on their visible, nmr and circular dichroism spectra and the X-ray structure analysis of  $\text{mer-[Co(N-Cm-L-Pyala)(D-Thr)]}\cdot 1/2\text{H}_2\text{O}$ .

The results from this study indicated that the overall stabilities of the isomers in Figure 1 are determined by a combination of electronic, structural and steric factors. If the coordination of the tetradentate ligands is considered first, there are two ways the group attached to the secondary nitrogen can coordinate as shown in Figures 2a and 2b. The coordination of the ligand in Figure 2b would produce

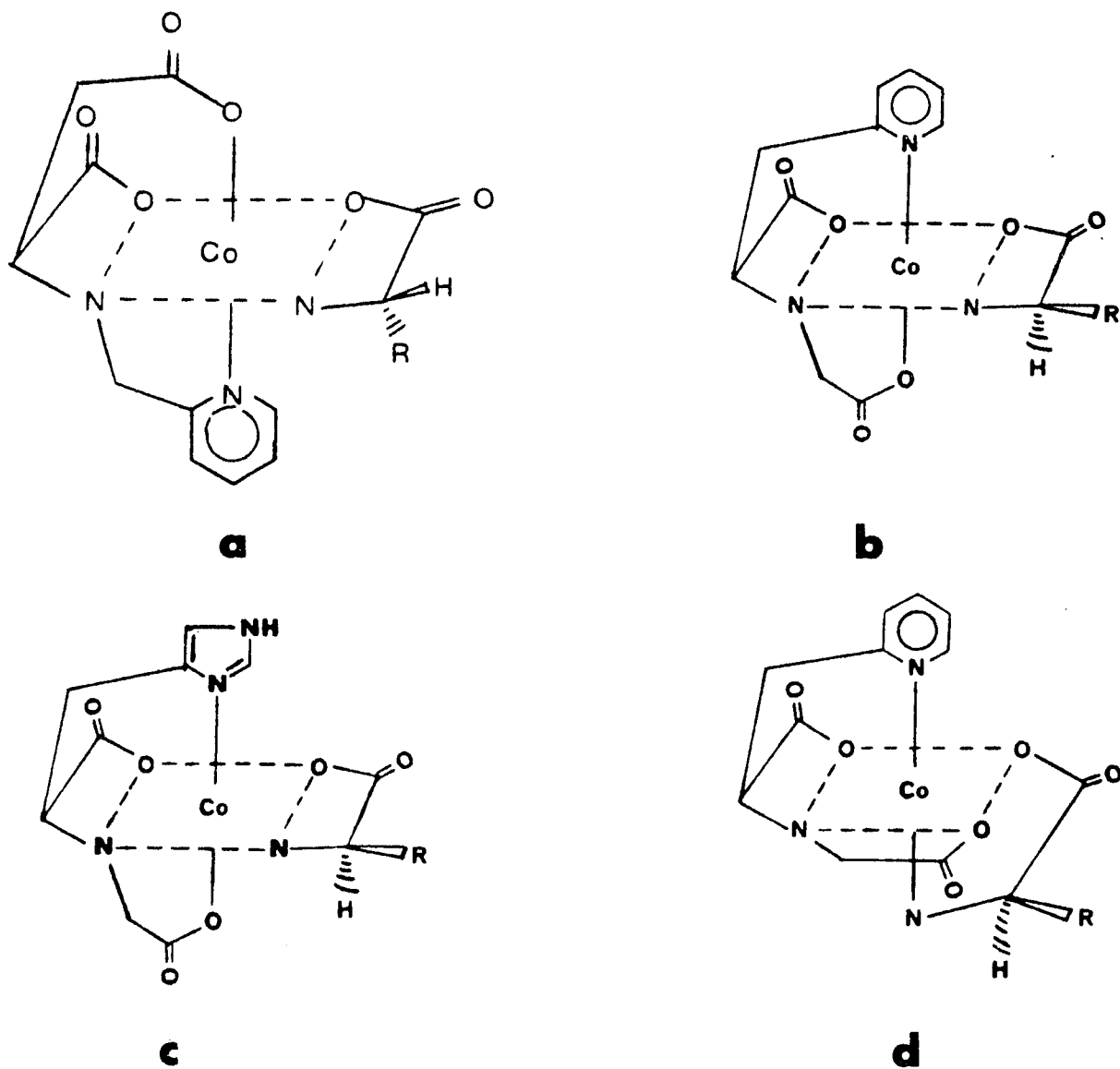


Figure 1. Various Co(III)N<sub>3</sub>O<sub>3</sub> complexes, a) fac-Co(PLASP)-(L-AA), b) fac-Co(N-Cm-L-Pyala)(D-AA), c) fac-Co(N-Cm-L-Hist)(D-AA) and d) mer-Co(N-Cm-L-Pyala)(D-AA)

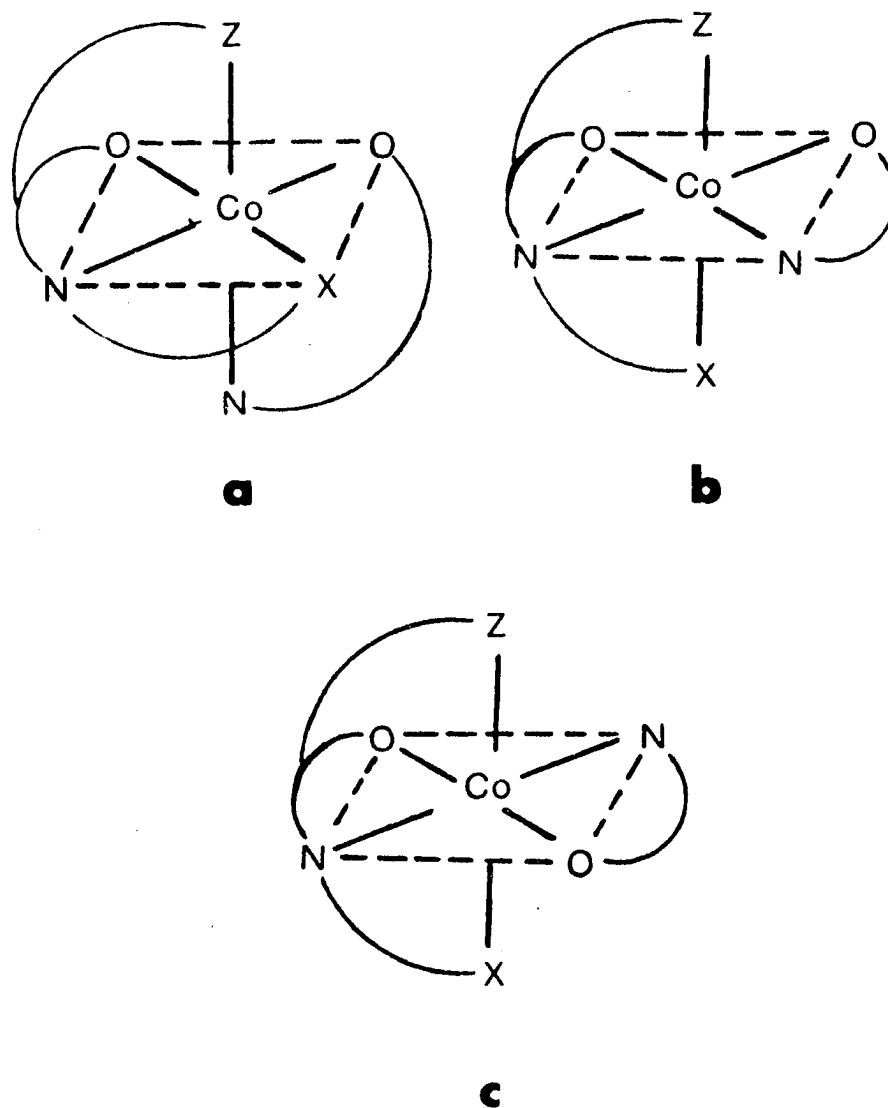


Figure 2. Various Co(III) mixed ligand structures for PLASP<sup>2-</sup> where X = pyridine and Z = CO<sub>2</sub><sup>-</sup>, N-Cm-L-Pyala<sup>2-</sup> where X = CO<sub>2</sub><sup>-</sup> and Z = pyridine and N-Cm-L-Hist<sup>2-</sup> where X = CO<sub>2</sub><sup>-</sup> and Z = imidazole

the least strain in the secondary nitrogen, C-N-C bond angle, while coordination as in Figure 2a would produce considerable strain in the C-N-C bond angle. Thus, based on strain in the bond angles, the coordination in Figure 2b is favored structurally over that in Figure 2a. If the coordination of the amino acidate is considered next, there are also two ways it can coordinate, as shown in Figures 2b and 2c. Coordination as in Figure 2b would be electronically favored over coordination as in Figure 2c since the amino group is coordinated trans to the oxygen of the carboxylate group. This mode of coordination is presumably favored by the amino groups avoiding coordination trans to each other. Thus, coordination as in Figure 2b is both electronically and structurally favored providing steric factors are not important. This was found to be the case for the Co(PLASP)(AA) complexes since only one structure (Figure 2b) was isolated for both enantiomers of valinate, phenylalaninate and asparaginate. However, for the Co(N-Cm-L-Pyala)(AA) and Co(N-Cm-L-Hist)(AA) complexes, steric factors appeared to have an important role in determining which geometry is preferred. In the facial isomer of these complexes

(Figures 1b and 1c) a D-amino acidate should have its  $\alpha$ -carbon and  $\alpha$ -CO<sub>2</sub><sup>-</sup> group pointing downward and away from the pyridine or imidazole group. This allows the R-group of the D-amino acidate to be in the favored equatorial position. On the other hand an L-amino acidate would have its  $\alpha$ -carbon and  $\alpha$ -CO<sub>2</sub><sup>-</sup> pointing upward toward the pyridyl or imidazole group. This conformation of the L-amino acidate chelate ring would allow its R-group to be in the favored equatorial position. However, examination of molecular models revealed that there is considerable interaction between the  $\alpha$ -CO<sub>2</sub><sup>-</sup> group of an L-amino acidate and the pyridyl or imidazole ring. Thus, the facial isomers of Co(N-Cm-L-Pyala)(D-AA) and Co(N-Cm-L-Hist)(D-AA) seemed to be sterically as well as electronically and structurally favored. This appeared to be the case since the only facial isomers isolated were fac-Co(N-Cm-L-Pyala)(D-AA) (in the cases of D,L-Val<sup>-</sup> and D,L-AsN<sup>-</sup>) and fac-Co(N-Cm-L-Hist)(D-AA) (in the cases of D,L-Val<sup>-</sup>, D,L-Thr<sup>-</sup> and D,L-AsN<sup>-</sup>) when D,L-AA<sup>-</sup> was used in the synthesis of the complexes. On the other hand, for the Co(N-Cm-L-Pyala)(AA) complexes, the meridional complex, Figure 1d, appeared to be favored if there is considerable steric

interaction between the amino acidate chelate ring and the pyridyl group. This appeared to be the case since only mer-Co(N-Cm-L-Pyala)(L-Val) was isolated when L-Val<sup>-</sup> was used in the synthesis and no evidence for the corresponding facial isomer was found. It was noted that the imidazole group is not as bulky as the pyridyl. The smaller size of the imidazole relative to pyridine would cause a lower degree of interaction between the imidazole and L-AA<sup>-</sup> chelate ring compared to that found in fac-Co(N-Cm-L-Pyala)(L-Val). This was consistent with the isolation of the fac-Co(N-Cm-L-Hist)(L-Val) complex using L-Val<sup>-</sup> in the synthesis of the complex. For the Co(N-Cm-L-Hist)(AA) complexes, the meridional isomer corresponding to that in Figure 1d was not isolated. This was attributed to strain in the secondary amino C-N-C bond angle and the possible tendency of amino and imidazole groups avoiding coordination trans to each other.

The differences in the overall peak intensities and shapes of the circular dichroism spectra of each series of complexes, Co(PLASP)(AA), fac- and mer-Co(N-Cm-L-Pyala)(AA) and fac-Co(N-Cm-L-Hist)(AA), were related to changes at the  $\alpha$ -carbon of the amino acidates. The CD

spectra of the  $\text{Co(PLASP)(AA)}$ ,  $\text{mer-Co(N-Cm-L-Pyala)(AA)}$  and  $\text{fac-Co(N-Cm-L-Hist)(AA)}$  were resolved into two contributions, one arising from the optically active portion of the amino acidate chelate ring (Y) and the other from the rest of the molecule (X). The X terms for each series were nearly identical to the observed spectrum of the corresponding  $\alpha\text{-AIBA}^-$  complex. The Y contribution was discussed in terms of amino acidate chelate ring bending. For all the complexes prepared, the sign of the low energy peak of the Y term is positive if the complex contains a D-amino acidate and negative if the complex contains an L-amino acidate.

In conclusion, the complexes in Figures 1a, 1b and 1c can be rationalized by the two criteria that 1) amino groups avoid coordinating trans to each other and 2) the X group (Figure 2) produces less strain in the chelate ring and C-N-C angle when coordinated trans to Z (Figure 2b). The two criteria above only apply to complexes in which steric factors are not significant. If steric factors are significant in isomers like Figure 1b then the isomer in Figure 1d is favored. It is hoped that these criteria can be applied to other  $\text{Co(III)N}_3\text{O}_3$  mixed ligand systems containing structurally similar ligands.



The work presented here has left questions such as a) is coordination of pyridyl or imidazole trans to nitrogen electronically preferred over coordination of pyridyl or imidazole trans to oxygen and b) is the  $\alpha$ -AIBA<sup>-</sup> chelate ring in the various complexes planar or bent, unanswered. The first question may be addressed by studying the coordination of the ligands in Figures 3a and 3b to Co(III). Since both the  $-\text{CH}_2-\text{CH}_2-\text{NH}_2$  and  $-\text{CH}_2-\text{CO}_2^-$  chelate rings are flexible, structural strain in the C-N-C angles probably will not be as significant as the electronic factors. The arrangement of the ligand as in Figure 3c would show coordination of amino trans to pyridine or imidazole is preferred while that as in Figure 3d would show coordination of oxygen trans to pyridine or imidazole is preferred. The second question can be answered by X-ray structure analyses of the Co(PLASP)-( $\alpha$ -AIBA), Co(N-Cm-L-Pyala)( $\alpha$ -AIBA) and Co(N-Cm-L-Hist)-( $\alpha$ -AIBA) complexes.

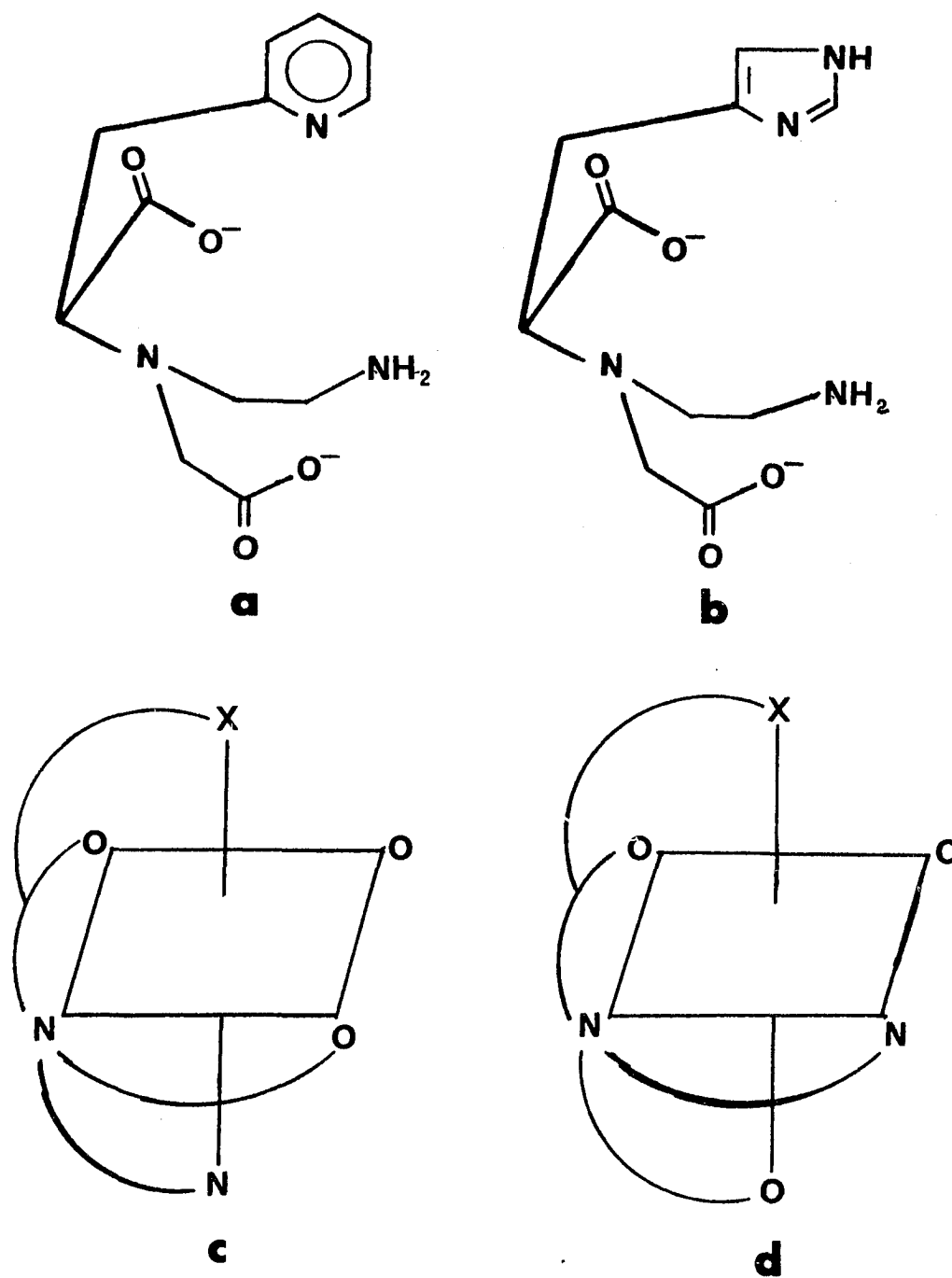


Figure 3. Two new potential ligands and their complexes with X = imidazole or pyridine

## LITERATURE CITED

1. Nakon, R.; Rechani, P. R.; Angelici, R. J. Inorg. Chem. 1973, 12, 2431.
2. Bedell, S. A.; Rechani, P. R.; Angelici, R. J.; Nakon, R. Inorg. Chem. 1977, 6, 972.

## ACKNOWLEDGEMENTS

I would like to sincerely thank Dr. Robert J. Angelici for his guidance and encouragement during this work. I wish to express my gratitude to Dr. Robert A. Jacobson, Dr. Don S. Martin and members of their research groups for help in collection of X-ray and spectral data. A special thanks is extended to Stephen R. Ebner and Man Sheung Ma for their many years of friendship and many valuable hours of helpful discussion. I am especially indebted to my parents for their love, support and encouragement given to me throughout my graduate study. I am also indebted to Paula J. Sievers for her kind understanding, patience and moral support extended to me during the writing of this dissertation. A very special thanks goes to Denise Wegter for her patience in typing this work.